DEVELOPMENT OF A SUBSIDENCE MODEL FOR ÇAYIRHAN COAL MINE

A THESIS SUBMITTED TO
THE GRADUATE SCHOOL OF NATURAL AND APPLIED SCIENCES
OF
MIDDLE EAST TECHNICAL UNIVERSITY

BY

M. ESENAY HACIOSMANOĞLU

IN PARTIAL FULFILLMENT OF THE REQUIREMENTS
FOR
THE DEGREE OF MASTER OF SCIENCE

IN

MINING ENGINEERING

JULY 2004

Approval of the Graduate School of Natural and Applied Sciences.

Prof. Dr. Canan Özgen
Director

I certify that this thesis satisfies all the requirements as a thesis for the degree of Master of Science.

Prof. Dr. Ümit Atalay
Head of Department

This is to certify that we have read this thesis and that in our opinion it is fully adequate, in scope and quality, as a thesis for the degree of Master of Science.

Prof. Dr.Erdal Ünal
Supervisor

Examining Committee Members

Prof. Dr. Bahtiyar Ünver (Hacettepe Univ., Mine)

Prof. Dr. Erdal Ünal (METU, Mine)

Prof. Dr. Tevfik Güyagüler (METU, Mine)

Assoc. Prof. Dr. Aydın Bilgin (METU, Mine)

Assist. Prof. Dr. İhsan Özkan (Selçuk Univ., Mine)

I hereby declare that all information in this document has been obtained and presented in accordance with academic rules and ethical conduct. I also declare that, as required by these rules and conduct, I have fully cited and referenced all material and results that are not original to this work.

Name, Last name: M. Esenay Hacıosmanoğlu

Signature :

ABSTRACT

DEVELOPMENT OF A SUBSIDENCE MODEL
FOR ÇAYIRHAN COAL MINE

Hacıosmanoğlu, Meryem Esenay
M.Sc., Mining Engineering Department
Supervisor: Prof. Dr. Erdal Ünal

September, 2004, 154 Pages

In this study, subsidence analyses were carried out for panels B14, B12, B10, B02; C12, C10, C08 of Çayırhan Lignite Mine using in-situ subsidence measurements.

Using the measurements from stations, installed both parallel and perpendicular to panel-advance direction, subsidence profiles were plotted as a function of time and distance from panel center. Horizontal displacement and strain curves were also plotted and compared with subsidence profiles.

There are various methods used for subsidence prediction. In this study however, a subsidence model was developed based on empirical model obtained from nonlinear regression analysis. During the analyses SPSS (V.10.0) software was used and the unknown parameters associated with subsidence function were determined for the stations above B14 panel. Since it was too complicated to take all the affecting factors into consideration, only the parameters which could be estimated by statistical evaluation were taken into account during analyses.

One significant contribution of this study to subsidence subject was the comparison of the subsidence values measured during this investigation with the values predicted by some other empirical methods.

In this study, the structural damages to the pylons installed on ground surface above retreating longwall panels were also investigated by the use of previous studies. Slope as well as horizontal strain changes caused by ground movements due to underground mining were determined.

Last but not least, it should be stated another significant contribution of this study to engineering was the collection of a significant database obtained from field measurements.

Keywords: Subsidence measurements, database, slope, horizontal displacement and strain, subsidence prediction, statistical analysis.

ÖZ

ÇAYIRHAN KÖMÜR MADENİ İÇİN TASMAN MODELİ GELİŞTİRİLMESİ

Hacıosmanoğlu, Meryem Esenay

Yüksek Lisans, Maden Mühendisliği Bölümü

Tez yöneticisi: Prof. Dr. Erdal Ünal

Eylül, 2004, 154 Sayfa

Bu çalışmada, yüzeydeki tasman ölçümlerini kullanarak Çayırhan linyit madenindeki B14, B12, B10, B02, C12, C10, C08 panolarına ait tasman analizleri yapılmıştır.

Pano ilerleme yönüne paralel ve dik olacak şekilde yerleştirilen istasyonlardan alınan ölçümler kullanılarak zamana ve pano merkezinden uzaklığa göre tasman profilleri çıkarılmıştır. Yatay deplasman ve birim deformasyon eğrileri de çizilmiş ve tasman profilleriyle karşılaştırılmıştır.

Tasmanın belirlenmesinde çeşitli yöntemler kullanılmaktadır. Bu çalışmada ise, görgül yaklaşıma dayanan bir tasman modeli doğrusal olmayan regresyon analizi kullanılarak geliştirilmiştir. Analizler surasında SPSS (V.10.0) programı kullanılmış ve fonksiyonla ilgili bilinmeyen parametreler B14 panosunun üzerindeki istasyonlar için belirlenmiştir. Başlangıçta tüm etkenleri dikkate almak çok güç olduğundan, analizler esnasında sadece istatistiksel değerlendirmeyle tahmin edilebilecek değişkenler dikkate alınmıştır.

Bu çalışmanın mühendisliğe önemli katkılarından biri, bu araştırma sırasında ölçülen tasman değerlerinin diğer ampirik yaklaşımlar kullanılarak tahmin edilen tasman değerleriyle karşılaştırılmış olmasıdır.

Bu çalışmada uzunayak madenciliği nedeniyle oluşan yapısal hasarların yüzeydeki pilonlar üzerindeki etkisi önceki çalışmalardan yararlanılarak araştırılmıştır. Yeraltı madenciliğinden kaynaklanan yer hareketlerinin sebep olduğu eğim ve yatay birim deformasyon değişimleri belirlenmiştir.

Son olarak, bu çalışmanın mühendisliğe diğer bir önemli katkısı, arazi ölçümleri kullanılarak oluşturulan kaydadeğer veri tabanıdır.

Anahtar Kelimeler: Tasman ölçümleri, veri tabanı, eğim, yatay deplasman ve birim deformasyon, tasman tahmini, istatistiksel analiz.

TO MY FAMILY

ACKNOWLEDGEMENTS

I wish to express my sincere appreciation to Prof. Dr. Erdal Ünal for his advice, support, constructive comments and contributions throughout this thesis.

I'm in great dept to İhsan Özkan for his significant contribution to this study.

Contributions of the members of the examining committee, Prof. Dr. Tevfik Güyagüler, Assoc. Prof. Dr. Aydın Bilgin, Prof. Dr. Bahtiyar Ünver, are thankfully acknowledged.

I would also like to express my thanks to my friends, Sinan & Başak İnal, Ahmet Karakaş & Sinem Şener, Aslı Sayılgan, Koray Önal, Medine Tuna, Muharrem Kılıç, Öykü Selimoğlu, Pınar Öneş, Pınar Taşcan, Reza Osgoui, Serpil Mesci, Tuğcan Tuzcu and Yasemin Yeşilay.

Thanks also go to all members of my family, my father (Mehmet Çetin Hacıosmanoğlu), my mother (Serap Hacıosmanoğlu), and my sister (Gülenay Hacıosmanoğlu).

TABLE OF CONTENTS

LIST OF TABLES

LIST OF FIGURES

LIST OF ABBREVIATIONS

a:	Subsidence factor
M:	Extraction thickness
W:	Extraction width
L:	Extraction length, Distance of subsidence trough margin to subsidence center
H:	Depth
s:	Subsidence
S:	Maximum subsidence
S_{max}:	Maximum possible subsidence
γ, θ:	Angle of draw from horizontal and vertical, respectively
α:	Dip of seam
u:	Displacement
R:	Radius of critical area
i:	Slope
k:	Curvature

CHAPTER 1

INTRODUCTION

1.1. GENERAL REMARKS

Being a dynamic operation, mining causes a continuous change in the topography over time. Therefore, systematic measurements are required to be able to evaluate and interpret the effects of the ground movement at the surface. Subsidence is one of the most important environmental effects of underground mining and depends on many factors. Therefore, prediction of ground movements and deformations caused by underground mining is an important aspect in determination and prevention or minimization of the damage.

1.2. OBJECTIVE OF THE THESIS

There are three main objectives of this thesis. Firstly, to prepare a database for the analysis of subsidence measurements carried out at the surface, over the retreating longwall panels at Çayırhan Coal Mine. Secondly, to determine structural damages to the power line pylons and propose precautions. Thirdly, to develop a mathematical model for subsidence prediction in panel B14 and use other empirical approaches to estimate subsidence profiles.

1.3. METHODOLOGY OF THE THESIS

Measuring stations were located at the surface, parallel and perpendicular to the panel axis to determine the vertical and horizontal displacements. Surface investigations were carried out, where fractures, erosions and pylon damages had occurred. Test poles were used to find out the amount of tilting.

After preparing the necessary tables using the measurement data, graphs were plotted to show absolute and differential components of subsidence, such as, vertical-horizontal displacement and strain profiles. Macros were prepared for the transformation and calculation processes. The angles, used for the determination of the shape of subsidence trough, can be determined by these profiles.

The function, that has been driven in this study for subsidence prediction is an exponential model consisting of time dependent and advance dependent components. There are many significant factors those should be taken into account in developing a mathematical model. These factors were taken into consideration by adding various parameters into the subsidence equation. These parameters were estimated by carrying out statistical analyses using the software SPSS Version 10.0. Further evaluations of the estimated parameters are required to come up with a decision on subsidence prediction.

1.4. THESIS OUTLINE

Following the Introduction Chapter, concepts of subsidence engineering, such as subsidence mechanism, factors influencing subsidence, subsidence prediction methods and a brief state-of-the art review are presented in the literature survey in Chapter 2. Chapter 3 gives information about the geology and the production process of the mine. In Chapter 4, the measurement procedure is explained. In Chapter 5, transformation and translation calculations of the distances, along and perpendicular to panel axis, are performed, and the results are tabulated; subsidence, horizontal displacement and strain profiles are compared. In Chapter 6 the exponential type mathematical model, developed in this study, is explained and the results associated with estimation of governing parameters are given and various empirical methods are tested.

CHAPTER 2

LITERATURE SURVEY

2.1. GENERAL

In this chapter, a comprehensive literature survey will be presented especially on significant subjects such as: i) subsidence engineering, ii) subsidence development, iii) the factors influencing subsidence, and iv) methods in predicting ground movement.

2.2. SUBSIDENCE ENGINEERING

Subsidence can be expressed as ground movements taking place because of extraction of mineral resources or abstraction of fluids. Mining subsidence is one of the most important impacts of mining on the environment. The field of subsidence engineering stretches from the firm rock at the mining horizon to the surface layer of loose ground. A comparison is done between subsidence engineering and strata control in Table 2-1.

Tasks of subsidence engineering can be classified as:

- Prediction of ground movements (possibility, magnitude, type, time, form)
- Determination of the movement effects (subsidence can have serious effects on natural features, surface structures, services and communications; can be responsible for flooding (Bell, 2000)).
- Prevention of the damage by means of appropriate mining improvements

- Protection studies

Table 2-1 Subsidence engineering and strata control comparison (Kratzsch, 1983).

	Interaction	Case	Model
Strata Control	between solid rock and roof supports & pillars	circumstances of disturbed load equilibrium (in vicinity of working)	load
Subsidence Eng.	between loose ground & structural foundations or shaft linings	influence of strata movements remote from underground workings	movement

2.3. SUBSIDENCE DEVELOPMENT

When the extraction reaches a certain size, the roof strata will cave in because of the disturbed stress field. The extent of deformation and displacement caused by the stress changes depends on the magnitude of the stresses and the cavity dimensions. In other words, removal of natural support because of underground cavities causes bending of successive layers under the influence of gravity and closing up of the cavity. So the collapsed roof beds and the packing material are gradually compressed by their own weight (compactional stage). This stage acts as the impulse for subsidence at the higher strata and at the surface.

The overlying strata continue to bend and break until the piles of the fallen rock fragments are sufficiently high to support the overhanging strata. At this time the overhanging strata does no longer cave, but bend and rest on the underlying strata.

A roof resting on packing material can be regarded as rheological medium which, in its time-dependent deformation behavior, approaches that of, for example, a visco-elastic Kelvin body consisting of an elastic Hookeian element (stress and strain are proportional) and a viscous Newtonian element (the relationship depends on the rate of deformation).

In a Kelvin body, the total stress acting to produce strain is given by:

$$\sigma = E\varepsilon + \eta(d\varepsilon/dt) \qquad [\ 2\text{-}1\ ]$$

where η is viscosity (Kratzsch, 1983).

Strata bending and subsidence develop upward until forming a subsidence basin at the surface. The extent of movement in the upper layers depends on the closing up. The whole overburden strata and the surface subsidence basin will further go through a period of compaction and gradually become stabilized (Peng, 1992).

Figure 2-1 is a schematic representation of subsidence development at different levels and Table 2-2 gives the interrelationship of rock-movement processes around mine excavations.

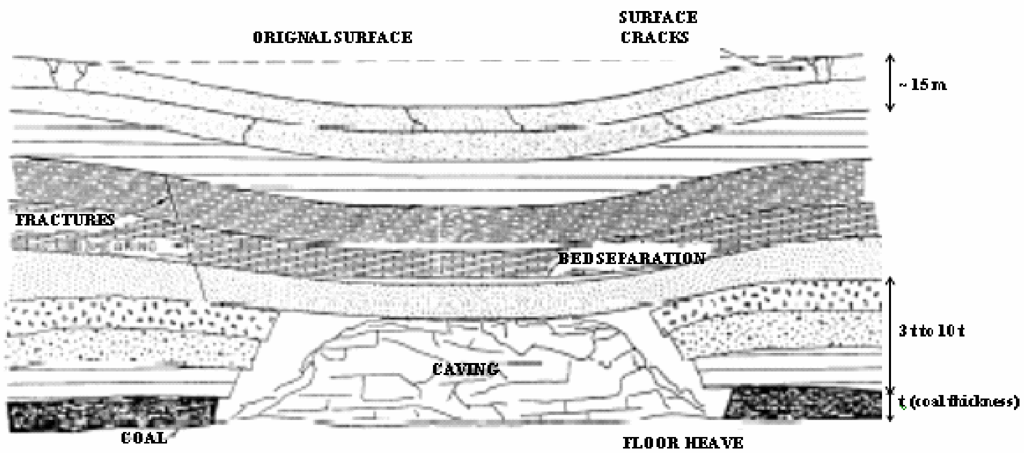

Figure 2-1 Strata disturbance caused by mining (Singh, 1992).

Table 2-2 Interrelationship of rock processes at the mining horizon.

Static equilibrium	**Stage 1**

Removal of natural support by the cavity of extraction	Artificially created disequilibrium of forces
Disturbed stress field (local disequilibrium)	
Liberation of strata energy and internal stress from depth pressure	
Strata movement and deformation - consumed by convergence (roof strata bend downward, floor heaves), rock fall, fracturing, heat of dynamic friction - stored as energy of elastic deformation	Forces of deformation operating in the **Transitonal Phase**
Gradual realignment of forces into a new equilibrium	
Visible and lasting shift in position of rock particles within mine excavation's sphere of influence (subsidence, displacement)	**Stage 2** Rock deformation established from the newly established equilibrium
Zonal deformation (extansion or compression horizontally, expansion or contraction vertically)	
Uneven stress distribution at different horizons (abutment pressure, stress relief)	
New equilibrium established as between external gravitational forces and internal rock stresses	

2.3.1. ZONES OF MOVEMENT

Six zones of movement above a longwall panel independent of time are shown in Figure 2-2. And also these special layers are defined as follows:

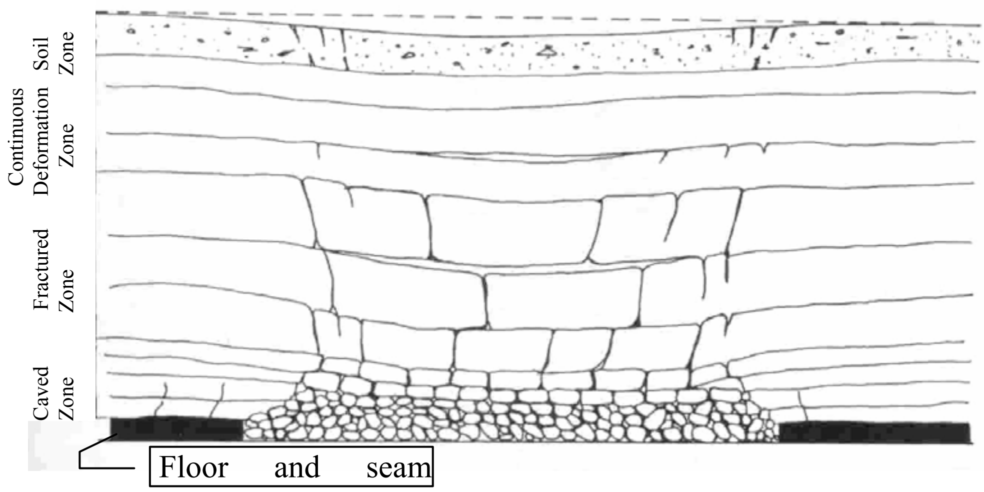

Figure 2-2 Zones of strata movement (Peng , 1992).

1. ***Floor layers*** arch elastically upwards upon the relief of the perpendicular load.

2. ***The seam and waste/packing layer*** is inelastically compressed both by the front abutment pressure on the solid ahead of the face and by the back abutment pressure on the mined-out goaf or on the pillars. Convergence in the workings can be divided into 3 zones of movement (Figure 2-3):

- *Convergence in the forefield (the zone in front of the face),* c_0, is caused by abutment pressure and its magnitude is about 10-20 % of the mining height. Settlement of immediate roof begins about 30-100 m ahead of the working face. Immediate roof is settled because of compression of the soft seam and protrusion of that part into the face area. At the same time the floor heaves at the seam edge.

- *Convergence in the face area,* c_1, is several tens of centimeters. The strata bend under their own dead weight. The floor heaves about 10-20 cm.

- *Post-convergence (after the face has gone through)*, c_2, is almost complete some 100 m to the rear of the last row props.

So the total convergence will be

$$C = c_0 + c_1 + c_2 \qquad [\ 2\text{-}2\ ]$$

This total convergence corresponds to the maximum possible subsidence (S_{max}) for flat seams:

$$S_{max} = C_{max} = a\,M \qquad [\ 2\text{-}3\ ]$$

where *a* represents the subsidence factor when the gob reached the critical size (Liu, 1981 in Peng, 1992), and it depends on the extraction system and strata-roof control methods. It amounts to 0.45-0.55 and 0.90-0.95 of seam thickness with stowing and caving respectively. This factor is related to rock properties by

$$a = 0.5\ (0.9 + P) \qquad [\ 2\text{-}4\ ]$$

where P is the coefficient for combined strata properties. Subsidence factor changes between 0.45-0.6, 0.6-0.8, 0.8-1 for hard, medium hard and soft rocks respectively.

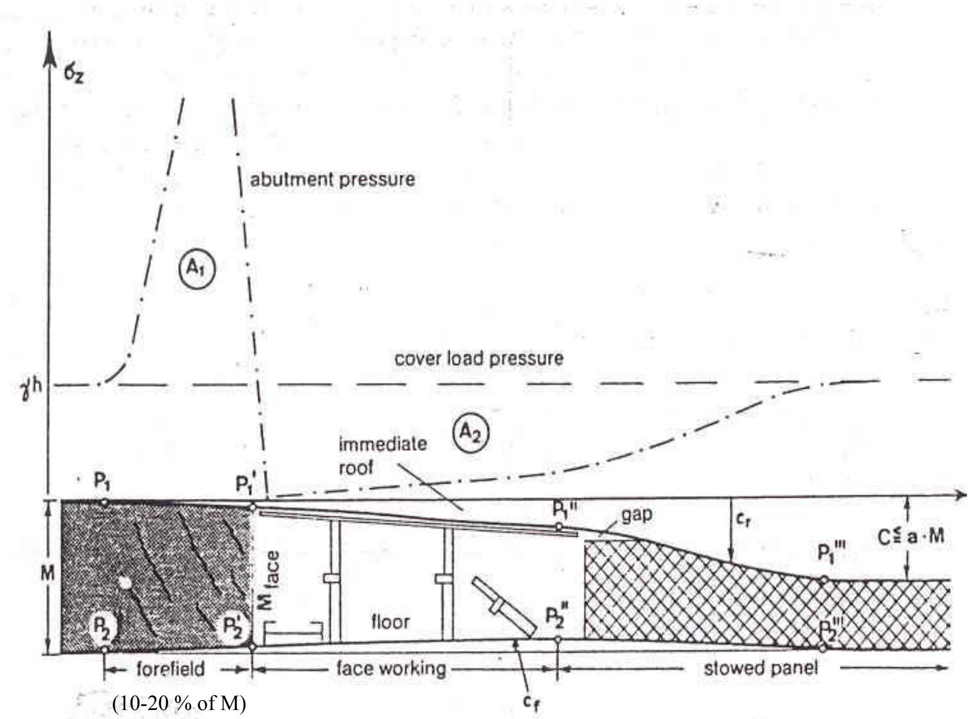

Figure 2-3 Convergence in the mine excavation, and the distribution of vertical rock pressure, in longwall mining – in case with stowing (Kratzsch,1983).

3. ***The immediate roof layer (caved zone)*** detaches itself from the more rigid main roof, breaks off, and falls in large pieces into the excavation (caves irregularly) and fills up the void (continuity and stratified beddings are lost). The height of the caved zone changes between 2 to 8 times the extraction height (Peng, 1992).

4. ***The main roof (*****fractured zone):**

Lower roof beds (the immediate roof and main roof) are exposed to high pressure, strong bending, and rapid development of movement. Consequently e*lastic stage* of deformation is soon passed and *elasto-plastic* deformation predominates.
Strata breakage and loss of continuity are the basic mechanisms in this zone. There will be a great increase in the porosity and permeability of the strata. Total height of fractured and caved zone changes between 20 to 30 times the mining height where height of the fractured zone for hard and strong strata is larger than that for soft and weak ones. Fractured zone may dome, horse saddle or is flat arch shaped (Peng, 1992).

Bending or shearing type roof breaking occurs in mining without pillars (up to 30 m behind the advancing face). In bending fracture, there will be a gradual settlement in a flat curve until wholly supported by the caved waste and by the compressed seam ahead of the face. Shear failure takes place either at right angles to the stratification by a punching effect over a hard seam edge (perpendicular shear) or, is broken up into several wedge-shaped blocks (thrust-fracture) while remaining parallel to stratification (slip separation) (Figure 2-4). In case of pillar working, sagging occurs in a wavy outline over rooms and pillars.

The factors influencing relative proportions of initial elastic bending and plastic movement of fractured blocks are bending resistance, brittleness, jointing pattern, perpendicular clamping pressure, rate of face advance, amount of bending (a function of seam thickness), and cover load (a function of depth) (Kratzsch,1983).

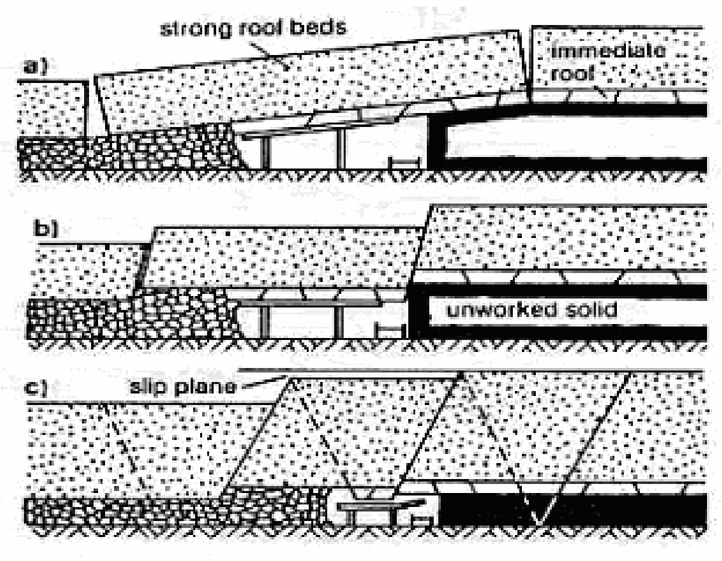

Figure 2-4 Principal types of main-roof break without pillars: a) bending fracture b) perpendicular shear c) thrust – fracture (Kratzsh, 1983).

5. ***The intermediate zone (continuous bending (deformation) zone)*** where elastic deformation and horizontal detachment processes predominate. Thick beds sag like a flat dish without breaking, maintaining continuity and the original forms. Some open fissures in the tension zone of the surface subsidence profile do not destroy the strata continuity.

6. ***The surface zone of loose overburden layers*** consists of soil and weathered rocks. It behaves in a predominantly inelastic and plastic manner in the formation of subsidence troughs. They have practically no tensile strength and follow the subsiding basement down as a flexible covering.
   When the face is nearby soil cracks open up and when it is far away they close back. Especially the cracks along the edges of the panel may remain open.

Figure 2-5 and Figure 2-6 show vertical and horizontal movement and deformation respectively.

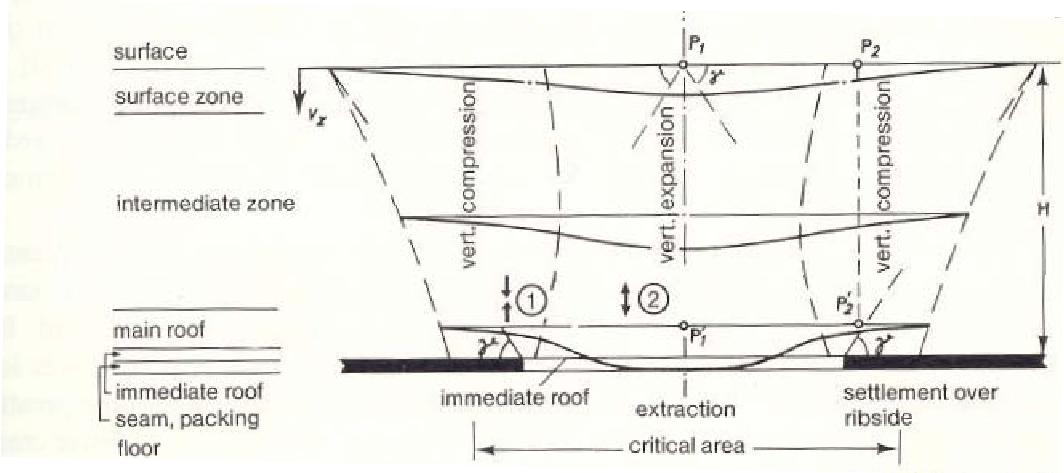

Figure 2-5 Vertical deformation of an undermined rock mass in flat-lying measures (Kratzsh, 1983).
① Additional pressure on the solid resulting from abutment and bending pressure
② load reduction and bed separation over the area of extraction

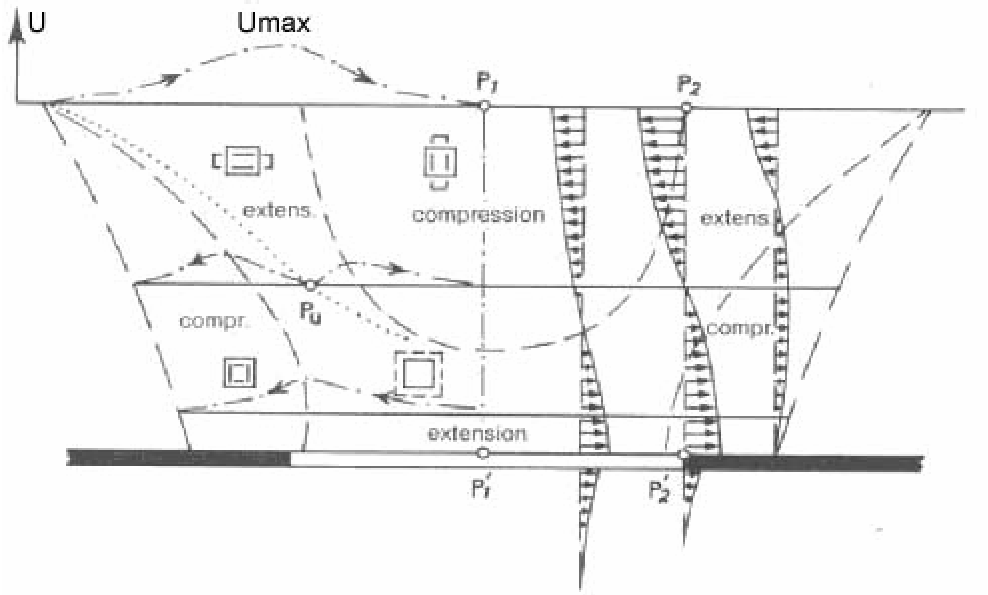

Figure 2-6 Horizontal deformation of a rock mass affected by underlying workings, with no bedding-plane slip (as a continuum) (Kratzsh, 1983).

2.3.2. THE COMPONENTS OF GROUND MOVEMENT

- **Vertical components:**

  - Vertical displacement (settlement, sinking, or lowering), *S*

    The amount of maximum possible subsidence for flat seams is given by Equation 2-3 and for inclined seams in Chapter 6.

  - Slope (tilt), *i* (the first derivative of the vertical displacement with respect to the horizontal distance)

    $$i_x = \frac{dS}{dx} \qquad [\ 2\text{-}5\ ]$$

  - Curvature (flexure), *k* (first derivative of the slope, or second derivative of the vertical displacement)

    $$k_x = \frac{d^2S}{dx^2} \qquad [\ 2\text{-}6\ ]$$

Vertical displacements cause little structural damage. Disruption of flow trough pipes and drainage patterns, alteration of grade of roads or railways are possible. Differential vertical settlements cause slopes to form and induce tilting.
Curvature causes arching in extended structures, which can lead to failure (Kratzsch, 1983).

- **Horizontal components:**

  - Horizontal displacement (lateral movement), U

$U_{max} = b\ S_{max}$ [2-7]

where *b* is the horizontal displacement coefficient and determined from the results of flat and wide seam extraction.
Its value lies in the range 0.13-0.4 and varies with seam inclination, but independent of rock property.

- Horizontal strain (extension, compression), ε (first derivative of the horizontal displacement with respect to the horizontal distance)

$$\varepsilon_x = \frac{dU_x}{dx} \qquad [\ 2\text{-}8\ ]$$

Principal horizontal deformations and their polar representation (tensile strain is positive, compressive strain is negative) are shown in (Figure 2-7):

- Shear strain

$$\gamma = \frac{dU_x}{dy} \qquad [\ 2\text{-}9\ ]$$

Uniform horizontal movements cause little damage, but brakes in pipes, communication lines, roads, and other features may occur.
Horizontal strains cause most of the structural damage. They cause tensile or shear cracks and buckling and induce distortion, fractures, or failure.

- **Twisting**

$$T = \frac{d^2S}{dxdy} \qquad [\ 2\text{-}10\ ]$$

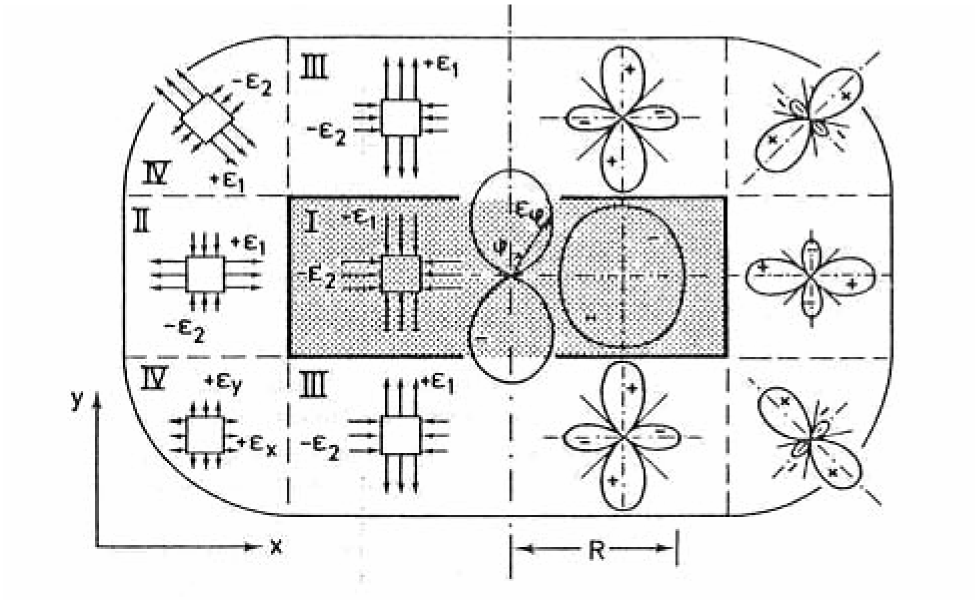

Figure 2-7 Tensile and compressive strain in a subsidence trough (Kratzsch, 1983).

Terminologies to define the characteristics of a subsidence profile are:

- **Angle of draw (angle of major influence, limit angle), γ (from horizontal) or θ (from vertical)** serves to define the limit of discernible movement at the edge of subsidence zone. θ varies from 4° to 45° and quoted about 35° in European and UK coalfields (Whittaker and Reddish, 1989). The diameter of the area of influence is equal to $2H \cot \gamma$ (or $\tan \theta$) (Figure 2-8, Figure 2-9).

- **Angle of critical deformation, δ** is the angle between the vertical line and the line connecting the opening edge and the point of critical deformation. It is about 10 degrees less than the angle of draw (θ).

- **Angle of break (fracture or slide), α** is the angle between the horizontal and the line connecting excavation edge with the point of maximum tensile strain (Figure 2-9). It shows little local variation and indicates the region of main structural damage or even breaks (in the form of open cracks or ground steps).

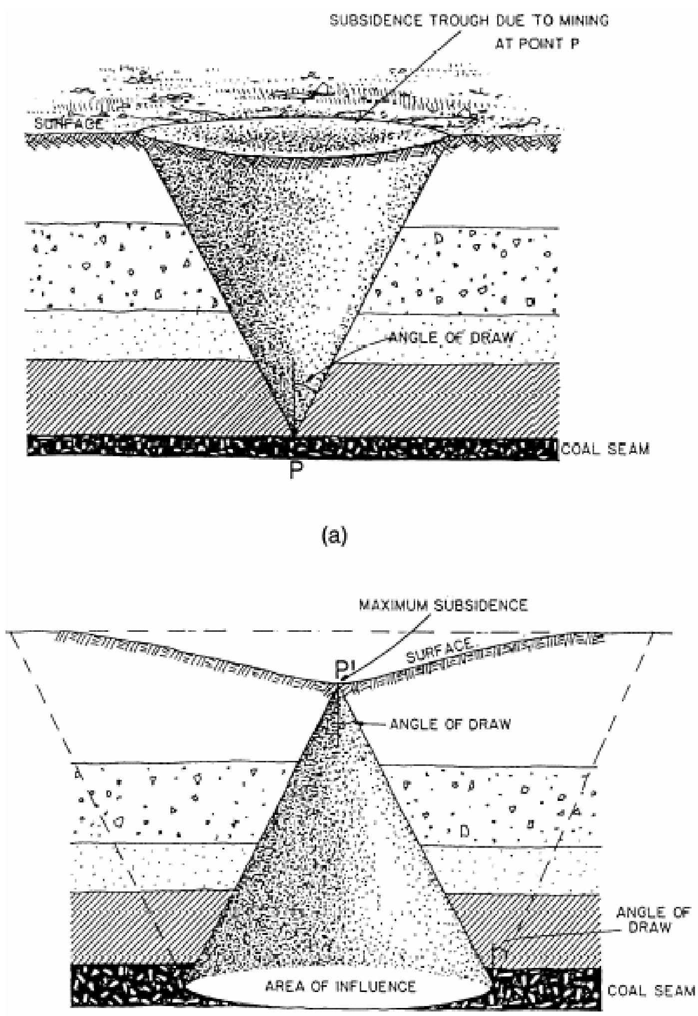

Figure 2-8 (a) Effect of mining to the surface (b) maximum subsidence at P' by mining area of influence (Singh, 1992).

- **Inflection Point (I.P.)** is the transition point between concave and convex portions of the subsidence profile (Figure 2-10). At this point, subsidence slope becomes its maximum value and curvature is equal to zero (Figure 2-9). Its distance from the edge of the opening, d, is generally equal to 0.4r (radius of major influence) (Peng, 1992).

- **Radius, r and angle of major influence, *β*.** Surface deformations are small beyond the distance greater than the radius of deformation. Tanβ is equal to H/r (Figure 2-10).

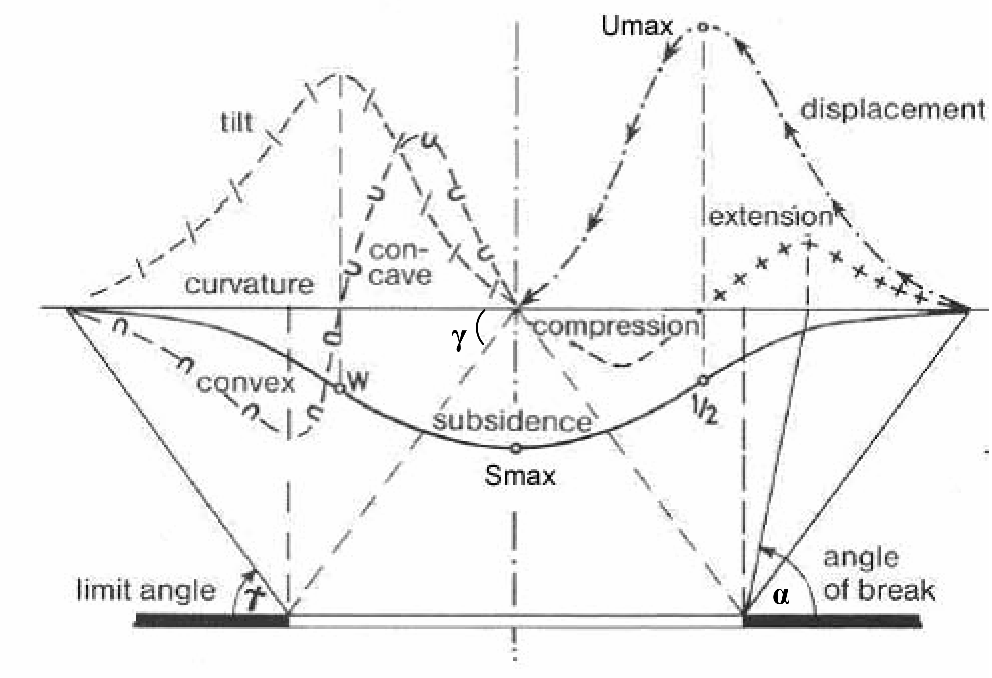

Figure 2-9 Vertical (left half) and horizontal (right half) components of ground movement over a critical area of extraction (Kratzsh, 1983).

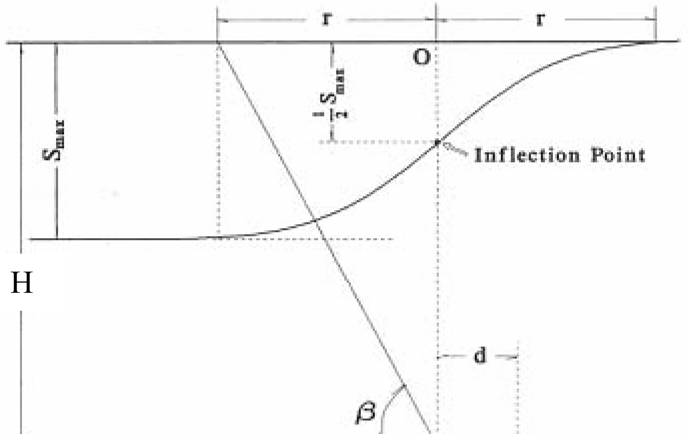

Figure 2-10 Radius (*r*) and angle of major influence (*β*) (Peng, 1992).

2.4. FACTORS INFLUENCING MINE SUBSIDENCE

Factors influencing subsidence can be divided into two major categories as mining related and geological factors. The first 5 factors are related to mining conditions and following ones with geological conditions.

2.4.1. MINING RELATED FACTORS

2.4.1.1. Extraction Thickness and Width

Subsidence will increase with increasing extraction thickness. Effected seam thickness (there may be pillars or unmined parts of coal) should be considered for the subsidence estimation. Slender (high height to width ratio) pillars are more close to failure. The full subsidence at the center is a linear function of the mining height.

Non-effective width is the maximum width of extraction up to which no significant symptom of subsidence occurs at the surface. Non-effective width to depth ratio (NEW) is varying between 0.2 and 0.8 in Indian coal fields depending on strata competence (Sheorey et al., 2000). *Critical width* is the minimum width that needs to be mined before the maximum possible subsidence is observed at the trough center. *Subcritical width* is less than critical width and the subsidence will be less than the maximum. *Supercritical width* is larger than the critical width and maximum possible subsidence is attained in a flat bottom shape (Singh, 1992) (Figure 2-11).

For a wider opening, the maximum subsidence will be larger and the subsidence basin wider (Figure 2-11).

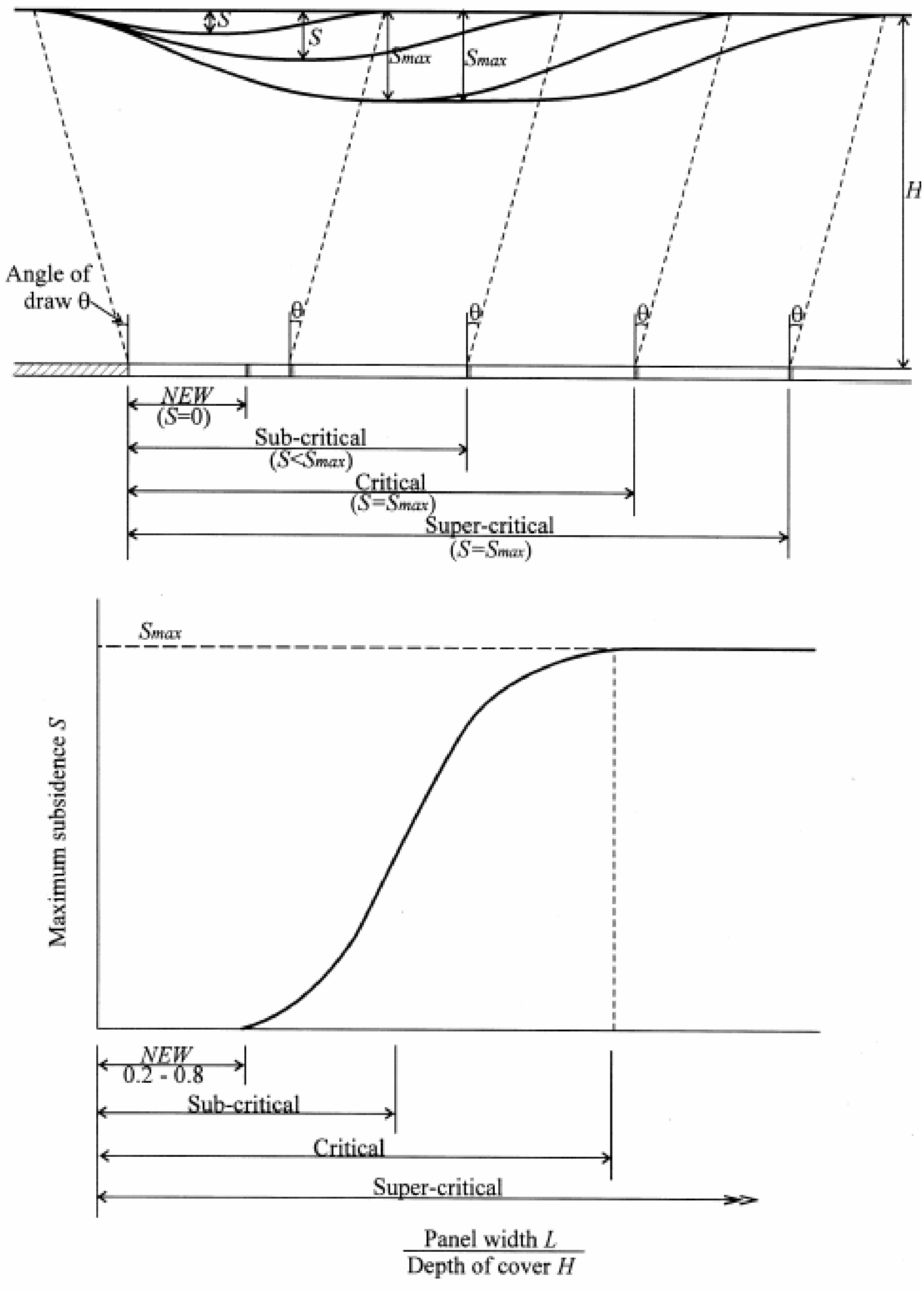

Figure 2-11 Width types (Sheorey et al., 2000).

Subsidence, vertical slope and horizontal strain profiles for different types of extraction widths are shown in Figure 2-12.

Width to depth ratios (W/H) of subcritical, critical and supercritical extractions for U.K. coal mining conditions were categorized by Whittaker and Reddish (1989):

$$
\begin{aligned}
&\text{Subcritical extraction} && \frac{W}{H} < 1.4 \\
&\text{Critical extraction} && \frac{W}{H} = 1.4 \qquad\qquad [\,2\text{-}11\,] \\
&\text{Supercritical extraction} && \frac{W}{H} > 1.4
\end{aligned}
$$

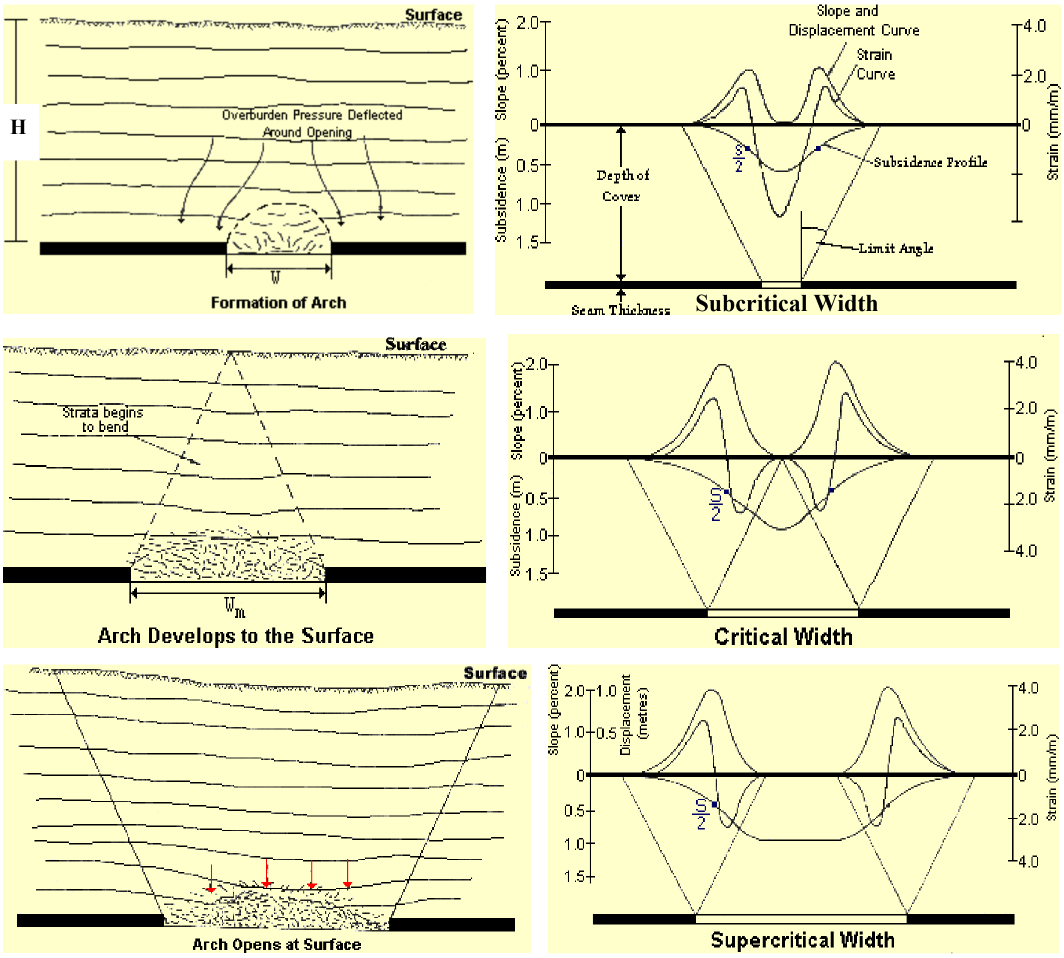

Figure 2-12 Surface and strata affects for a subcritical, critical, supercritical width of extraction.

Diameter of area of influence – the area at the base of the conical shape having its apex at point P - defines critical width of the workings. The critical width (causing full amount of subsidence) at a smaller depth (H') can be found out using the cone (Figure 2-13).

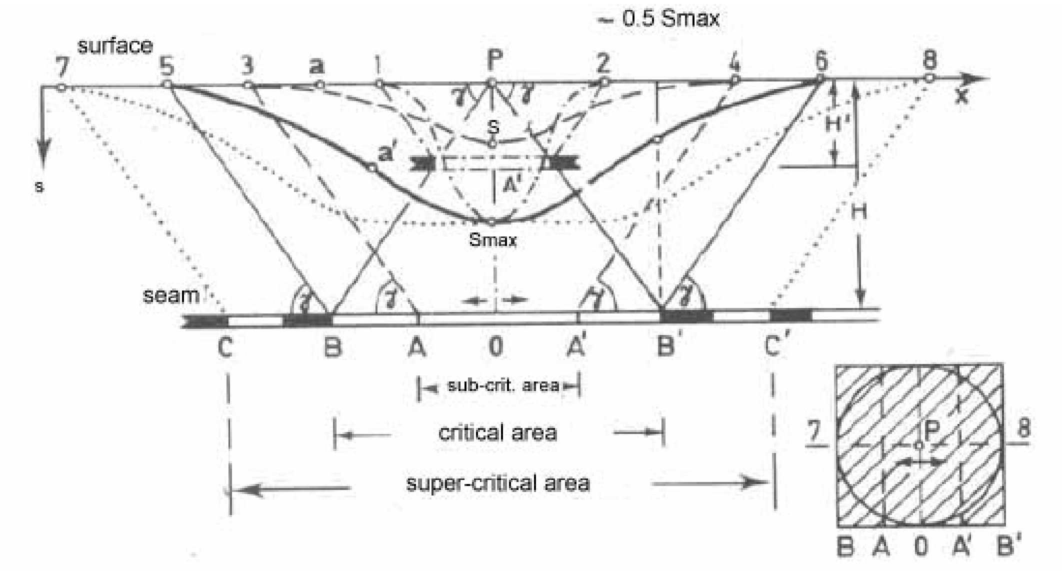

Figure 2-13 Trough profiles for subcritical, critical and supercritical areas (Kratzsh, 1983).

Various trough profiles are compared in Figure 2-13 and Figure 2-14.

Strata pressure arching across a longwall extraction in relation to extraction width is illustrated in
Figure 2-15.

Maximum observed subsidence is 90% of the mining height in several European coalfields and especially in UK. This amount of subsidence only occurs with supercritical extractions (Whittaker et al., 1991).

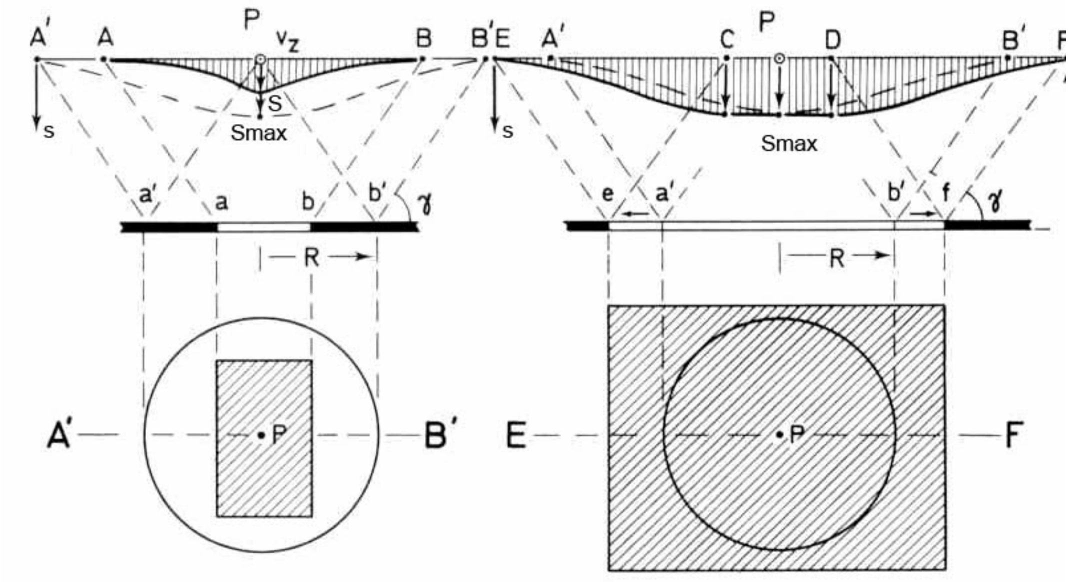

Figure 2-14 Subcritical (left) and supercritical (right) trough profiles and areas compared with critical trough (dashed line) and area (circular) (Kratzsh, 1983).

2.4.1.2. Multiple-Panel Mining

The likelihood of subsidence events increase because of the disturbance of the adjacent strata in a case of multiple worked-out mining horizons. Maximum slopes in a subsidence trough generally range between 0.002 to 0.02, but may reach 0.15 for multiple seam extraction (Singh, 1992).

2.4.1.3. Mining Depth

Instability caused by mining reaches the surface through the overburden, and the depth affects the velocity and period of the surface movements. When mining depth is smaller than 50 m, surface movements last for 2-3 months only, if it is between 500 to 600 m, surface movements may last for 2-3 years.

The total amount of subsidence does not appear to be changed; that is, subsidence amount is independent of depth (Orchard, 1964 in Singh, 1992).

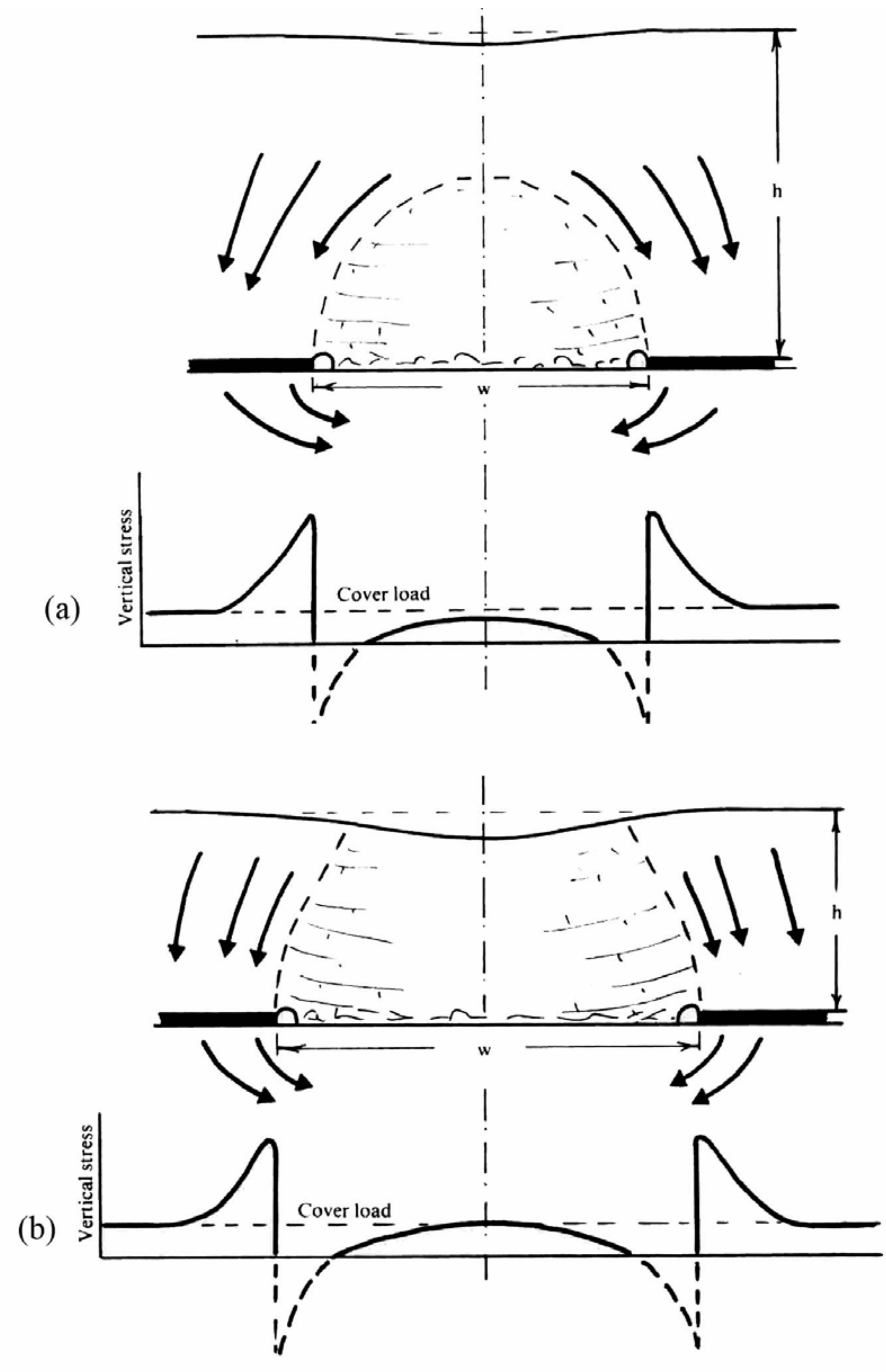

Figure 2-15 Pressure arch formation in relation to sub-critical (a) and super-critical (b) extractions (Whittaker and Reddish, 1989).

2.4.1.4. Mining Method

Comparison of mining methods is presented in Table 2-3.

- ***Permanent Pillars.*** Pillars are used as permanent and natural support, but they may be deformed later by the overlying weight. Long-term deformation (time factor in relation to failure and flow criteria) behavior should be taken into consideration. As a result of room and pillar mining two common forms of subsidence may arise:
  - sink-hole type subsidence resulting from collapsed mine junctions
  - widely saucer-shaped depression if pillar failure occurs (Whittaker and Reddish, 1989).

  Movement depends on the:
  - pillar size
  - percentage of recovery
  - whether or not the gob is backfilled (Peng, 1992).

- ***Filling (stowing).*** The disturbed rock mass caused by longwall mining comes to rest again within 1 to 3 years of mining, leaving a flat shaped subsidence trough (Kratzsch, 1983).

- ***Caving.*** Roof layer breaks off and fills the excavation as a heap rubble which provides a yielding underlay (self-stowing medium) for the main mass of overlying rock. This method causes most severe movement, and the fractured zone heights are largest. Subsidence is about 70% to 95% of the excavation thickness since immediate layers increase in bulk as they break up. The first segment of the roof collapses when the excavation length reaches 10 - 50 m (Kratzsch, 1983). It is an advantage of this method that the overburden movement and damage will be completed and the gob will be compacted and restabilized in a limited time period. So in the future there will not be subsequent major movements.

Table 2-3 Mining Methods.

Manner of working	Treatment of roof		
	With permanent pillars (partial extraction)	With filling	With caving (total extraction)
In long fronts		Longwall mining	Longwall caving
		Rill stoping	
		Overhand stoping	
		Underhand stoping	
In chambers	Chamber working		Chamber working with caving
	Room or stall workings	Room and temporary pillar	Room and pillar with caving
	Pillared open stopes		Open-stope caving
		Sublevel stoping	Sublevel caving
In Blocks			Block caving
In single faces		Bench stoping	
		Overhand shrinkage stoping	
		Cross-cut stoping	Cross-cut stoping with caving

2.4.1.5. Inclined seam mining

According to the examination in the north Staffordshire coal fields of U.K., the maximum subsidence point is located by intersecting the normal of the center of the longwall extraction with the surface.

Seam gradient not only shifts the individual subsidence trough to the dip side but also causes asymmetry of the trough. The boundaries of the trough are defined by two different influence angles for the rise and dip (see App. E). On the longitudinal cross-section, the trough is symmetrical to the vertical with the influence angle being the same for a level seam extraction (Lin et al., 1992). seam A seam dip angle based mining subsidence model is introduced by Huayang et al. (2002).

2.4.2. GEOLOGICAL FACTORS

2.4.2.1. Bedrock Conditions

Major fissures encourage the concentration of tensile strain and are opened up causing localized erosion of surface soils. The nature of bedrock influences the scale of the problem. Fissuring is generally occurred in the region over the rib side, i.e. in the tensile zone (Whittaker et al., 1991).

2.4.2.2. Roof Property and Stratigraphic Sequence

Strength and type of cover rock conditions greatly influence the magnitude and limits of subsidence (Whittaker and Reddish, 1989). Height of overburden movement is affected by rock properties and stratigraphic sequence. Hard and brittle strata are more likely to produce cracks and fractures than the soft and plastic strata.

Fractures in the soft and plastic strata will close up with time, thereby slightly reducing the fractured zone height. In the hard/strong and medium hard/strong strata, the fractured zone height ones formed does not show any conspicuous changes with time (Peng, 1992).

Overburden movements having different stratigraphic sequences are compared in Table 2-4.

2.4.2.3. Hydrogeological effects

Localized drainage giving rise to significant lowering of the water table can result in appreciable subsidence. Drainage gradients, patterns and groundwater flow may change because of opening or closing of bedrock fissures. Localized erosion features can occur at the surface above such bedrock fissures.

Shearer (1998) introduced the Interbed Drainage Package, which has been developed for the MODFLOW model, allowing the calculation of land subsidence due to the extraction of groundwater.

2.4.2.4. Tectonic conditions

Geological faulting can give rise to anomalous subsidence profiles. Faults tend to cause appreciable concentration of subsidence strain at the surface. They can also exhibit time-dependent behavior which tends to be aggravated by mining subsidence.

2.4.2.5. Surface topograpy

Tensile strains become more marked on hilltops and decrease in valleys (Singh, 1992). Significant fissuring can occur at the steep hillsides and substantial fissuring can introduce slope stability problems (Whittaker et al., 1991).

Table 2-4 Subsidence mechanisms for different types of overburden (Peng, 1992).

Hard/Strong	Soft/Weak	Soft/Weak (lower) Hard/Strong (upper)	Hard/Strong (lower) Soft/Weak (upper)
• caving in blocks • small and slow convergance • Once broken the fractures cannot fully close back up again and cannot recover to the impermeable conditons • Fractured zone height: 20-30 times the mining height	• immediate roof caves completely right after support advance • rapid development of subsidence. • caved and frctured zones cannot fully develop, fractures can easily be closed again, restoring its impermeable conditions • Fractured zone height: 9-11 times the mining height • sometimes upward development of the fractured zone is restricted by the weathered portions of the bedrock.	• immediate roof caves right after undermining • hard/ strong strata either subside very slowly or overhang with little convergance	• After caving of the lower portion of the overburden, the soft and weak strata immedately bend and subside thereby restricting the upward development of the fractured zone.

2.4.3. TIME FACTOR

Subsidence has active and residual phases. Active phase refers to the movements occurring simultaneously with the mining operations. Residual subsidence is the part of the surface deformation that occurs following the cessation of mining (or in case of longwall mining, after an underground excavation has reached its critical width). The magnitude of residual subsidence appears to be of the general order of 5-10 % of the maximum subsidence. Duration of the residual subsidence is of particular importance from the standpoint of structural damage at the surface. Subsidence as a function of time is shown in Figure 2-16

Longwall mining with caving induces subsidence rapidly. However, using pillars may give rise to surface instability many years afterwards. The long-term stability of mine pillars is extremely difficult to determine (Singh, 1992).

There are three elements acting collectively to produce subsidence (Whittaker and Reddish, 1989):

- Closure due to elastic (time-independent) deformation
- Closure due to inelastic (time-dependent) deformation
- Closure under gravitational force of the overlying rocks

Subsidence at a time is (Jeremic, 1985):

$$\frac{s_t}{s} = 1 - e^{-ct} \qquad [\ 2\text{-}12\ ]$$

where:

s_t = subsidence at time of observation;

s = maximum subsidence;

t = time of observation of subsidence in progress;

c = coefficient of velocity of strata displacement (dependent on the lithological units and geological structural conditions).

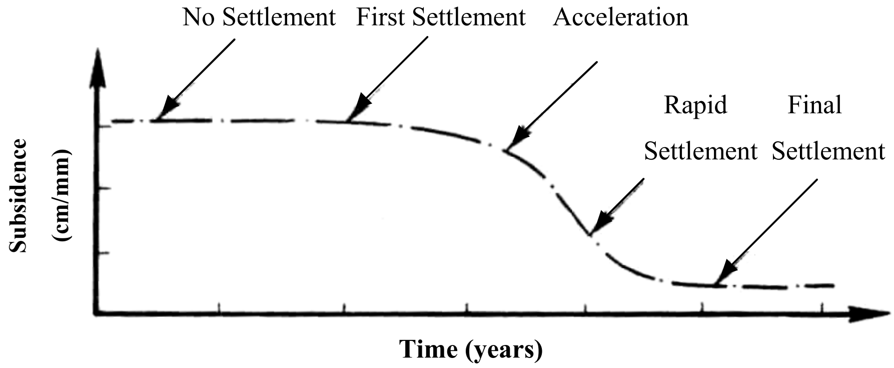

Figure 2-16 Time dependent subsidence (Jeremic, 1985).

Various time functions for subsidence prediction are presented in Appendix E.

2.5. PREDICTION OF GROUND MOVEMENT

2.5.1. EMPIRICAL AND SEMI-EMPIRICAL METHODS

Empirical methods are based on a combination of experience and the detailed analysis of a large number of observed ground movements to predict future subsidence effects. These type of methods are a good choice to predict subsidence in the regions where initial data were taken, but their geographic extension is usually restricted (Peng, 1992).

The material properties of the overburden rocks and simplifying assumptions to simulate complex field problems cause difficulty while using this method (Aston et al., 1987).

2.5.1.1. Graphical Method

This method is derived from the analysis of an extensive field analysis of an extensive field database collected over many years from a variety of mining conditions. So, they rely on compilation and a summary of case histories in graphical form. The best known example is developed by NCB, where subsidence values have been related graphically to variable parameters, e.g. depth, tilt, thickness, surface topography and seam geometry, etc. (Bahaguna et al., 1991). The data were summarized in the form of a series of non-dimensional graphs, where the subsidence is related to the ratio of the longwall face width to the depth of working and subsidence parameters (vertical displacement and horizontal strains) are calculated from this ratio (Aston et al., 1987).

2.5.1.2. Profile Function Method

This method is based on a curve fitting procedure that employs a mathematical profile function to match the predicted profiles with observed profiles. The use is simple and little input data needed. Profile functions are easy to calibrate with field data. However, they can only be applied to simple two-dimensional problems of rectangular exctraction (Bahaguna et al., 1991). This technique has been applied successfully in Poland, Hungary and Russia (Hood et al., 1983).

$S(x) = S\ f(B, x, c)$ (Aston, 1987) [2-13]

where:
B = control parameter for the range of function
x = horizontal distance from panel centre
c = a constant

The functions may be in hyperbolic, exponential or trigonometrical form.

- **Donetz Trigonometrical Function** (The Russian Profile-curve Method) makes use of a formula derived from an empirically obtained ratio between subcritical and critical extraction areas A_{sub} and A_{crit}. The equation gives fairly close agreement with measured subsidence values in Donetz and some other European coalfields (Figure 2-17).

$$s = S\left[1 - \frac{x}{L} + \frac{1}{2\pi}\sin\left(2\pi\frac{x}{L}\right)\right] \qquad [\ 2\text{-}14\ ]$$

$$S = aM\cos\alpha\sqrt{n_1 n_2} \qquad [\ 2\text{-}15\ ]$$

In Equation 2-15 convergence *aM* normal to the stratification is projected to the vertical).

$$n_1 = 0.9\frac{I_s}{H_m} \quad n_2 = 0.9\frac{I_d}{H_m} \qquad [\ 2\text{-}16\ ]$$

$$\frac{S}{S_{\max}} = \sqrt{\frac{A_{sub}}{A_{crit}}} \qquad [\ 2\text{-}17\ ]$$

where:

x	= distance of calculation point from the centre of the subsidence trough (m)
L	= distance of trough margin from the centre of the subsidence trough (m)
α	= dip of seam
S_{max}	= maximum possible subsidence occuring at critical width (m)
S	= maximum subsidence (m)
s	= subsidence at any point P along the profile (m)
A_{sub}, A_{crit}	= subcritical and critical areas of extraction (m^2)
n_1, n_2	= constants for the particular mine geometry

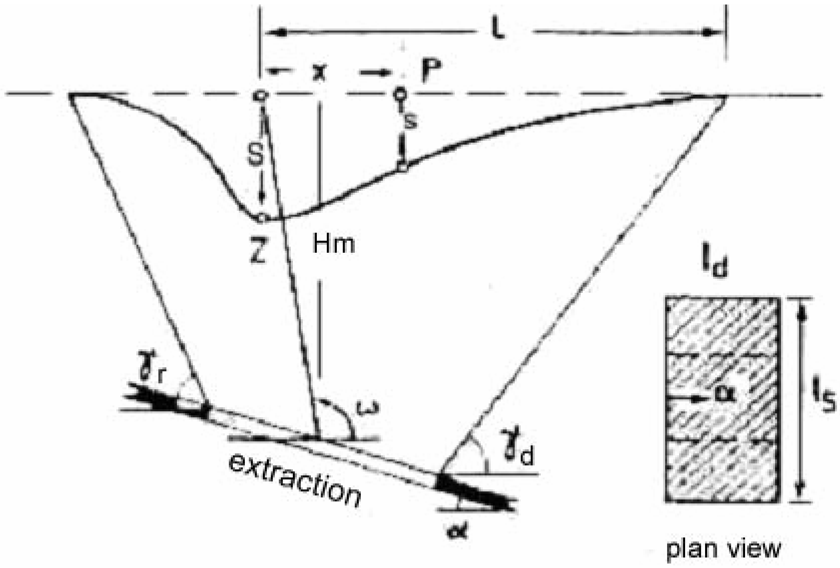

Figure 2-17 Trough profile of Donetz function (Kratzsch, 1983).

- **Polish Profile Function** is developed on the basis of data in upper Silesian coalfields.

$$s = S_{\max} \exp(-nx^2) \qquad [\ 2\text{-}18\ ]$$

where:

$$n = \frac{S_{\max}}{R^2 \bar{c}} \qquad [\ 2\text{-}19\ ]$$

$\bar{c}$ = the average roof-bed settlement

R = radius of critical area

- **Hungarian Profile Function** produces a relatively flatter and wider subsidence trough because the observations in the Hungarian field indicate the transition point to be not over the face edge but over the margin zone of the stowed goaf (Figure 2-18).

$$s = S \exp\left(\frac{-x^2}{2l^2}\right) \qquad [\ 2\text{-}20\ ]$$

where:

$$S = S_{\max} \frac{W}{2R} \qquad [\ 2\text{-}21\ ]$$

l = distance of the transition point from the center of the panel

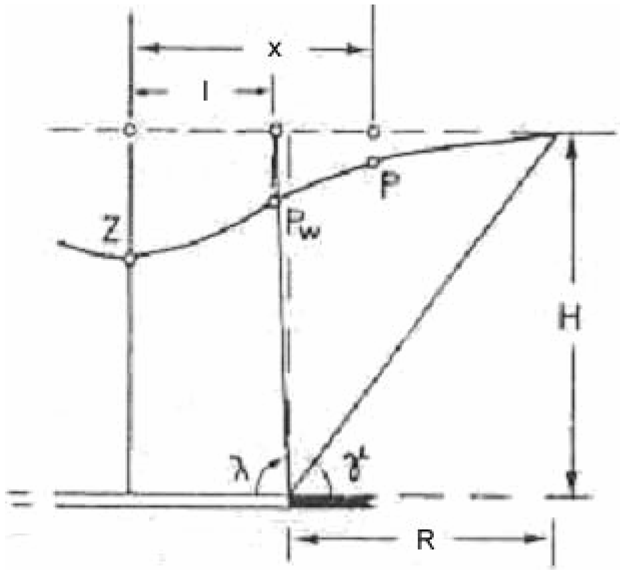

Figure 2-18 Hungarian and Polish profile function (Kratzsch, 1983).

- **Niederhofer's Profile Function (The Programmed Profile-Curve Method)** is useful for inclined seams and complex geometry with the help of computers.

$$s = S\left[1 - \left(\frac{x}{p}\right)^2\right]^2 \qquad [\ 2\text{-}22\ ]$$

where p is half width of subsidence profile.

- **Indian Profile Function** is developed for Indian coal mines. Estimated subsidence trough is broader than the observed one.

  For subcritical widths:

$$s = Se^{-\left[\frac{nx^2}{p^2 - x^2}\right]} \qquad [\ 2\text{-}23\ ]$$

  For critical widths:

$$s = Se^{-\left[\frac{nx^4}{p^4 - x^4}\right]} \qquad [\ 2\text{-}24\ ]$$

  where n is given by the Equation 2-19 and p is the half width of the subsidence profile.

- **Hyperbolic Function** gives fairly satisfactory results in British coalfields

$$s = \frac{S}{2}\left[1 - \tan h\left(\frac{2x}{R}\right)\right] \qquad [\ 2\text{-}25\ ]$$

- **Trigonometrical Profile Function** is valid only for European coalfields

$$s = S\sin^2\left[\frac{\pi}{4}\left(\frac{x}{R} - 1\right)\right] \qquad [\ 2\text{-}26\ ]$$

2.5.1.3. Influence Function Method

The principle of the influence function is based on extraction of a finite element Q which results in an individual subsidence trough. The trough is generally symmetrical to the vertical line passing through the trough center P as shown in Figure 2-19 and this approach is defined in Equation 2-27 (Lin et al., 1992 a).

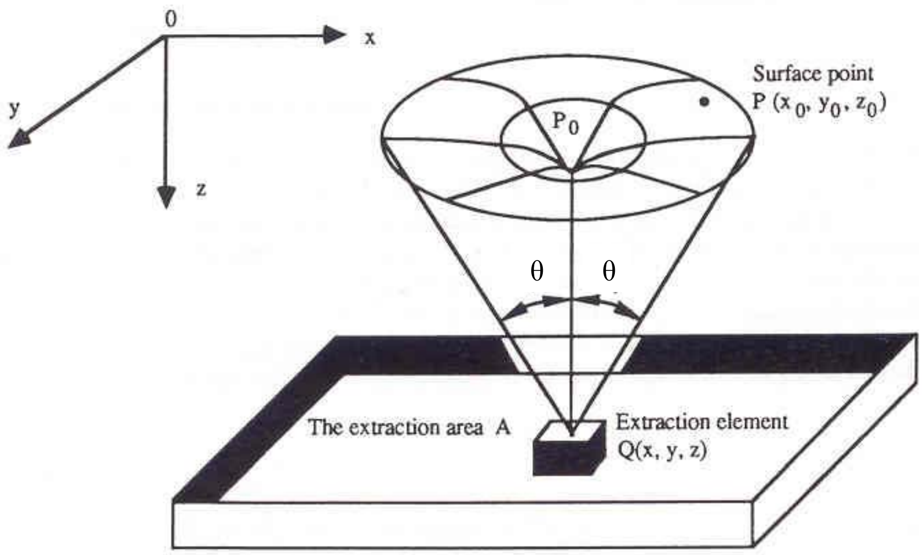

Figure 2-19 Extraction element based subsidence influence function (Lin et al., 1992 a).

$$S = \iint_A f(x_0, y_0, z_0, x, y, z)dxdy \qquad [\ 2\text{-}27\ ]$$

where $f(x_0, y_0, z_0, x, y, z)$ is the influence density.

Total subsidence at a point P is due to the sum of the influence of each element extracted (Figure 2-20). The amount of relative subsidence at point P is

$$S(i) = S / S_{\max} = \int_A \int k_z dA \qquad [\ 2\text{-}28\ ]$$

and this value is called as influence factor or weighting factor (Ren et al., 1987).

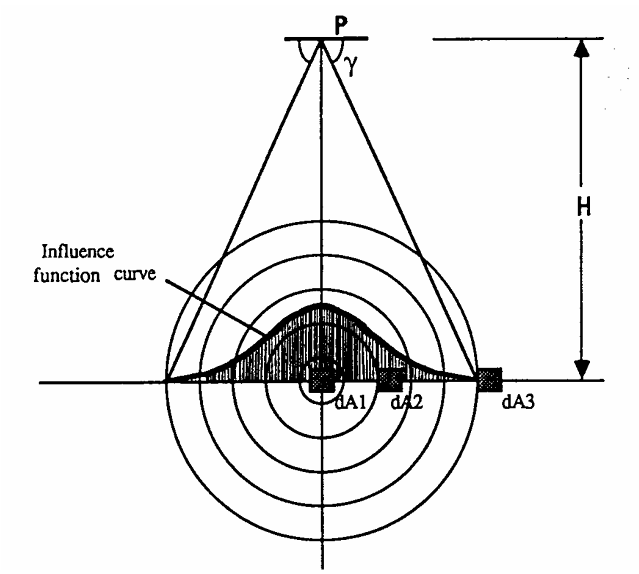

Figure 2-20 Surface point based influence function (Ren et al.,1987).

Some influence functions (k_z) are listed below.

- **Knothe's Method (Probability/Stochastic Influence Function Method)** based on a Gaussian distribution probabilities

$$k_z = \frac{1}{R^2}\left[e^{-\left(\frac{\pi x^2}{R^2}\right)} \right] \qquad [\ 2\text{-}29\ ]$$

Normal subsidence profile (in polar form):

$$s = S\left[e^{\left(-\frac{\pi r_2^2}{R^2}\right)} - e^{\left(-\frac{\pi r_1^2}{R^2}\right)} \right] \qquad [\ 2\text{-}30\ ]$$

- **Keinhorst's Method** makes use of a formula which gives a simplified subsidence profile. The profile function is:

$$k_z = \frac{2}{3\pi} \frac{\tan^2 \alpha}{(\tan^2 \alpha - \tan^2 \theta)} \frac{1}{R^2} \qquad [\ 2\text{-}31\ ]$$

where

θ = angle of influence of the outer zone (angle of draw)

α = angle of break of the inner zone

R = H cot θ

- **Bals' Method** (Figure 2-21) Figure 2-21is based on Newtonian gravitatioanal law, where the influence on the surface is inversely proportional to the square of distance of the particular element.

$$k_z = \frac{C}{R^2 + h^2} d\alpha \qquad [\ 2\text{-}32\ ]$$

and in usable form:

$$k_z = \frac{C}{h^2} \frac{1}{4} (\sin^2 \alpha_m + 2\alpha_m) \qquad [\ 2\text{-}33\ ]$$

where:

C = constant

α_m = angle of influence measured to the vertical

- **Beyer's Method** (Figure 2-21)

$$k_z = \frac{3S}{\pi R^2} \left[1 - \left(\frac{r}{R} \right)^2 \right]^2 \qquad [\ 2\text{-}34\ ]$$

- **Sann's Method** (Figure 2-21) predicts a trough with a deeper central area

$$k_z = 2.256 \frac{1}{r} e^{-4r^2} \qquad [\ 2\text{-}35\ ]$$

- **Erhhardt and Sauer Method**

$$k_z = 0.1392 e^{-0.5 r^2} \qquad [\ 2\text{-}36\ ]$$

- **Litwiniszyn's Method** is based on probability considerations, and well supported by field and experimental observations, this method has also been varified with the theory of stochastic rock movements. This method has further been modified by Kochmanski.

$$k_z = \frac{nS}{R^2} \exp\left[-n\pi \left(\frac{r}{R} \right)^2 \right] \qquad [\ 2\text{-}37\ ]$$

where n is usually equal to 1

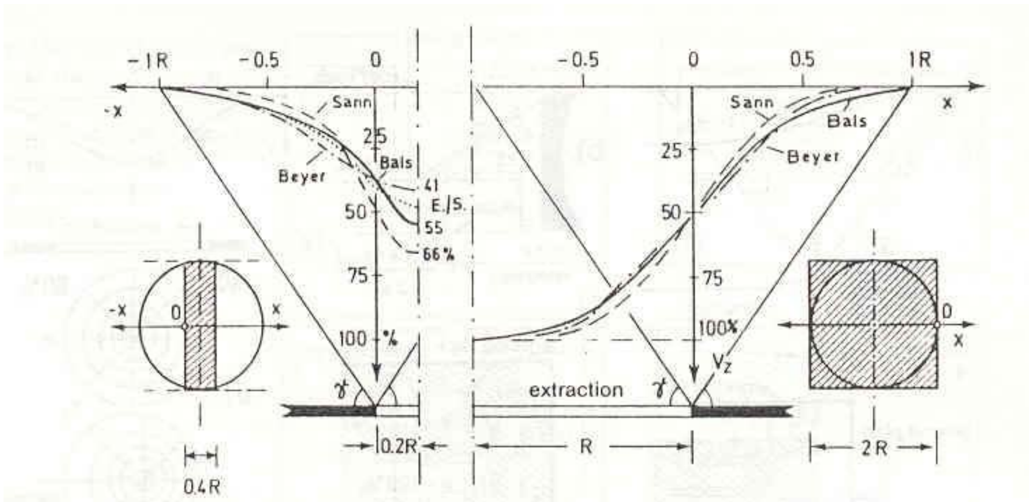

Figure 2-21 Comparison of influence function models for subcritical and critical widths (Kratzsch, 1983)

Merits of the influence function methods are:

- Applicable to complex mine geometry (profile function method can only be applied to regular openings)
- Can be mathematically validated
- Applicable to various types of mining situations
- Some factors other than mine geometry can be used in the form of complementary functions
- Time factor can be taken into consideration
- Functional methods have been further enhanced by incorporating suitable supplementary functions for different parameters

Demerits of the influence function methods are:

- More complicated then profile functions when an extensive area of irregular configuration is encountered
- overburden is assumed a homogeneous, isotropic., symetrical subsidence profiles about the trough centre predicted → not always the case*
- The inflection point is located just above the ribside → not always the case*

*can be overcomed by modifications

Use of complementary influence functions eliminates computational difficulties experienced with the conventional influence functions (Sutherland and Munson, 1984).

2.5.1.4. Incremental Design

Future conditions are predicted from changes in current operations. This process requires an existing database and derivation of equations.

2.5.1.5. Stochastic Models

The stochastic model describes behavior of a collection of discrete members or particles within a medium and may therefore be applied to soils and specialized events such as block caving (Aston et al., 1987).

2.5.2. ANALYTICAL TECHNIQUES

2.5.2.1. Closed Form Elastic Solution

It is assumed that the strata displacement behaves according to one of the constitutive equations of continuum mechanics. In this context, continuum theories evolved from the analysis of displacement discontinuity produced by a slit in an infinite half-space elastic media. It is developed for three types of underground excavation based on elastic ground conditions:

- Non-closure
- Partial closure
- Complete closure

Closed form solutions can be used for transversely isotropic ground conditions in two and three dimensions (Aston et al., 1987).

2.5.2.2. Numerical Methods

They are based on numerical approximations of the governing equations, i.e. the differential equations of equilibrium, the strain-displacement relation, the stress-strain equation and the strength-stress relationship. Finally, induced displacements and stresses are produced. They can be considered as the most rigorous and sophisticated subsidence prediction techniques (Garcia and Meres, 1997). The numerical methods used for subsidence analysis are presented as follows:

- **Finite Element Method (FEM)** can simulate non-homogeneous, non-linear material behavior and complicated mine geometries (Aston et al., 1987). Structural analysis of the overburden and gob is made by dividing and subdividing it into individual structural elements because of the stresses in the overburden body experience strains and get displaced. The amount of displacement of each element depends on the level of stress and material properties of each element. The effect of regular and large numbers of geological discontinuities such as joints faults bedding planes, etc., and different types of the rock layers in the overburden , can be taken in the account as the finite element mesh spread all over the body of the overburden. However, this makes the method more voluminous and time consuming. Although it is reported that highly non-linear problems are best handled by codes using an explicit solution technique, the FEM is not suitable for analyzing discontinuous deformation (Cui et al., 2000).

  Analytical or mechanistic methods based on computerized mathematical models using FEM had limited success.

- **Distinct Element Method (DEM)** represents a discontinuous system of a blocky rock mass. It is suitable for modeling a jointed rock mass where deformation mechanism is mainly block separation, rotation or slip, and there are large relative movements. So this method is suitable only for discontinuous deformation, such as caved zone and fractured zone (Cui et al., 2000).

- **Finite Difference Method (FDM)** can be used for large strain non-linear cases. Yielding and flow of materials and deformation of grid are permitted by Lagrangian calculation scheme. Alejano et al. (1999) used “FLAC” (Fast Lagrangian Analysis of Continua), based on FDM modeling technique, to predict subsidence trough due to flat and inclined seam mining.

- **Boundary Element Method (BEM).** The element mesh is not spread all over the body of the overburden but only at the boundary (on the ground surface). It is more suitable for cases where geological discontinuities are comparatively less (Bahaguna et al., 1991). Heasley and Barton (1999) presented several case studies in which a mechanics-based boundary element program (LAMODEL) is used to calculate both the underground convergence and the resulting surface subsidence. LAMODEL calculates the displacements and stresses for user defined pillar geometries in flat lying seams using a laminated overburden model (Aksoy et al., 2004)

Continuum methods (FEM, BEM, FDM, displacement discontinuity (DDM)) fail completely, even with elosto-plastic analysis performed using realistic rock mass strengths inputs, assuming that such inputs are possible for each bed. DEM will possibly the best, but again this will require rock characterization of each bed and this is usually not possible. Numerical modeling generally ignores the possibility of each bed having different horizontal in situ stresses (Sheorey et al., 2000).

2.5.2.3. Mechanistic Models

Void-volume Model. Actions of discrete deformational and collapse mechanisms are primary modes of influencing subsidence development. Actual collapse mechanisms must be known and physical models constructed. Effect of scaling factors raise questions, since different types of material behavior are involved in the collapse mechanism.

2.5.2.4. State-of-art:

- A hyperbolic tangent profile was shown by Hood et al. (1983) to serve as an accurate predictive tool for subsidence behavior in two adjacent longwall panels in Illinois. Also surface curvatures could be predicted above the panels using that function.

- Based on fuzzy probability measure, the theories for both the two- and three-dimensional problems are developed and applied to ground movement analysis by Wenxiu (1991).

- Cui et al.(2001), Kwinta (1996), Jarotz et al. (1990) used and reviewed time function analysis for the prediction of rock mass subsidence See App. E for details).

- Yong and Sung (2005) introduced subsidence estimation and prediction using artificial neural network because of the complexity of subsidence mechanism. ANN is an appropriate tool for this kind of problems. They developed ANN program using Visual Basic and constructed ANN model using the results of numerical analyses.

CHAPTER 3

INFORMATION ABOUT ÇAYIRHAN MINE SITE

3.1. GENERAL INFORMATION

Çayırhan Lignite Mine is located in the western part of Ankara province (125 km from Ankara), between the townships Beypazarı and Nallıhan (30 km from Beypazarı).

The method of mining is fully mechanized, retreating, back caving, longwall mining. This is the first fully mechanized longwall coal mine in Turkey.

The coal reserve of the mine is about 415 million tones. There are two workable coal seams in Çayırhan region.

3.2. GEOLOGY

Çayırhan lignite basin is formed by old miocene series, named as M1, M2, M3, and M4 from bottom to top and Pliocene formation (composed of sandstone and gypsum) over them (Figure 3-1).

Coal seams are located in M1 formation. There is a light brown colored limestone layer of 5-6 m over the coal seams and 7-8 m green colored clay-stone layer below the seams. Under clay-stone there is a 15-20 m thick layer of volcanic brecia. Also a third coal seam is found 140-160 m below the workable seams.

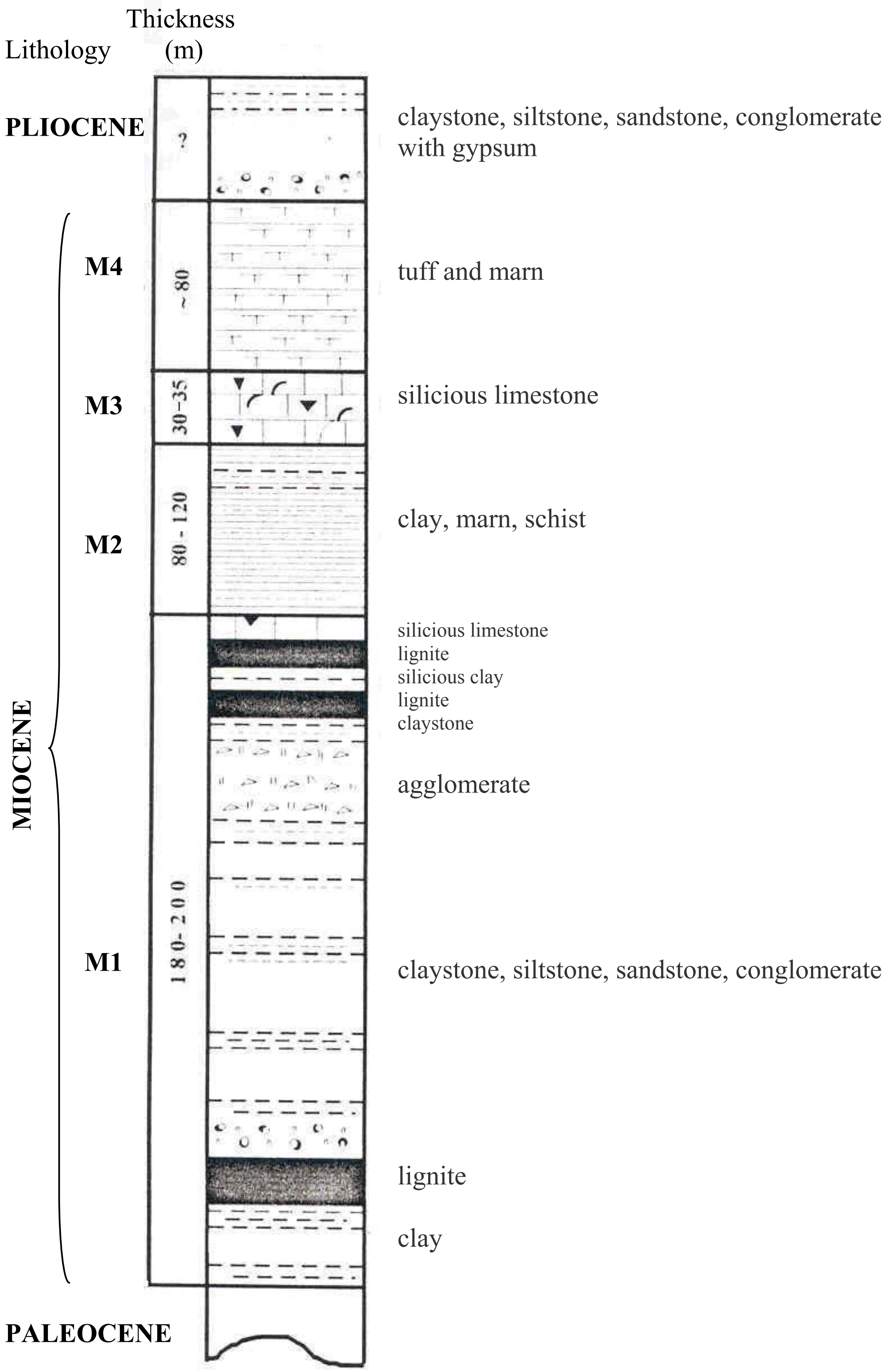

Figure 3-1 Generalized stratigraphic section (Dalgıç, 1996)

M2 formation consists of clay and marn at a thickness of 80-120 m. There are 2 bituminous schist layers of 20 m at the top and bottom.

M3 is the hardest formation composed of beige colored siliceous limestone and having a thickness about 30-35 m. This is the major aquifer zone in the field. Many cavities and fractures at the bottom levels are enabling collection of water.

Majority of the area is covered with M4 formation composed of grey, red, green and beige tuffs. Despite their hard structure, they are going to break into parts when subjected to water. Therefore, 15-20 cm of clastic portions cover the surface. The thickness of this formation is about 80 meters and consists of silica of 5-10 cm at the bottom layers.

The two main normal faults, Davutoğlan fault and North fault, in north-west and south-east direction are almost parallel and about 1.5-2 km apart from each other.

3.3. PRODUCTION

Mining Sectors B and C are located between the Davutoğlan and North faults, and Sector D is located at the eastern part. Sectors A and F are located at the southern part of the Davutoğlan fault. Layout of the sectors are displayed in Figure 3-2.

The layout of the panels in Sector B and Sector C above which subsidence measurements were carried out are shown in Figure 3-3 and Figure 3-4. Panels working at the same time are colored same.

In Sector B, thickness of the upper coal seam is about 1.70 m and the lower one is about 1.80 m. The interburden thickness is changing between 1.20-150 m. In this sector two seams are mined simultaneously with the upper face leading the lower face by about 20-35 m. Excavation thicknesses are 1.80 m and 1.90 m for the upper and lower seams respectively.

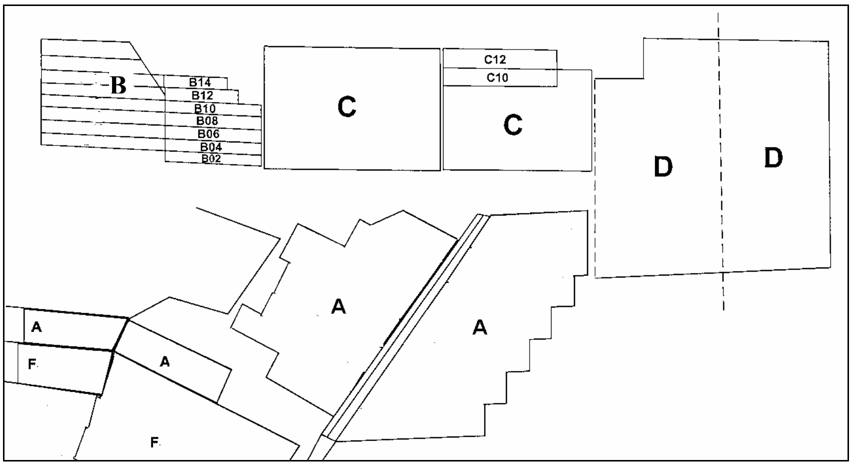

Figure 3-2 Layout of the sectors in Çayırhan Coal Mine

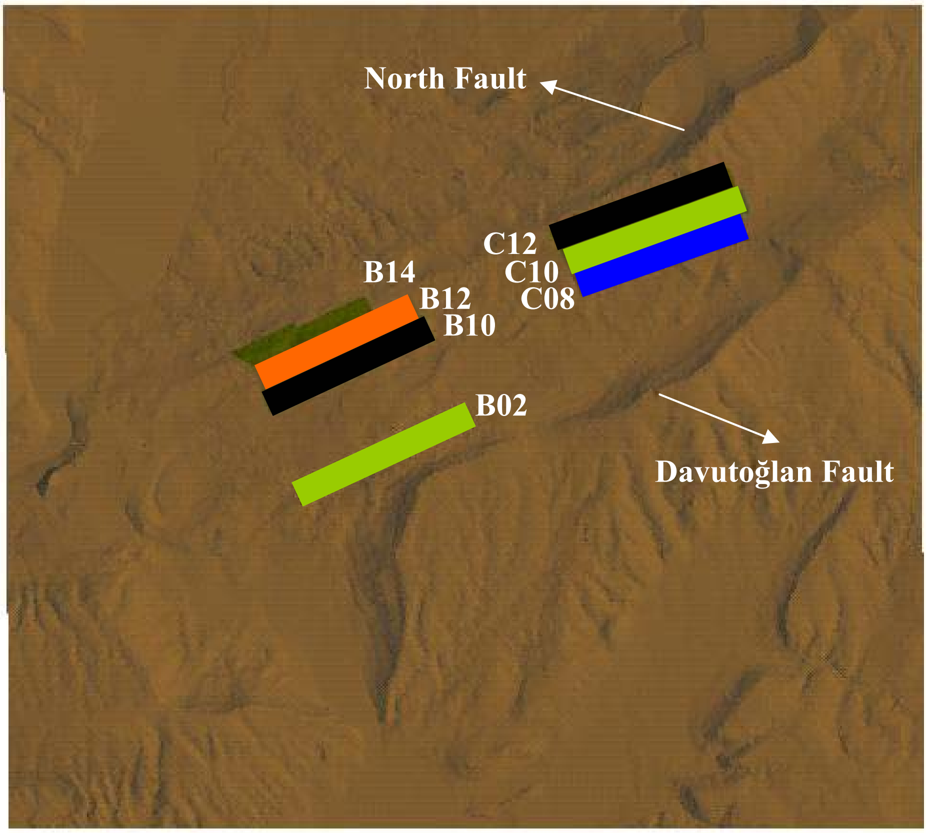

Figure 3-3 Topography and the layout of the panels above which subsidence measurements were carried out (top view).

In Sector C, thickness of the upper coal seam is about 1.75 m and the lower one is about 1.80 m. The interburden thickness is about 70 cm. The panel length and width of the Sector C are 1700 and 220 meters respectively and it is divided into 13 panels.

Because of the thin interburden layer, production is performed through one fully mechanized longwall face, in Sector C. Galleries have approximately 25 m^2 cross-sectional area. Yearly production is about 3,120,000 tons in this sector.

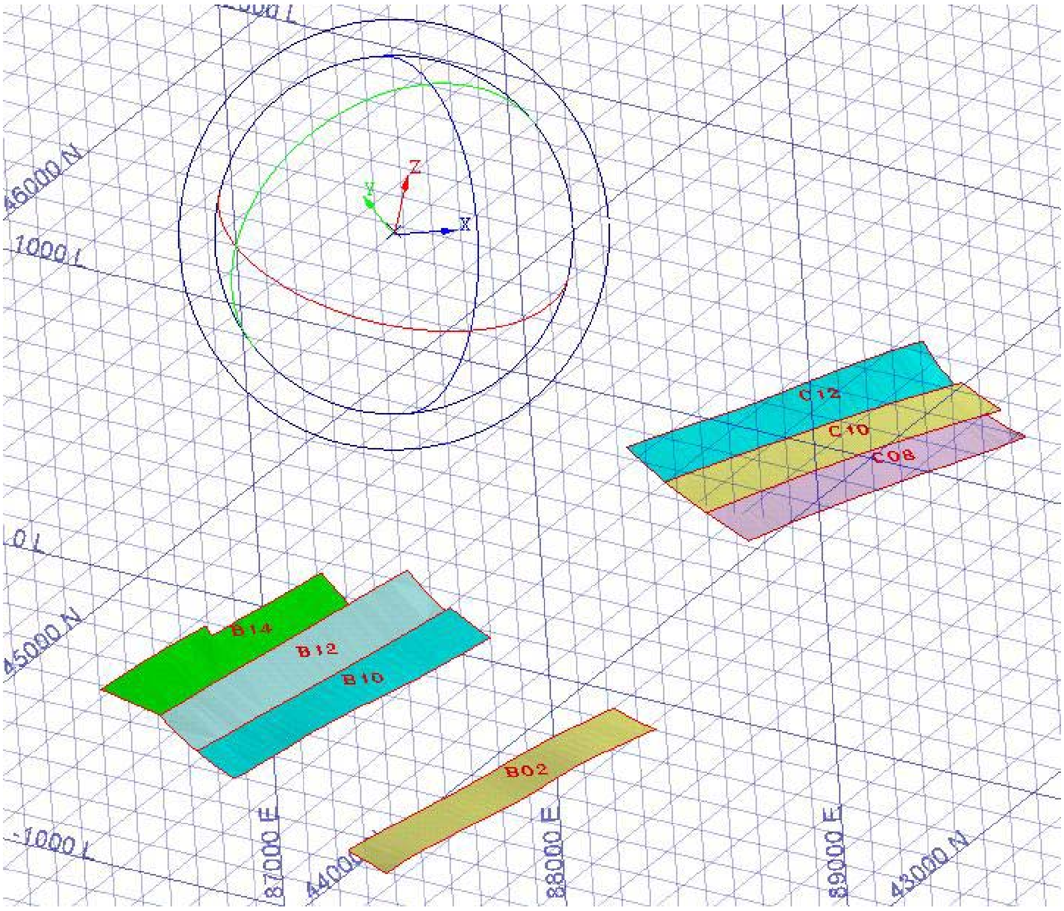

Figure 3-4 Virtual sphere rotation of the panels using Vulcan software.

CHAPTER 4

SUBSIDENCE MEASUREMENTS ABOVE LONGWALL PANELS

4.1. SUBSIDENCE MEASUREMENTS

Knowledge of subsidence engineering is of considerable importance to the planning and development of the surface in the subsided regions.

The subsidence investigations have been initiated in order to find solution to the damage of pylons above panel B14 due to subsidence occurred as a result of retreating longwall faces. Surface subsidence measurements above B14 panel began in June 1997, and continued until November 1997. Surface measurement stations were established along two main survey lines, one parallel to the centerline of the longwall panel (longitudinal direction) and the other across the extraction width (transverse direction).

Figure 4-1 shows the layout of the survey lines and the location of vertical and horizontal cracks above B14 panel. Distance between the stations along the survey lines BB', CC' and AD was about 30 m. Number of stations along CC' were increased later. 37 measuring stations were located at 10 meters intervals along EE'. Measurements at the stations were taken in three mutually perpendicular directions. The results of measurements were evaluated in terms of subsidence, slope, displacement and horizontal strain.

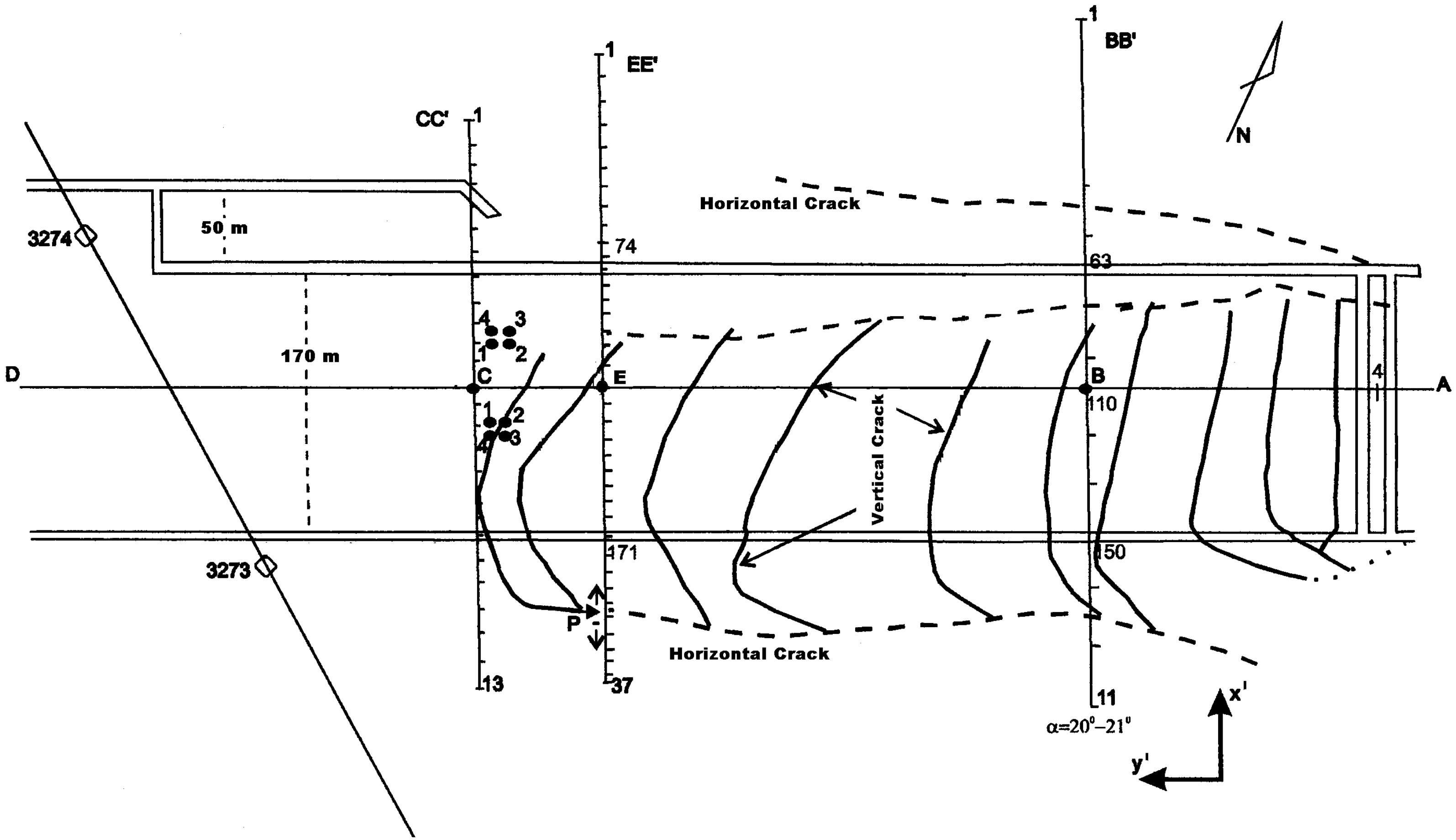

Figure 4-1 Measurement stations, longitudinal/transverse lines along the stations and the surface cracks above panel B14 (Unal et al., 1998).

During the second stage of measurements, carried out between December 1998 and June 2003, the surface movements occurring above panels B12, B10, B02 and C12, C10, C08 were measured. The steps related with the measurements (carrying out measurements, evaluation of measurements and interpretation of the results) will be explained in detail in Chapter 5. Table 4-1 and Table 4-2 present number of survey stations along longitudinal (A) and transverse (B, C, D, E) lines, above the panels stated above. An example of raw data obtained from measurement stations is given in Table 4-3. Position of measurement stations are displayed in the figures in Chapter 5.

Table 4-1 Number of surface stations along survey lines over Sector B.

B12				B10			B02				
A	B	C	D	A	B	C	A	B	C	D	E
ABCD + 44	B + 17	C + 20	D + 20	ABC + 32	B + 15	C + 10	ABCDE + 32	B + 9	C + 9	D + 8	E + 7

Table 4-2 Number of surface stations along survey lines over Sector C.

C08				C10					C12			
A	B	C	D	A	8	B	C	D	A	B	C	D
ABC + 20	B + 10	C + 8	D + 8	ABCD + 42	"8" + 8	B + 10	C + 8	D + 10	ABCD + 35	B + 13	C + 13	D + 11

Table 4-3 Example raw data for B line of panel B02.

Meas. Date	**08.08.2001**			**22.08.2001**			**27.08.2001**		
	X	**Y**	**Z**	**X**	**Y**	**Z**	**X**	**Y**	**Z**
1	87527.692	42962.416	763.144	87527.627	42962.452	763.212	87527.663	42962.427	763.172
2	87539.571	42936.864	767.466	87539.522	42936.905	767.501	87539.578	42936.885	767.503
3	87556.329	42900.802	771.264	87556.227	42900.828	771.229	87556.365	42900.790	771.254
4	87565.756	42880.440	773.302	87565.668	42880.494	773.321	87565.812	42880.456	773.295
5	87576.302	42857.813	775.076	87576.278	42857.848	775.105	87576.446	42857.848	774.995
B	87588.111	42832.340	777.530	87588.149	42832.357	777.540	87588.305	42832.416	777.261
6	87602.019	42802.517	783.668	87601.988	42802.565	783.655	87602.207	42802.747	783.391
7	87621.166	42761.295	795.617	87621.059	42761.380	795.626	87621.240	42761.422	795.534
8	87643.533	42713.285	803.816	87643.434	42713.368	803.799	87643.509	42713.328	803.778
9	87654.047	42690.757	801.880	87653.992	42690.795	801.858	87654.054	42690.776	801.888

Table 4-3 Number of surface stations over Sector C (cont.).

Meas. Date	01.09.2001			15.09.2001			01.10.2001		
	X	Y	Z	X	Y	Z	X	Y	Z
1	87527.646	42962.443	763.226	87527.767	42962.310	763.137	87527.644	42962.293	763.240
2	87539.562	42936.901	767.552	87539.715	42936.637	767.371	87539.557	42936.505	767.410
3	87556.372	42900.808	771.232	87556.551	42900.373	770.373	87556.254	42899.968	770.132
4	87565.926	42880.440	773.054	87565.747	42879.837	771.083	87565.251	42879.579	770.602
5	87576.621	42857.909	774.607	87576.499	42857.639	772.300	87575.795	42857.391	771.900
B	87588.522	42832.501	776.779	87588.099	42832.238	774.683	87587.353	42832.005	774.240
6	87602.243	42802.969	782.824	87601.368	42803.019	780.575	87600.551	42802.998	780.267
7	87621.194	42761.730	795.342	87620.373	42762.787	794.376	87619.612	42762.551	794.020
8	87643.484	42713.394	803.780	87643.274	42713.605	803.578	87643.033	42713.776	803.551
9	87654.028	42690.814	801.878	87653.864	42690.897	801.759	87653.668	42691.068	801.769

4.2. EFFECTS OF GROUND MOVEMENT

Various effects of ground movement (such as cracks occurred parallel and perpendicular to panel advance direction) that had occurred at the surface in Çayırhan coal mine due to retreating longwall panels are shown in Figure 4-2, Figure 4-3, Figure 4-4, Figure 4-5, Figure 4-6, Figure 4-7.

Results of the investigations related with the damage to the power line pylons (3273 and 3274) as surface structures over the panel B14 are presented in Chapter 5. A sample pylon deformation is shown in Figure 4-8.

Figure 4-2 Vertical movement above Sector C.

Figure 4-3 Vertical sliding about 3.5 m inside the influence area of B10 panel.

Figure 4-4 Erosion above an old working area of Sector A.

Figure 4-5 Cracks seen at the surface above B14 panel.

Figure 4-6 Cracks along the hill side above B14 panel.

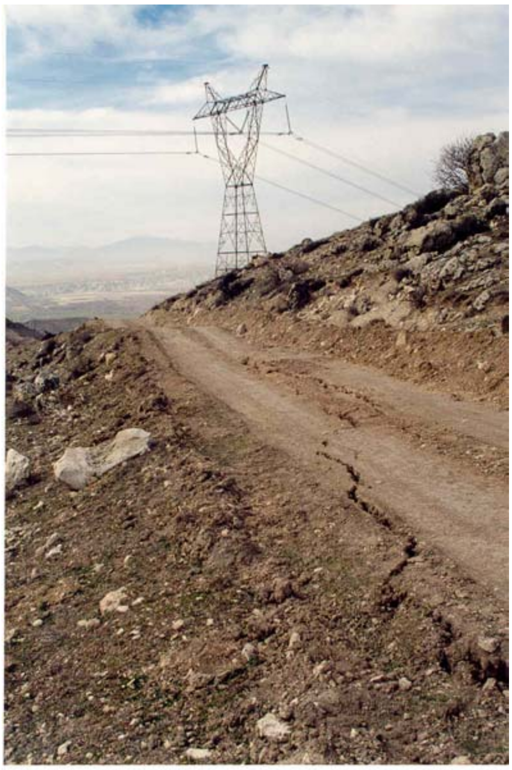

Figure 4-7 Cracks above B14 panel.

Figure 4-8 Pylon deformation above B14 panel.

4.3. INSTRUMENTATION

Surveying equipments (such as electronic-distance-meter (EDM), theodolite (Figure 4-9), leveling rod, reflector assembly) and the stations consisting of concreted iron rods are used for measurement of vertical and horizontal movements.

The surveying system selected for measurement and observation of vertical and horizontal movements of the survey stations is the conventional surveying system. This system is established to make periodic leveling of the subsiding points for the vertical displacements from some bench marks on the stable ground and triangulation from a base line for the horizontal displacement.

EDM is mounted on the top of the theodolite by an adopter before surveying work. Other instrument assemblies are a single prism set with coaxial target plate, a tripod, and a telescopic prism pole. Precision of EDM is 5 mm/km.

Coordinate values of the survey stations were determined by taking coordinates of the reference stations into consideration (Unver, 1993).

Figure 4-9 Measurement instrumentation.

CHAPTER 5

EVALUATION OF MEASUREMENTS

5.1. DATABASE PREPARATION

The steps of algorithm used in this study for preparation of database are presented in sections given below. There are a total of four steps and each step consists of information related to both surface and underground measurements.

Step 1: Determination of location of surface stations and position of longwall faces.

In this step 3D coordinates, namely X-Easting, Y-Northing and Z-Elevation, of the subsidence stations as well as position of the longwall faces and gate roads are measured. For this purpose:

i. Surface measurements are carried out at stations which are located parallel and perpendicular to panel axis.
ii. Underground measurements are carried out along head- and tail-gates, and the faces. Figure 5-1 shows the location of faces (of the panels B02, B10, B12, C08, C10 and C12 above which subsidence measurements are carried out) while advancing. Measurements to determine the face locations shown in this figure were taken monthly.

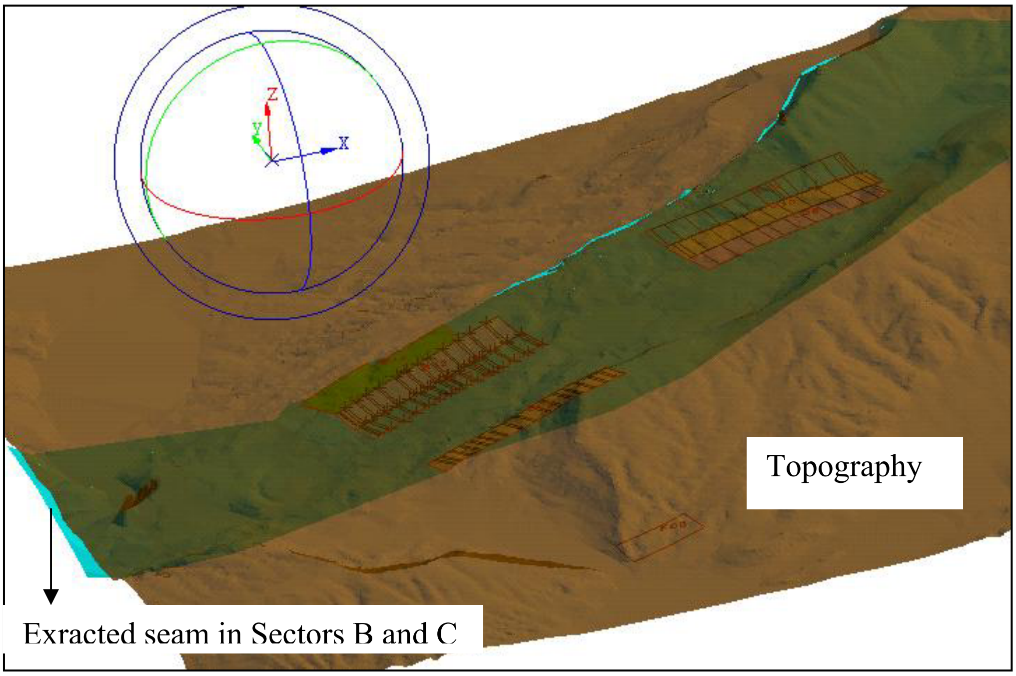

Figure 5-1 Face advance lines.

Step 2: Drawing best lines for surface and underground measuring points.

For this purpose:

i. Longitudinal and transverse lines passing through the surface stations are drawn according to the surface measurements. Figure 5-2 shows the surface measuring stations and related best lines. These lines are drawn and their equations are determined by adding trendline using the graphing utilities in Excel.

ii. Using underground measurements the location of the head- and tail-gates are drawn and center lines of the panels are determined by taking the average of head- and tail-gate lines. Figure 5-3 and Figure 5-4 show measuring points along head- and tail-gates, best lines passing through these points, and the centerline of the panels related with subsidence measurements in Sectors B and C, respectively. The equations of the gate roads and centerlines are also presented. Additionally, surface measurement stations above the panels can be seen in these figures.

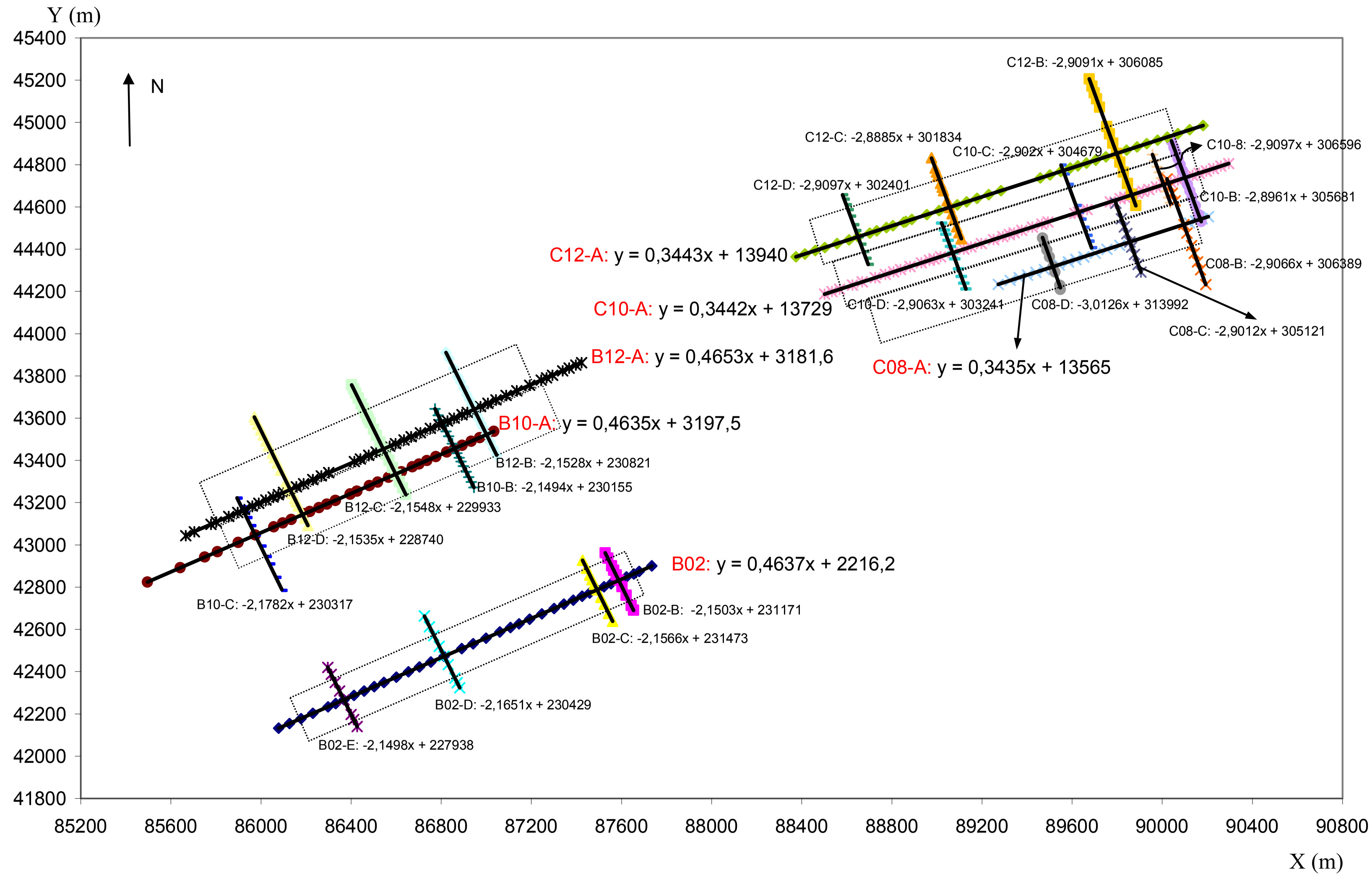

Figure 5-2 Best lines for the surface stations

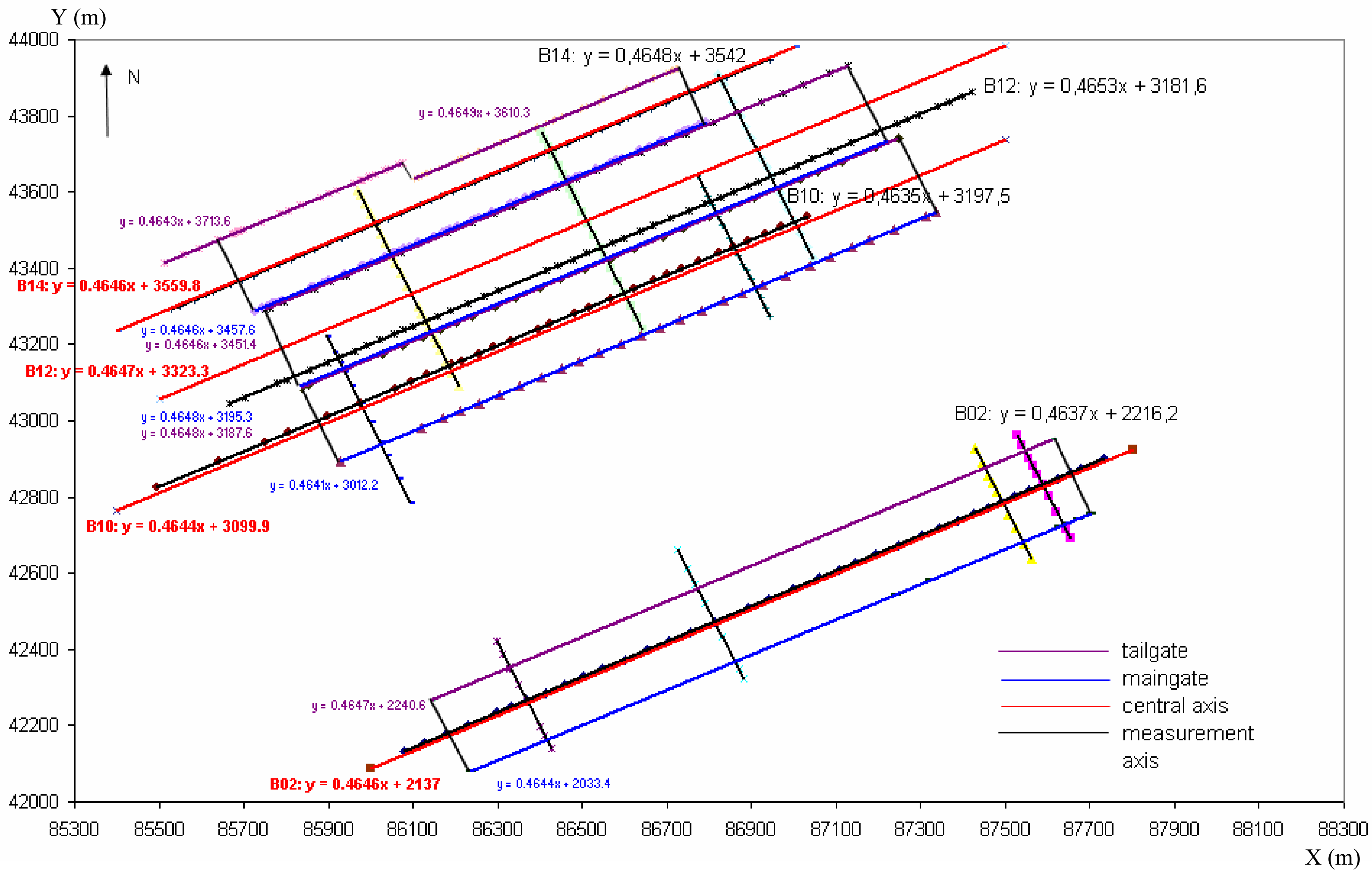

Figure 5-3 Outlines and centerlines of the panels in Sector B.

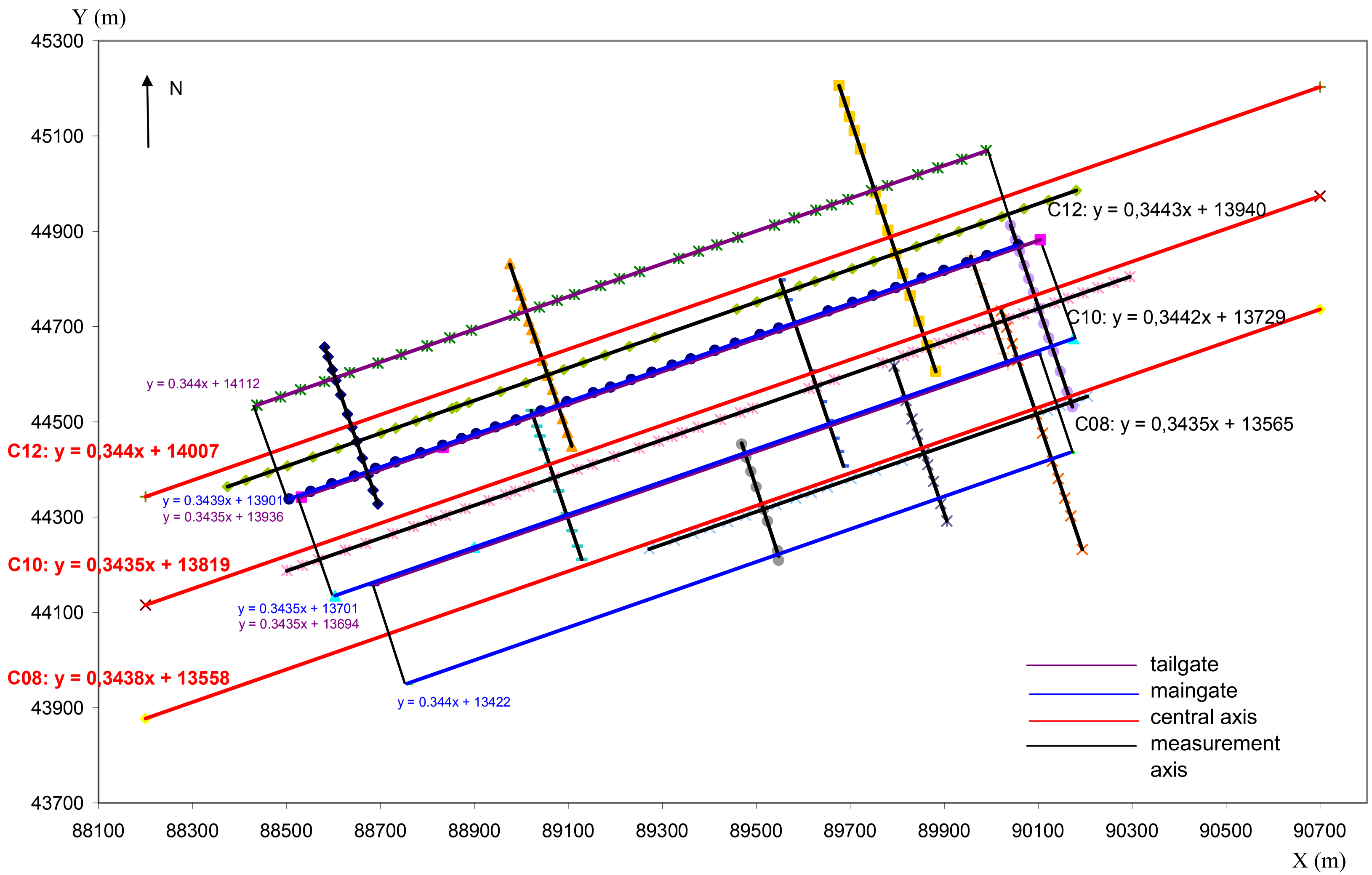

Figure 5-4 Outlines and centerlines of the panels in Sector C.

Step 3

After determination of face intersection points with panel centerline at surface measurement dates (3.1), transformations are carried out with respect to new coordinate system (3.2).

3.1 Determination of Face Intersection Points from Underground Measurements.

Intersection points of face advance lines with the panel centerline (coordinates of face center) are determined using VULCAN software. X coordinates of face centers of panel B02 at face advance measurement dates are presented in Table 5-1.

Table 5-1 Coordinates of the face centers of panel B02 at underground measurement dates.

Date	X_{front}	X_{back}
01.09.2001	87573.991	87596.509
01.10.2001	87485.988	87508.449
01.11.2001	87375.852	87398.057
01.12.2001	87274.857	87295.316
31.12.2001	87195.356	87215.816
01.02.2002	87092.493	87114.212
01.03.2002	87003.326	87025.066
01.04.2002	86877.177	86896.424
01.05.2002	86761.746	86782.426
01.06.2002	86640.540	86660.543
01.07.2002	86551.884	86570.521
01.08.2002	86479.560	86501.793
31.08.2002	86401.037	86421.642
01.10.2002	86319.484	86339.354
01.11.2002	86235.551	86254.284
24.11.2002	86187.414	86205.374

The steps related with underground measurements, namely: locating measuring points, drawing gate roads and face advance lines and determination of front-back face intersection points with panel centerline, are covered in Figure 5-5 for panel B02 (from May 2002 until the end of production).

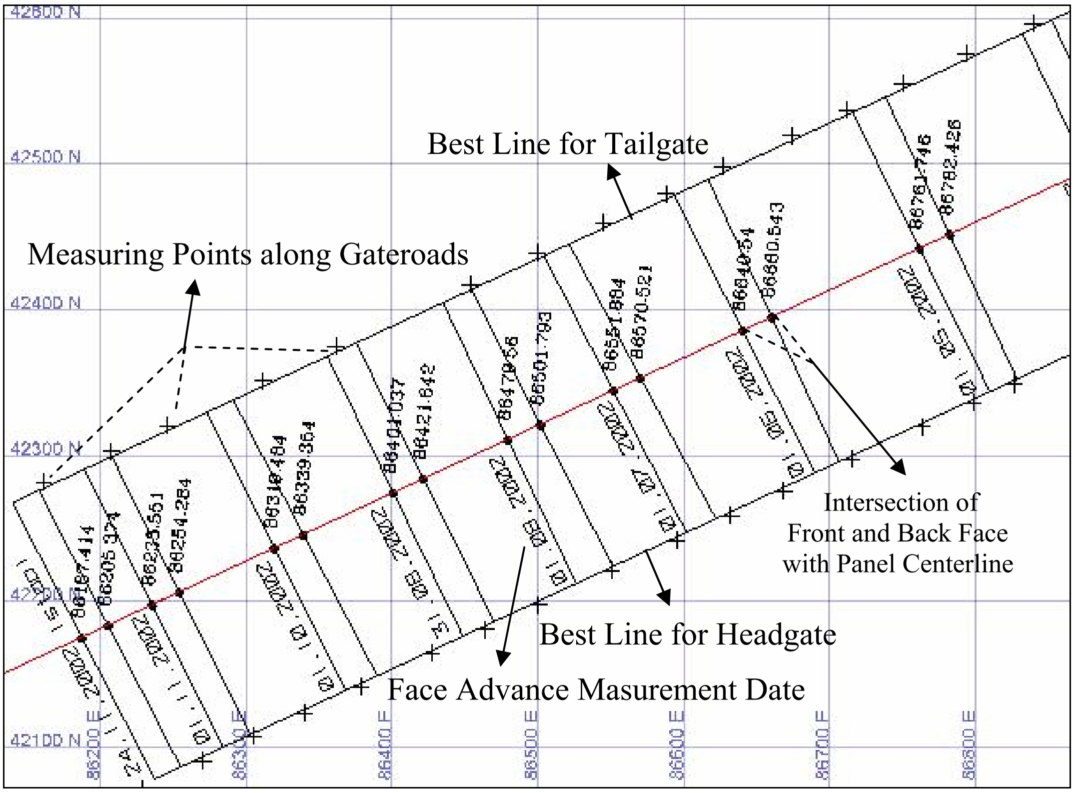

Figure 5-5 Steps related with underground measurements.

Coordinates of the intersection points at subsidence measurement dates are found by interpolation, to make it possible to calculate the distance between the face and the surface stations. Table 5-2 presents this interpolation process for B line of panel B02. First part of the table gives the coordinates of face centers found by underground measurements. The interpolated coordinates at surface measurement dates are presented in the second part of the table.

Table 5-2 Determination of coordinates of the face centers at surface measurement dates using interpolation, for B line of panel B02.

Underground Measurments			Calculated Locations by Interpolation		
Date	X_{front}	X_{back}	Date	X_{front}	X_{back}
04.08.2001	87655.113	87655.113	08.08.2001	87644.393	87647.369
			22.08.2001	87603.325	87617.701
			27.08.2001	87588.658	87607.105
01.09.2001	87573.991	87596.509	01.09.2001	87573.991	87596.509
			15.09.2001	87532.923	87555.414
01.10.2001	87485.988	87508.449	01.10.2001	87485.988	87508.449

3.2 Transformation of original locations (X and Y coordinates) into X' and Y' coordinates which show location of the measuring stations with respect to longitudinal and perpendicular axes of longwall panels.

For this purpose, the distances of the surface stations from face center are transformed as being parallel (Y') and perpendicular (X') to the panel axis.

Before transformation process, the planar components of the vector connecting the surface station and the face center should be determined by taking the difference between station coordinates (X, Y) and face center coordinates (X_{int}, Y_{int}). This process is called as translation, where the origin of the XY coordinate system is shifted to the face center. Since the coordinates of face center becomes (0, 0) in the translated system, translated coordinates of the stations (ΔX, ΔY) are equal to the distances from the face center parallel to X and Y axes.

In transformation process, translated vectors are projected into X' and Y' axes using the unit vectors of the new coordinate system given in Equations 5-1 and 5-2 (*i* and *j* are unit vectors along translated coordinate axes, ΔX and ΔY, respectively):

$$\vec{n}_{X'} = -\sin\theta\,\vec{i} + \cos\theta\,\vec{j} \qquad [5\text{-}1]$$

$$\vec{n}_{Y'} = -\cos\theta\,\vec{i} - \sin\theta\,\vec{j} \qquad [5\text{-}2]$$

X' coordinate of the station is the sum of the components of ΔX and ΔY along X':

$$X': \quad (X-X_{int})(-\sin\theta) + (Y-Y_{int})\cos\theta$$

$$= \Delta X(-\sin\theta) + \Delta Y \cos\theta \qquad [5\text{-}3]$$

Y' coordinate of the station is the sum of the components of ΔX and ΔY along Y':

$$Y': \quad (X-X_{int})(-\cos\theta) + (Y-Y_{int})(-\sin\theta)$$

$$= \Delta X(-\cos\theta) + \Delta Y(-\sin\theta) \qquad [5\text{-}4]$$

Translated (ΔX-ΔY) and the transformed (X'-Y') coordinate systems are shown in Figure 5-6.

X' coordinate is equal to the perpendicular distance of the station from the panel centerline. Y' coordinate is equal to the distance of the station parallel to panel axis from the face center. The matrix form of this statement is given in Equation 5-4, where f_j (Y' coordinate of face center at jth measurement date) values are equal to 0 and therefore, y_{ij} (Y' coordinate of ith station at jth measurement date) values are equal to yf_{ij} (distance of the ith station to the face center parallel to Y' at jth measurement date).

$$\begin{bmatrix} y_{11} & y_{21} & . & . & . & y_{m1} \\ y_{12} & y_{22} & . & . & . & y_{m2} \\ . & . & . & . & . & . \\ . & . & . & . & . & . \\ . & . & . & . & . & . \\ y_{1n} & y_{2n} & . & . & . & y_{mn} \end{bmatrix} - \begin{bmatrix} f_1 & f_1 & . & . & . & f_1 \\ f_2 & f_2 & . & . & . & f_2 \\ . & . & . & . & . & . \\ . & . & . & . & . & . \\ . & . & . & . & . & . \\ f_n & f_n & . & . & . & f_n \end{bmatrix} = \begin{bmatrix} yf_{11} & yf_{21} & . & . & . & yf_{m1} \\ yf_{12} & yf_{22} & . & . & . & yfm_2 \\ . & . & . & . & . & . \\ . & . & . & . & . & . \\ . & . & . & . & . & . \\ yf_{1n} & yf_{2n} & . & . & . & yf_{mn} \end{bmatrix} \qquad [5\text{-}4]$$

$$\cong \begin{bmatrix} yf_1 \\ yf_2 \\ . \\ . \\ . \\ yf_n \end{bmatrix} \textit{along} \quad \textit{transverse lines}$$

Distances to the face center will be equal for the stations along the same transverse line (Y' coordinates of the stations are same), if the transverse line passing through the stations is exactly perpendicular to the panel axis (parallel to X' axis). However, it should be noted that, the distance to the face will change slightly for each station along the same transverse line. Therefore, the relative distances of the stations to the face (yf) are found one by one instead of assuming these values being equal.

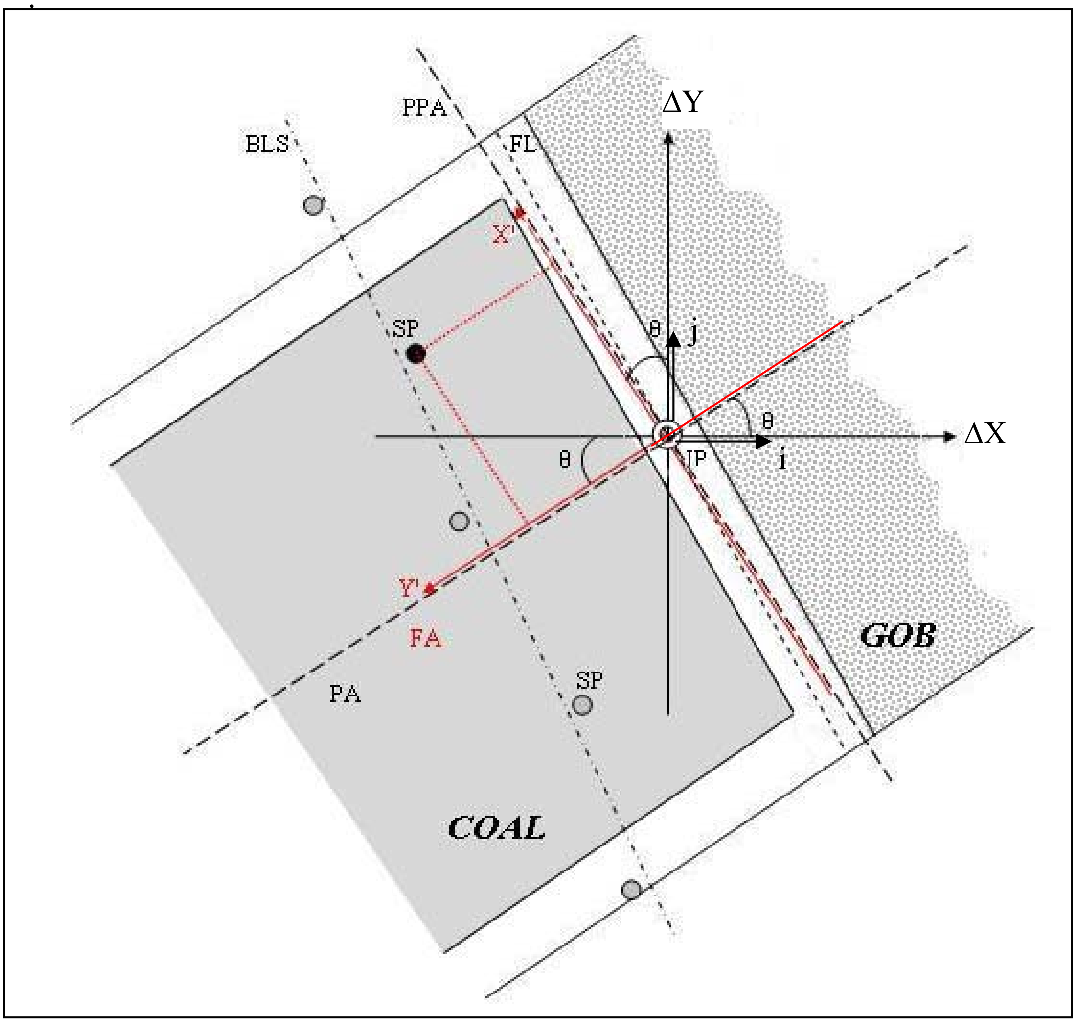

SP: Station point	BLS: Best line for the stations
PA: Panel axis (longitudinal)	PPA: Perpendicular line to the panel axis
FL: Face line	IP: Intersection point between PA & FL
FA: Face advance direction	θ: Angel of the panel axis from X axis

Figure 5-6 Translation and transformation processes.

Since longitudinal lines deviate from the center of the panel, the centerline of the panels are used to calculate the perpendicular distances (X') to the face advance.

Step 4: Calculation of horizontal displacement along X' and Y' axes and subsidence.

Table 5-3 below presents the steps stated above.

Table 5-3 Tabulation of results for panel B02.

5-3 a.

①		②		③	④	⑤
Panel Start		**Panel End**		**m**	**Angle of Panel Axis (θ)**	**n**
X_{ps}	Y_{ps}	X_{pe}	Y_{pe}			
87655.113	42857.183	86187.414	42175.363	0.4645	24.917	2137

①, ②: X (Easting) and Y (Northing) coordinates of panel start and end.

③ ⑤: Slope (m) and the constant (n) in the panel centerline equation ($mx+n$).

④: Angle of panel axis from Easting (X axis): θ = atan m.

5-3 b.

①'	②'	③'	④'	⑤'	⑥'	⑦'	⑧'
Meas. No	**Meas. Date**	**Time (days)**	$X_{int. front}$	$X_{int. back}$	**Dist. btw. Fr. and B. Face**	**Gob L. (of Fr. F.)**	**Fr. Face Adv.**
1	08.08.2001	0	87644.393	87647.369	3.281	11.820	0.000
2	22.08.2001	14	87603.325	87617.701	15.851	57.103	45.283
3	27.08.2001	19	87588.658	87607.105	20.340	73.276	61.456
4	01.09.2001	24	87573.991	87596.509	24.829	89.448	77.628
5	15.09.2001	38	87532.923	87555.414	24.800	134.731	122.911
6	01.10.2001	54	87485.988	87508.449	24.766	186.483	174.664

①': Measurement Number.

②': Measurement Date.

③': Time (Days passed since the initial measurement date).

④': X coordinate of Front Face Intersection with Panel Centerline ($X_{int.\ front}$).

⑤': X coordinate of Back Face Intersection with Panel Centerline ($X_{int.\ back}$).

④' and ⑤' are calculated using interpolation.

⑥': Distance between Front and Back Face: $(X_{int.\ front} - X_{int.\ back}) / -\cos\theta$

⑦': Gob Length of Front Face: $(X_{int.\ front} - X_{ps}) / -\cos\theta$

⑧': Front Face Advance. It is the difference between the gob length at the measurement date and the gob length at the first measurement date.

5-3 c.

①' ①'' ②'' ③'' ④'' ⑤'' ⑥'' ⑦'' ⑧''

Meas. No	Station No 1							
	X	Y	Z	X'	Disp. along X'	Y' (yf)	yd	S
1	87527.692	42962.416	763.144	149.121	0.000	59.405	0.000	0.000
2	87527.627	42962.452	763.212	149.181	0.060	14.165	0.044	0.068
3	87527.663	42962.427	763.172	149.144	0.022	-2.029	0.022	0.028
4	87527.646	42962.443	763.226	149.165	0.044	-18.193	0.030	0.082
5	87527.767	42962.310	763.137	148.994	-0.128	-63.530	-0.023	-0.007
6	87527.644	42962.293	763.240	149.030	-0.091	-115.163	0.095	0.096

Meas. No	Station No 2							
	X	Y	Z	X'	Disp. along X'	Y' (yf)	yd	S
1	87539.571	42936.864	767.466	120.943	0.000	59.397	0.000	0.000
2	87539.522	42936.905	767.501	121.001	0.058	14.141	0.027	0.035
3	87539.578	42936.885	767.503	120.959	0.016	-2.074	-0.015	0.037
4	87539.562	42936.901	767.552	120.980	0.037	-18.239	-0.007	0.086
5	87539.715	42936.637	767.371	120.677	-0.267	-63.549	-0.035	-0.095
6	87539.557	42936.505	767.410	120.623	-0.320	-115.103	0.164	-0.056

Meas. No	Station No 3							
	X	Y	Z	X'	Disp. along X'	Y' (yf)	yd	s
1	87556.329	42900.802	771.264	81.178	0.000	59.392	0.000	0.000
2	87556.227	42900.828	771.229	81.244	0.067	14.190	0.082	-0.035
3	87556.365	42900.790	771.254	81.152	-0.026	-2.091	-0.028	-0.010
4	87556.372	42900.808	771.232	81.165	-0.013	-18.278	-0.042	-0.032
5	87556.551	42900.373	770.373	80.695	-0.483	-63.540	-0.021	-0.891
6	87556.254	42899.968	770.132	80.453	-0.725	-114.852	0.419	-1.132

Table 5-3 Tabulation of results for panel B02 (cont.).

Meas. No	Station No 4							
	X	Y	Z	X'	Disp. along X'	Y' (yf)	yd	s
1	87565.756	42880.440	773.302	58.739	0.000	59.421	0.000	0.000
2	87565.668	42880.494	773.321	58.825	0.086	14.195	0.057	0.019
3	87565.812	42880.456	773.295	58.730	-0.009	-2.092	-0.058	-0.007
4	87565.926	42880.440	773.054	58.668	-0.072	-18.361	-0.154	-0.248
5	87565.747	42879.837	771.083	58.196	-0.543	-63.228	0.262	-2.219
6	87565.251	42879.579	770.602	58.171	-0.568	-114.422	0.821	-2.700

Meas. No	Station No 5							
	X	Y	Z	X'	Disp. along X'	Y' (yf)	yd	s
1	87576.302	42857.813	775.076	33.775	0.000	59.390	0.000	0.000
2	87576.278	42857.848	775.105	33.817	0.042	14.114	0.007	0.029
3	87576.446	42857.848	774.995	33.746	-0.029	-2.211	-0.145	-0.081
4	87576.621	42857.909	774.607	33.728	-0.047	-18.568	-0.330	-0.469
5	87576.499	42857.639	772.300	33.535	-0.241	-63.627	-0.105	-2.776
6	87575.795	42857.391	771.900	33.606	-0.169	-114.636	0.638	-3.176

Meas. No	Station No B							
	X	Y	Z	X'	Disp. along X'	Y' (yf)	yd	s
1	87588.111	42832.340	777.530	5.698	0.000	59.412	0.000	0.000
2	87588.149	42832.357	777.540	5.698	-0.001	14.087	-0.042	0.010
3	87588.305	42832.416	777.261	5.685	-0.013	-2.252	-0.208	-0.269
4	87588.522	42832.501	776.779	5.671	-0.027	-18.657	-0.441	-0.751
5	87588.099	42832.238	774.683	5.611	-0.087	-63.446	0.054	-2.847
6	87587.353	42832.005	774.240	5.714	0.016	-114.423	0.829	-3.290

Meas. No	Station No 6							
	X	Y	Z	X'	Disp. along X'	Y' (yf)	yd	s
1	87602.019	42802.517	783.668	-27.208	0.000	59.363	0.000	0.000
2	87601.988	42802.565	783.655	-27.152	0.057	14.088	0.008	-0.013
3	87602.207	42802.747	783.391	-27.079	0.129	-2.360	-0.267	-0.277
4	87602.243	42802.969	782.824	-26.893	0.316	-18.659	-0.394	-0.844
5	87601.368	42803.019	780.575	-26.479	0.730	-63.169	0.379	-3.093
6	87600.551	42802.998	780.267	-26.154	1.055	-114.172	1.129	-3.401

Meas. No	Station No 7							
	X	Y	Z	X'	Disp.	Y'	yd	s
1	87621.166	42761.295	795.617	-72.660	0.000	59.366	0.000	0.000
2	87621.059	42761.380	795.626	-72.538	0.122	14.144	0.061	0.009
3	87621.240	42761.422	795.534	-72.576	0.084	-2.211	-0.121	-0.083
4	87621.194	42761.730	795.342	-72.277	0.383	-18.471	-0.209	-0.275
5	87620.373	42762.787	794.376	-70.973	1.687	-63.455	0.091	-1.241
6	87619.612	42762.551	794.020	-70.866	1.794	-114.418	0.880	-1.597

Table 5-3 Tabulation of results for panel B02 (cont.).

Meas. No	Station No 8							
	X	Y	Z	X'	Disp. along X'	Y' (yf)	yd	s
1	87643.533	42713.285	803.816	-125.625	0.000	59.308	0.000	0.000
2	87643.434	42713.368	803.799	-125.508	0.117	14.079	0.055	-0.017
3	87643.509	42713.328	803.778	-125.576	0.049	-2.144	0.004	-0.038
4	87643.484	42713.394	803.780	-125.505	0.119	-18.322	-0.001	-0.036
5	87643.274	42713.605	803.578	-125.225	0.399	-63.504	0.100	-0.238
6	87643.033	42713.776	803.551	-124.969	0.656	-115.109	0.247	-0.265

Meas. No	Station No 9							
	X	Y	Z	X'	Disp. along X'	Y' (yf)	yd	S
1	87654.047	42690.757	801.880	-150.485	0.000	59.264	0.000	0.000
2	87653.992	42690.795	801.858	-150.428	0.058	14.014	0.034	-0.022
3	87654.054	42690.776	801.888	-150.471	0.014	-2.207	-0.014	0.008
4	87654.028	42690.814	801.878	-150.426	0.060	-18.371	-0.007	-0.002
5	87653.864	42690.897	801.759	-150.281	0.204	-63.541	0.107	-0.121
6	87653.668	42691.068	801.769	-150.044	0.442	-115.187	0.213	-0.111

①", ②" and ③" : Raw data (3-D coordinates).

④" : Distance to the centerline of the panel (X').

It is calculated as follows:

$(X-X_{int.\ front})\ (-\sin\theta) + (Y-Y_{int.\ front})\cos\theta$

where $Y_{int.\ front} = m\ X_{int.\ front} + n$

= (①"-④') (-sin④) + (②" -m④'-n) cos④

⑤" : Change in X'.

It is the change in distance along X', relative to the first measurement date.

⑥" : Distance to the face center (yf).

$(X-X_{int.\ front})$ (-sin④) + $(Y-Y_{int.\ front})\cos\theta$

= (①"-④') (-cos④) + (②" -m④'-n) (-sin④)

⑦" : Displacement in Y' direction (yd) . Calculation of "yd" is explained in

Figure 5-7 by illustrations.

⑧" : Subsidence (s)

③', ⑥', ⑦', ⑧', ④", ⑤", ⑥", ⑦", ⑧" are calculated using macro (code written in Excel to calculate these values automatically for all stations).

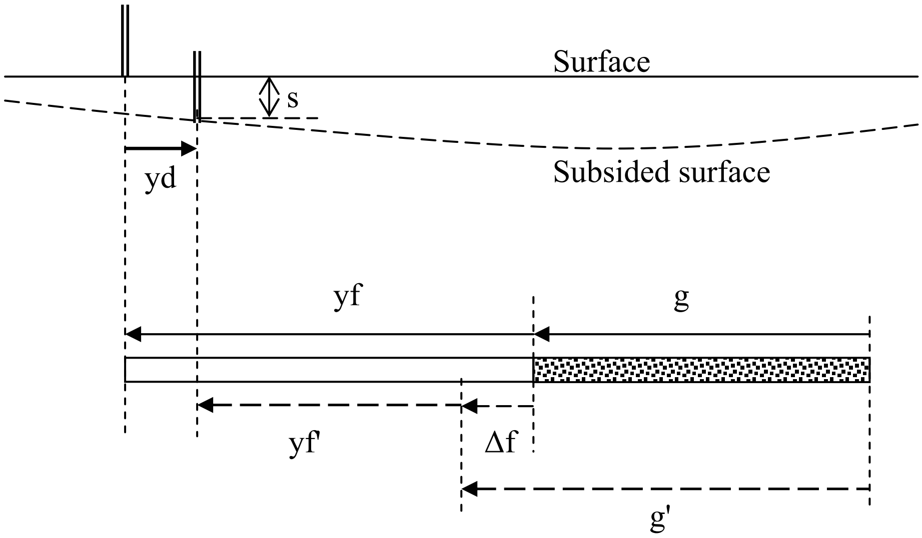

or

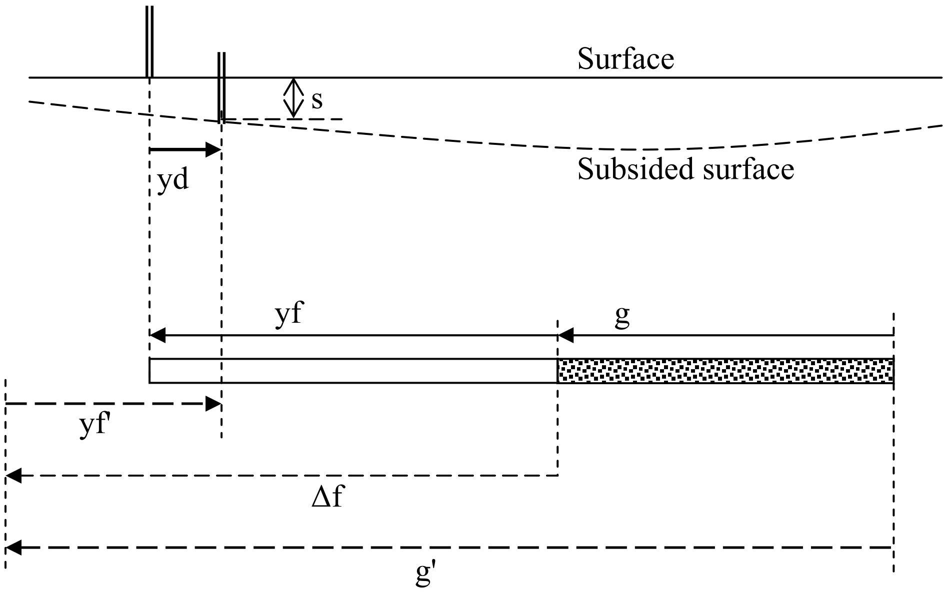

g, g': Gob length (initial, after movement)	**yd:**Displacement of the station
yf, yf': Distance to the face (initial, after movement)	**Δf:** Face advance

Figure 5-7 Displacement of a station after movement

As it can be seen in Figure 5-7:

Figure 5-7

$\Delta f = g' - g$ and $yd = (yf' + g') - (yf + g) = (yf' - yf) + \Delta f$ [5-3]

5.2. EVALUATION OF SUBSIDENCE PROFILES

The subsidence profiles relative to the initial measurement of the survey line are plotted according to distance from the panel center and time. Graphs are also prepared to show the original surface line, final subsidence trough, the face below and the angle of draw.

Figure 5-8, Figure 5-9, Figure 5-10 and Figure 5-11 for B line over panel B02 are example graphs and the rest of graphical forms obtained from measured values are presented in Appendix-B.

In Figure 5-8, subsidence is plotted versus time for each station along B line of panel B02. Location of the stations with respect to face center (Y') is also given at each measurement date in the graph. In Figure 5-9, subsidence profile is plotted along the same transverse section for each subsidence measurement date.

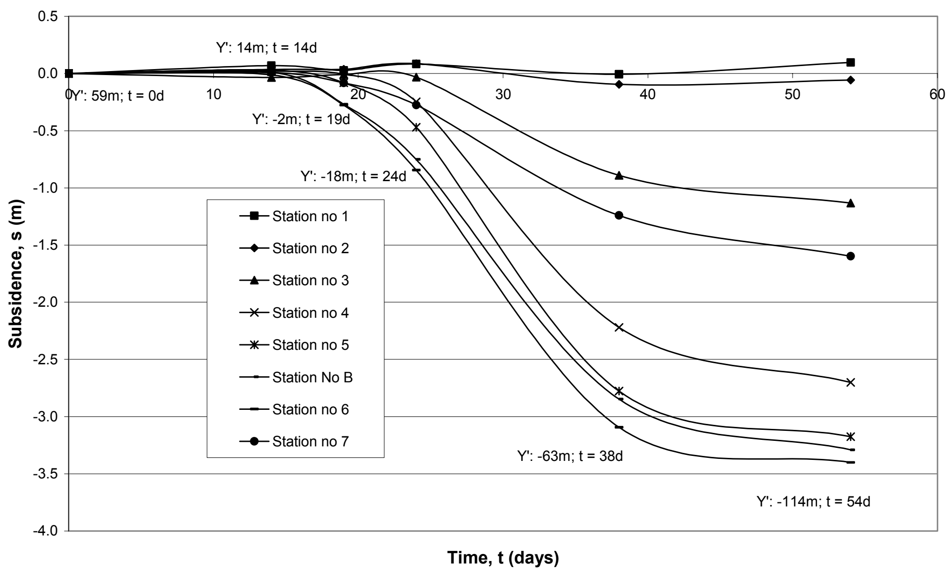

Figure 5-8 Subsidence versus time graph for the stations along B line of panel B02.

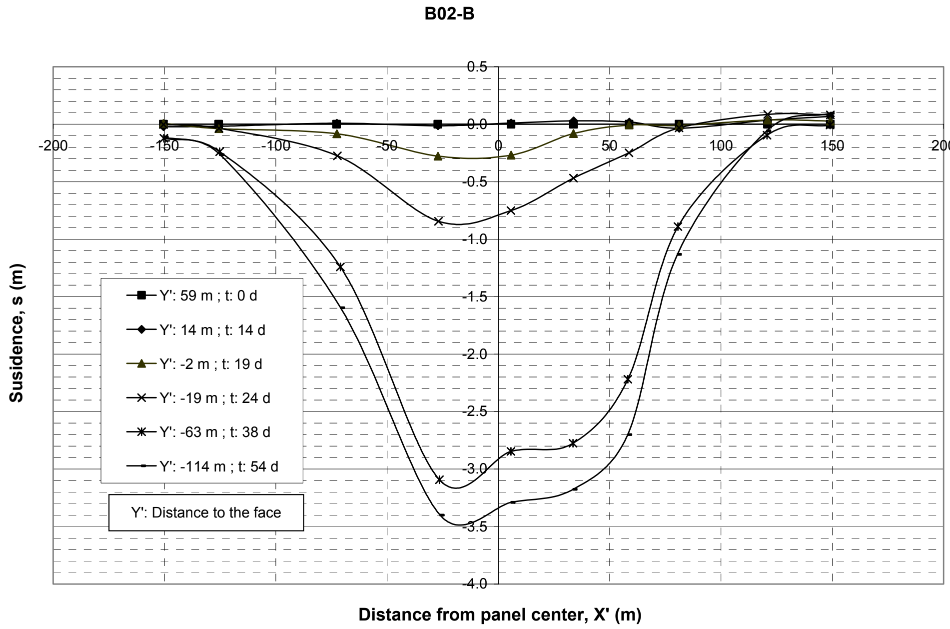

Figure 5-9 Subsidence versus distance from panel center, along B line of panel B02.

Section view of BB' line, showing topography, subsidence profile at the last measurement date (54. day) and the extracted coal seam, is given in Figure 5-10.

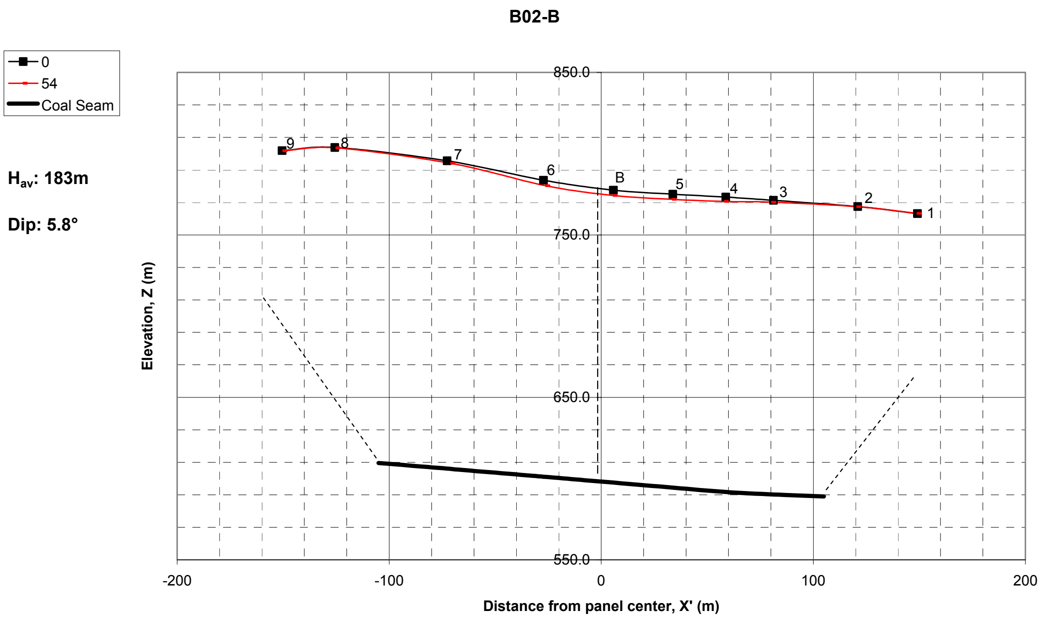

Figure 5-10 BB' section of panel B02 (Original-subsided surface and coal seam).

In Figure 5-11, horizontal displacement profiles are plotted versus time for each station along BB'.

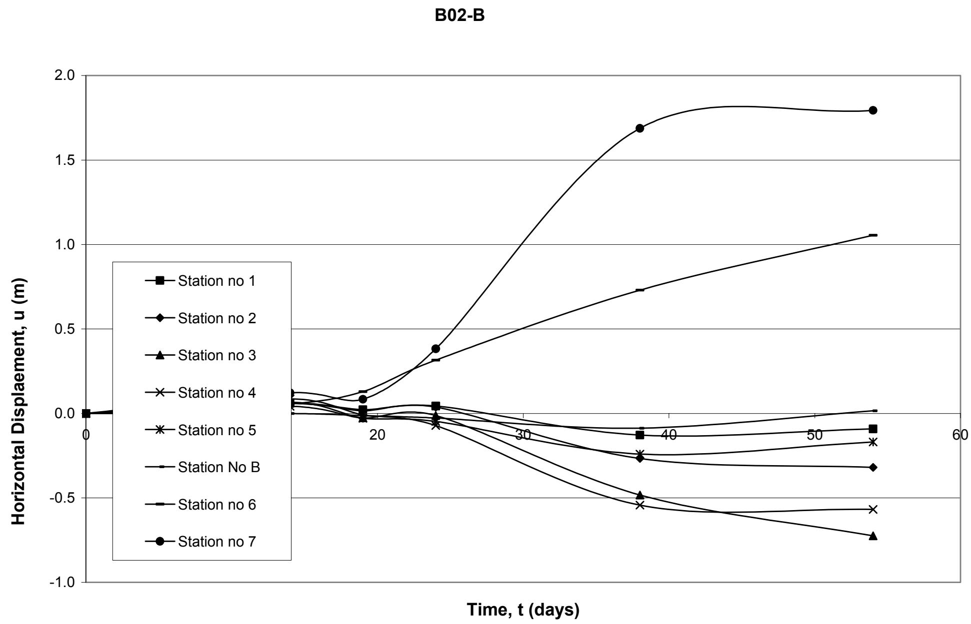

Figure 5-11 Horizontal displacement versus time along B line of panel B02.

Table 5-4 presents mining depth, seam dip, maximum subsidence and maximum horizontal displacement values, which are demonstared by the Figures in Appendix B.

Figure 5-12 demonstrates the subsidence, vertical strain and, horizontal displacement profiles. As it can be seen from the figure, vertical strain and horizontal displacement profiles are similar. Centroidal y axis shows subsidence and horizontal displacement values (absolute displacements), the secondary axis right hand side shows for subsidence slope and horizontal strain (differential movements). From the flatter part for maximum subsidence, it can be concluded that this width is supercritical.

Table 5-4 Production date of the panels, mining depth, seam dip, maximum subsidence and horizontal displacement values.

Transverse Section	Information	B12	B10	B02	C12	C10	C08
		12.1998 – 11.1999	02.2000 – 05.2001	09.2001 – 11.2002	11.1999 – 01.2001	04.2001 – 03.2002	07.2002 – 06.2003
B	H (m)	160	180	183	-	220	198
	Dip (°)	19	4	6	-	1	5
	S_{max} (m)	3.7	3.6	3.5	2.2	2.8	2.3
	U_{max} (m)	0.414 -0.634	1.387 -1.452	1.794 -0.725	0.702 -0.902	0.264 -0.546	0.452 -0.725
C	H (m)	172	198	172	120	191	195
	Dip (°)	17	0	6	17	2	5
	S_{max} (m)	3.4	-	2.5	3.2	3.0	3.4
	U_{max} (m)	0.763 -1.805	-	1.013 -0.363	0.882 -1.463	0.772 -1.096	1.133 -1.434
D	H (m)	180		179	150	162	
	Dip (°)	18		6	11	3	
	S_{max} (m)	3.4		3.2	2.7	3.4	
	U_{max} (m)	1.184 -0.921		0.619 -1.087	0.912	1.106 -1.614	
E	H (m)						
	Dip (°)						
	S_{max} (m)						
	U_{max} (m)						

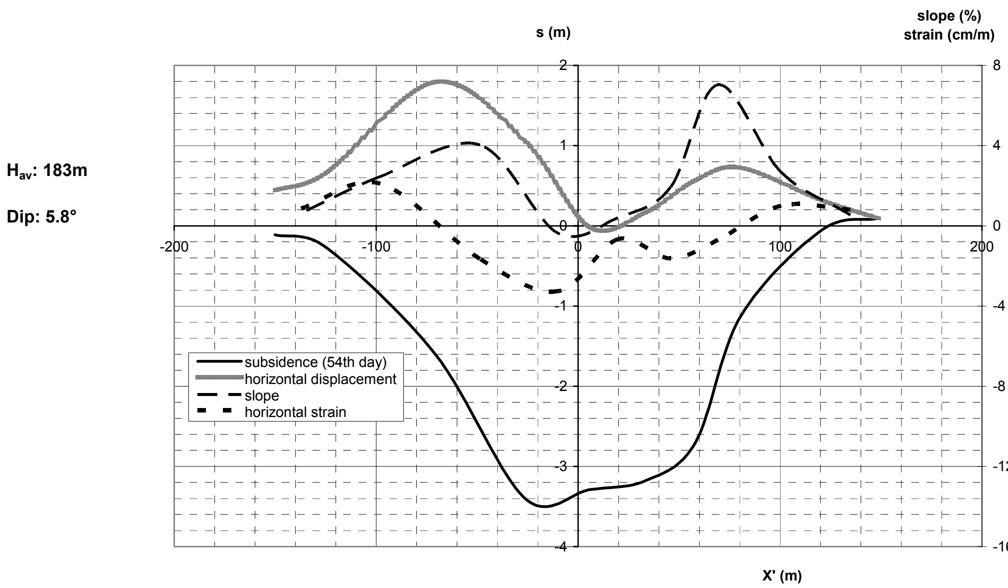

Figure 5-12 Subsidence, horizontal displacement and slope profiles along B02 panel along B line.

5.3. PREVIOUS STUDIES

5.3.1. SUBSIDENCE STUDIES ABOVE A13 PANEL

Ünver (1993) carried out subsidence studies above A13 panel having a width of 220 m and a length of 865m. Average mining depth was 180 m, monthly face advance was 55-70 m. Concrete packing with 1.5 m in width and 3.2 m in height was applied at the goaf side of the main gate. The seam inclination was changing between 0 and 10 degrees in this panel.

AD line was laid down in the longitudinal direction, EH and IK lines in the transverse direction (Figure 5-13).

Results are presented as follows:

- The development of the subsidence, along the longitudinal section, can be seen in Figure 5-14, where Sa, Sb, Sc, Sd and Se are the profiles of 500, 600, 800, and 865 m face advance, respectively. First considerable ground movement at the surface of A-13 panel was seen 240 m ahead from the panel start border. The amount of subsidence did not change after 500 m of face advancement.
- The maximum subsidence was 2.3 m and 2.11 m along AD and IK lines, respectively.
- Subsidence factor is 0.87 for this panel.
- The maximum horizontal displacements above the solid part and goaf were 11.5 cm and 22 cm respectively.
- The maximum slope in the longitudinal direction is 30.8 mm/m above the panel start side and 54 mm/m above the panel finish side.
- The maximum compressive strain is 3.83 mm/m, and maximum tensile strain is 4.4 mm/m and 6 mm/m at the dip and rise sides, respectively.

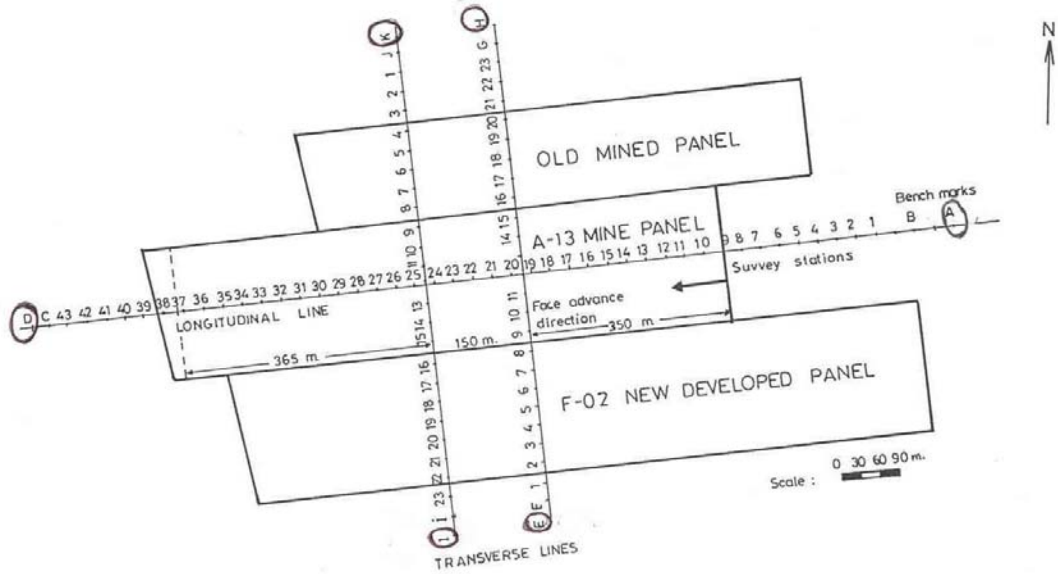

Figure 5-13 Layout of subsidence stations (Unver, 1993).

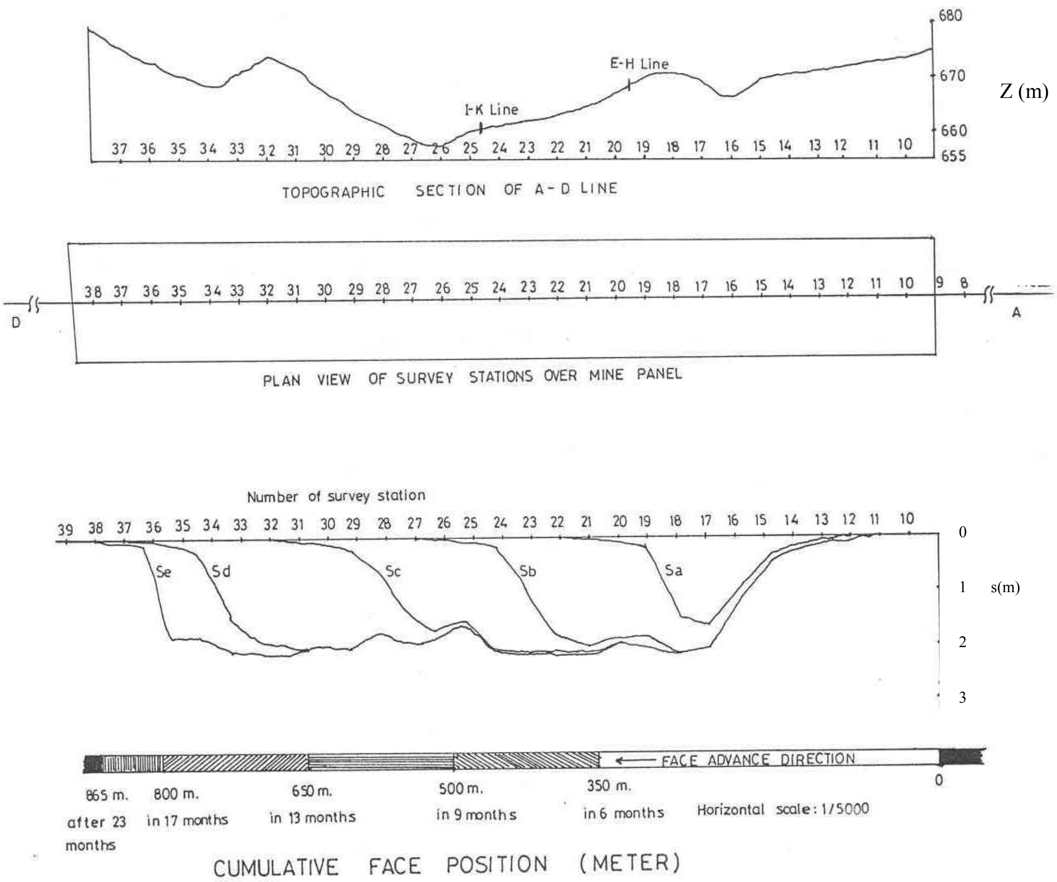

Figure 5-14 Longitudinal cross section of the A13 panel (Unver, 1993).

5.3.2. SUBSIDENCE STUDIES ABOVE B14 PANEL

As stated in Chapter 4.1, subsidence investigations above panel B14 have been initiated due to damage of pylons caused by underground mining. Layout of the survey lines and power-line pylons were shown in Chapter 4.1. Coordinate systems used in the analysis of ground movements are shown in Figure 5-15. The difference between the coordinate systems used for subsidence studies (Unal et al., 1998) above B14 panel and those used in this study (for panels B02, B10, B12, C08, C10 and C12) is that the origin is located at the intersection of the longitudinal and transverse lines (for B14 panel) instead of locating them at the face center.

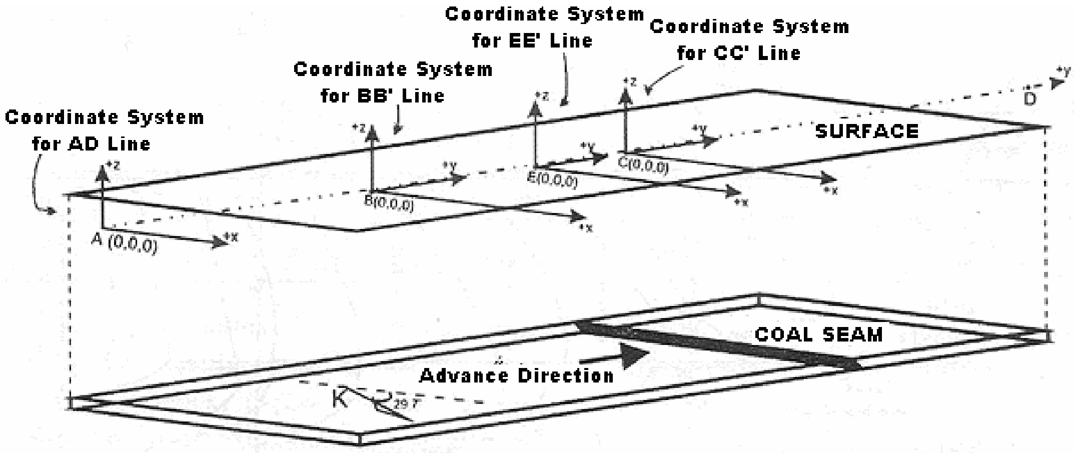

Figure 5-15 Coordinate systems used for subsidence studies above B14 panel (Unal et al., 1998).

Subsidence profiles obtained at different measurement dates along AD section of panel B14 are plotted in Figure 5-16. In addition, subsidence, horizontal movement and differential movements are shown in Figure 5-17 and Figure 5-18 for BB' and CC' sections, respectively.

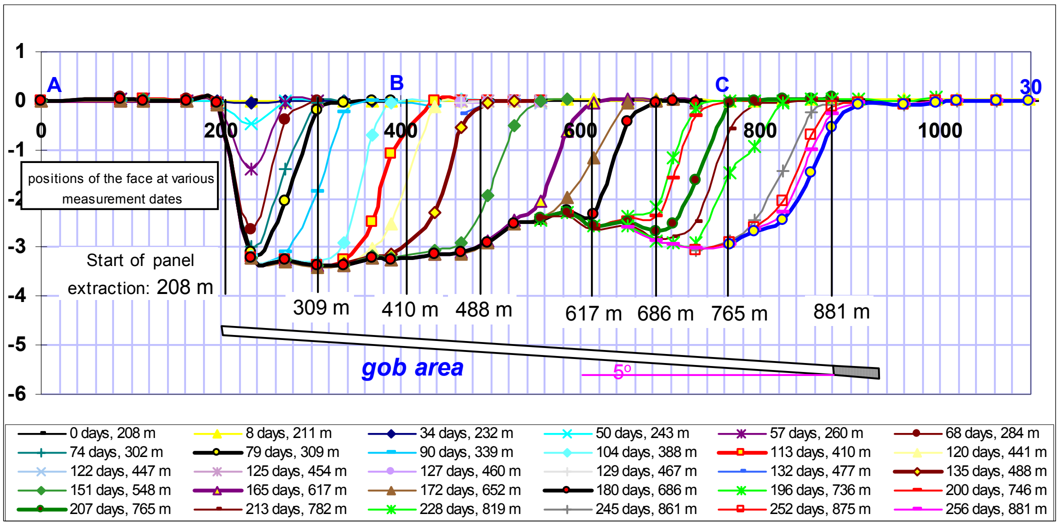

Figure 5-16 Subsidence profiles along AD section of panel B14 (Unal et al., 1998).

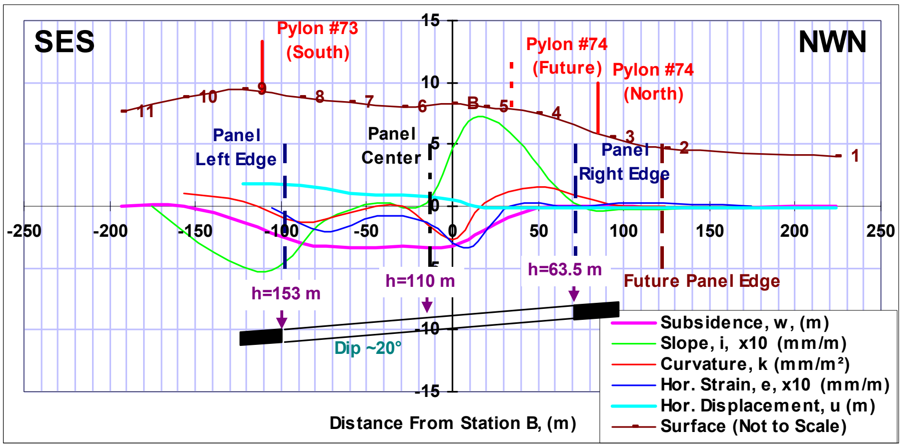

Figure 5-17 Profiles along BB' section of panel B14 (Unal et al., 1998).

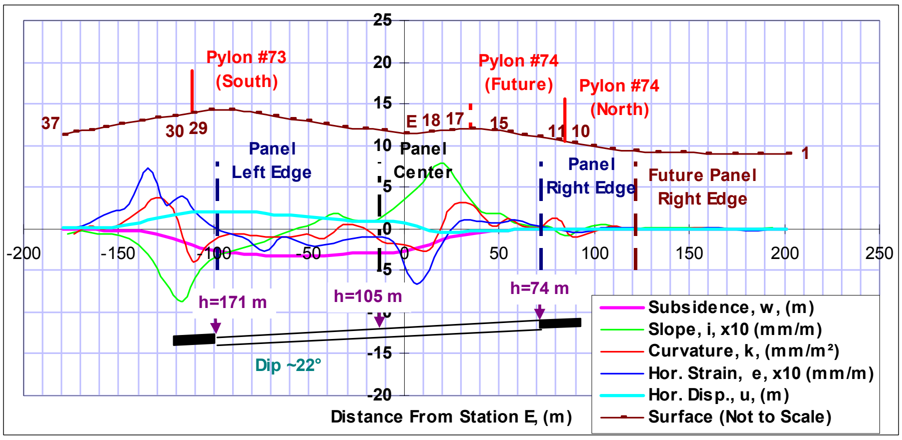

Figure 5-18 Profiles along EE' section of panel B14 (Unal et al., 1998).

According to the measurements carried out by Unal et al.(1998), the maximum subsidence along the longitudinal and transverse sections were about 3.3 m. The maximum slope along AD section was determined as -80 mm/m. Fractures along BB' section occurred between St.2 and St.3 which are outside of the panel edge, and between St.3-St.4, St.9-St.10 located inside of the extraction area. Maximum slope occurs 20 m right side of station E, between St.17 and St.18 (80mm/m) and 118 m left side of St.E between St.29 and St.30 (-85 mm/m). Maximum horizontal compressive strain (65 mm/m) occurs between St.E and St.18.

The ground slope and strains developed due to retreating longwall faces are likely the cause of damage to the electrical power lines. For protection of pylon deformation above panel B14 and for providing stability of pylons, the following alternatives are suggested (see Appendix D for details).

- **Alternative 1.** Instead of relocating both the damaged pylons, use another power transmission route outside of the area of subsidence.

- **Alternative 2.** Move both of the pylons into the region of B14 panel, but strengthen their base to be able to resist the surface tilt.

- **Alternative 3.** When panel width increased to 220 meters from 170 meters pylon No: 3274 should be observed closely and the pylon No: 3273 should be transferred firstly to a location outside of the panel influence area (40-60 m away from recent location), and then back to a location inside the panel (70 m away from recent location)

- **Alternative 4.** To establish a new power transmission route.

CHAPTER 6

ANALYSIS OF MEASUREMENTS

6.1. NEWLY DEVELOPED MATHEMATICAL MODEL

6.1.1. REVIEW OF CONVERGENCE MODEL

The mathematical model developed in this study is partly based on the convergence model developed by Ünal et al (2001). In both, subsidence and convergence models, face advance and time, were considered as main parameters controlling the subsidence and convergence.
The convergence was modeled by the product of two functions as follows:

$$U = U_I U_{II} \tag{6-1}$$

where

$$U_I = A + Be^{c/(t+1)} \tag{6-2}$$

$$U_{II} = K(1+e^{-x_1/6D})^{E/h_{t1}} + L(1+e^{-x_2/6F})^{G/h_{t2}} \tag{6-3}$$

Finally, the relation for the mathematical representation of convergence becomes:

$$U = (A + Be^{c/(t+1)})[K(1+e^{-x_1/6D})^{E/h_{t1}} + L(1+e^{-x_2/6F})^{G/h_{t2}}] \tag{6-4}$$

where *A, B, C, D, E, F, G, K, L* are coefficients found by statistical analyses,t is time (days), x_1 is and x_2 are the distances of upper and lower face to the the measuring station in meters. The distance between the upper and lower face was reported to be changed 25 to 40 meters for double seam extraction (Figure 6-1).

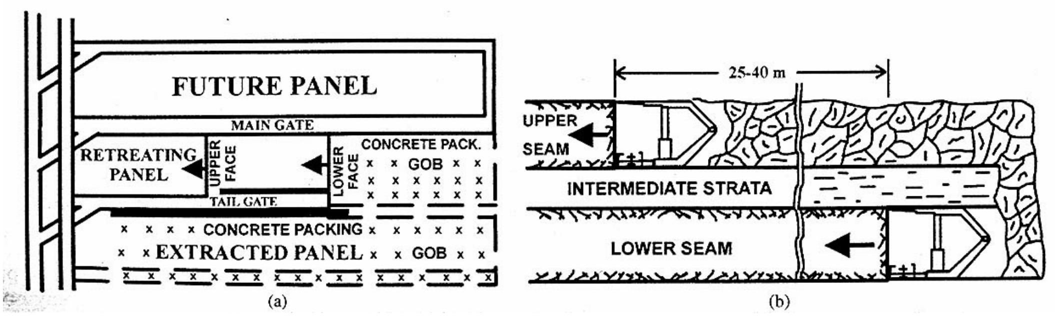

Figure 6-1 (a)Plan view of longwall panels and positions of gate roadways, and (b)section view showing the upper and lower seams and position of longwall faces in Çayırhan Lignite Mine (Unal et al., 2001).

Related with this concept, dynamic loads causing convergence are shown in Figure 6-2. Rock mass-conditions in the roof and floor of the mine can be evaluated as good. Roof of the upper seam caves in large pieces. Interburden layer becomes the roof of the lower face and itcaves in small pieces. Roof control problems usually occur when of the interburden thickness decreases down to 0.4 m (Dalgıç, 1996).

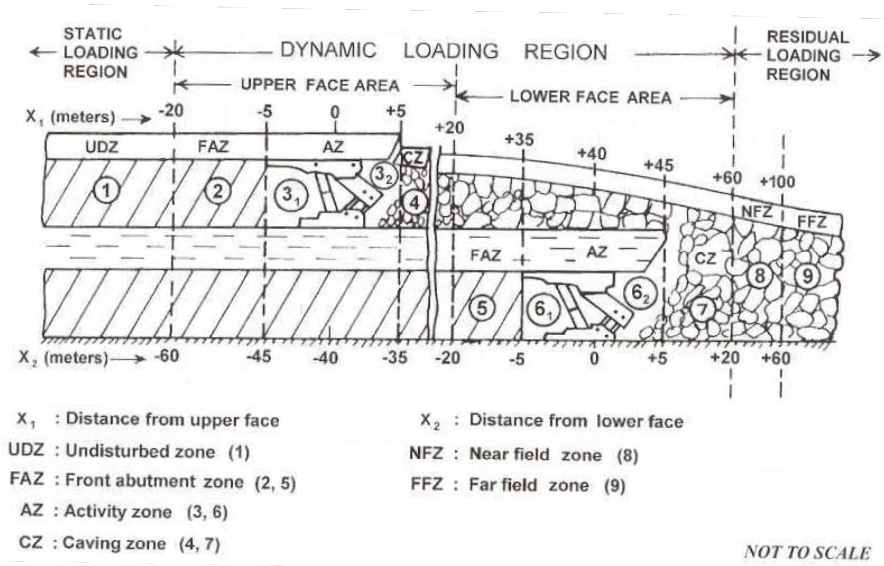

Figure 6-2 Loading regions (Unal et al., 2001).

6.1.2. SUBSIDENCE MODEL

It has been seen in the literature that, diagrams were developed and subsidence profiles were suggested on the basis of depth, height and inclination of extraction. As stated in the previous part, the subsidence model in this study is based on face advance and time. Various mathematical models were tested by SPSS (V10) using the subsidence measurements above Panel B14 and the exponential mathematical model derived in order to predict subsidence-time characterization is:

$$U = (A + Be^{-C/(t+1)}\left\{[D(1+e^{-x_1/9{,}71E})^{(-\mu/F)}] + [G(1+e^{-x_2/7{,}28H})^{(-\mu/K)}]\right\} \quad [6\text{-}5]$$

where

A,B,C,D,E,F,G,H,K,μ are constant coefficients

t is time (days)

x_1 is distance of the surface measuring station to the upper face (m)

x_2 is distance of the surface measuring station to the lower face (m)

The equation can be redefined as:

$$S = S_I(S_2 + S_3) \quad [6\text{-}6]$$

where

$$S_I = [A + Be^{-c/(t+1)}] \quad [6\text{-}7]$$

$$S_2 = [D(1+e^{-x_1/9{,}71E}]^{(-\mu/F)} \quad [6\text{-}8]$$

$$S_3 = [G(1+e^{-x_2/7{,}28H}]^{(-\mu/K)} \quad [6\text{-}9]$$

$[Be^{-c/(t+1)}]$ term in Equation 6-7 is the time dependent component of subsidence. Equations 6-8 and 6-9 are face-distance dependent components of subsidence caused by upper face and lower face advance, respectively.

Since the face advance is dependent on time, Equation 6-4 can be divided into following components:

i. Subsidence caused by upper face advance

$$S_{UA} = A[D(1+e^{-x_1/9,71E}]^{(-\mu/F)} \quad [6\text{-}10]$$

ii. Subsidence caused by lower face advance

$$S_{LA} = A[G(1+e^{-x_2/7,28H}]^{(-\mu/K)} \quad [6\text{-}11]$$

iii. Time dependent subsidence caused by upper face

$$S_{Ut} = [Be^{-c/(t+1)}][D(1+e^{-x_1/9,71E}]^{(-\mu/F)} \quad [6\text{-}12]$$

iv. Time dependent subsidence caused by lower face

$$S_{Lt} = [Be^{-c/(t+1)}][G(1+e^{-x_2/7,28H}]^{(-\mu/K)} \quad [6\text{-}13]$$

So, Equation 6-6 becomes:

$$U = [U_{UA} + U_{Ut}] + [U_{LA} + U_{Lt}] \quad [6\text{-}14]$$

It is expected that the region near to the center of the panel will be more affected by advance and near the edges by time.

6.1.3. STATISTICAL EVALUATION OF THE MODEL

SPSS (V.10) is used for the estimation of parameters. Firstly, measured subsidence, time and distance to the face values (x1, x2) are listed in different columns. Secondly, subsidence value is defined as dependent parameter and A, B, C, D, E, F, G, H, K are defined as the coefficients of the equation, for nonlinear regression analysis. Then the subsidence equation is written in terms of t, x1, x2 and coefficients (Equation 6-4). While writing the equation a reasonable value for μ should be estimated for statistical anlysis.

Lastly, the coefficients of the equation is estimated by running the program. The assumed μ values and the program outputs (estimated values of the coefficients and R^2 values) are presented, for 10 stations along BB' section of panel B14, in Table 6-1. It can be seen from Figure 6-3 that, there is a linear relationship between the distance of the stations to the face center and the μ values predetermined for statistical analyses.

Table 6-1 Estimated coefficients of the model using nonlinear regression analysis, for BB' line over panel B14.

St. No	Distance to the Panel Center	μ	A	B	C	D	E	F	G	H	K	R^2
1	224.266	61.75	0.48	0.19	0.23	0.00	3.36	18.78	0.02	0.29	564.00	0.9994
2	123.690	37.50	0.35	0.51	0.26	0.07	1.59	28.91	0.00	0.05	48.00	1.0000
3	92.605	21.85	0.01	0.00	9.96	0.21	0.36	0.01	1.31	2.81	28.85	0.9994
4	49.582	12.85	0.05	0.06	-0.08	0.22	3.38	0.74	0.71	2.20	17.70	1.0000
5	18.440	5.75	0.43	0.41	0.82	0.51	3.98	2.28	0.64	1.13	0.10	0.9998
B	0.000	0.30	1.16	0.64	1.00	1.20	2.03	0.09	0.65	0.26	0.03	1.0000
6	23.310	5.50	1.27	0.61	0.39	0.28	2.47	0.29	1.47	1.05	9.17	1.0000
7	59.307	16.85	1.26	0.52	0.04	0.78	2.58	2.33	1.10	0.55	62.82	1.0000
8	89.023	27.85	1.12	0.52	15.28	0.80	0.20	0.00	1.07	3.08	19.67	1.0000
9	122.034	37.85	0.76	0.39	49.48	0.18	0.20	0.00	1.03	3.71	23.48	1.0000

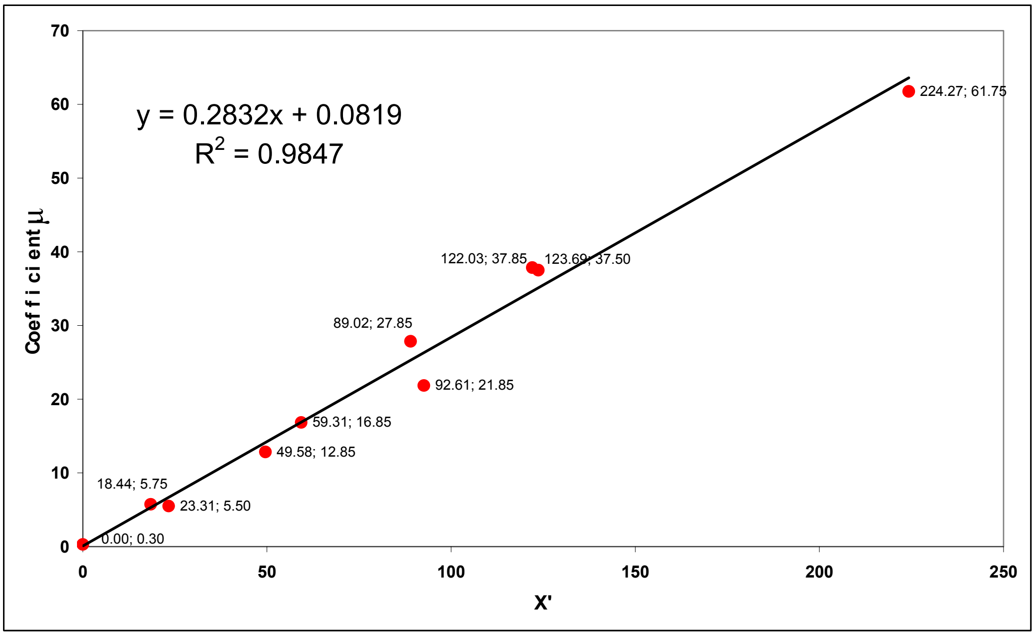

Figure 6-3 Relationship between X' and the coefficient μ, determined for BB' line of panel B14.

Subsidence values are calculated by putting the estimated values of coefficients into the equation and these predicted values are compared with actual ones in Table 6-2 for the stations along BB' line.

Table 6-2 Comparison of measured and predicted subsidence values of the stations 1 to 9, along BB' line over panel B14.

Date	Time (days)	Face Adv. (m)	St1		St2		St3		St4		St5	
			Meas. Subs. (m)	Pred. Subs. (m)	Meas. Subs. (m)	Pred. Subs. (m)	Meas. Subs. (m)	Pred. Subs. (m)	Meas. Subs. (m)	Pred. Subs. (m)	Meas. Subs. (m)	Pred. Subs. (m)
02.06.1997	0	-160	0.000	0.000	0.000	0.000	0.000	0.000	0.000	0.000	0.000	0.000
10.06.1997	8	-157	0.000	0.000	0.000	0.000	0.000	0.000	0.000	0.000	0.002	0.000
06.07.1997	34	-135	0.000	0.000	0.000	0.000	0.000	0.000	0.000	0.000	-0.003	0.000
20.08.1997	79	-58	0.000	0.000	0.000	0.000	0.000	0.001	0.002	0.001	0.008	0.006
31.08.1997	90	-28	0.000	0.001	0.005	0.005	0.003	0.002	0.006	0.006	0.007	0.027
14.09.1997	104	20	0.010	0.010	0.046	0.046	0.010	0.010	0.037	0.037	0.150	0.135
23.09.1997	113	42	0.016	0.016	0.060	0.060	0.019	0.019	0.046	0.060	0.196	0.209
30.09.1997	120	74	0.017	0.017	0.064	0.064	0.023	0.023	0.080	0.080	0.713	0.715
15.10.1997	135	120	0.018	0.018	0.065	0.065	0.024	0.025	0.086	0.095	0.917	0.919
31.10.1997	151	180	0.018	0.018	0.065	0.065	0.025	0.025	0.104	0.102	0.949	0.953
14.11.1997	165	249	0.018	0.018	0.065	0.065	0.025	0.025	0.104	0.104	0.960	0.962
21.11.1997	172	284	0.018	0.018	0.065	0.065	0.025	0.025	0.104	0.104	0.965	0.963
29.11.1997	180	320	0.018	0.018	0.065	0.065	0.025	0.025	0.104	0.104	0.965	0.963

Date	Time (day)	Face Adv. (m)	StB		St6		St7		St8		St9	
			Meas. Subs. (m)	Pred. Subs. (m)	Meas. Subs. (m)	Pred. Subs. (m)	Meas. Subs. (m)	Pred. Subs. (m)	Meas. Subs. (m)	Pred. Subs. (m)	Meas. Subs. (m)	Pred. Subs. (m)
02.06.1997	0	-160	0.000	0.000	0.000	0.000	0.000	0.000	0.000	0.000	0.000	0.000
10.06.1997	8	-157	0.000	0.000	-0.001	0.000	0.007	0.000	-0.007	0.000	-0.003	0.000
06.07.1997	34	-135	0.000	0.000	-0.005	0.000	0.003	0.000	-0.009	0.000	-0.005	0.000
20.08.1997	79	-58	0.007	0.000	0.006	0.003	0.018	0.006	0.010	0.009	0.003	0.005
31.08.1997	90	-28	0.003	0.007	0.011	0.029	0.040	0.041	0.038	0.051	0.028	0.027
14.09.1997	104	20	0.692	0.692	1.094	1.091	1.081	1.081	1.157	1.222	0.282	0.280
23.09.1997	113	42	2.476	2.476	2.487	2.488	2.343	2.343	2.148	2.190	0.659	0.658
30.09.1997	120	74	3.006	3.006	2.983	2.983	2.930	2.930	2.677	2.697	0.974	0.977
15.10.1997	135	120	3.172	3.168	3.228	3.227	3.281	3.279	2.940	2.939	1.204	1.197
31.10.1997	151	180	3.192	3.199	3.272	3.284	3.344	3.353	2.979	2.986	1.258	1.262
14.11.1997	165	249	3.213	3.212	3.288	3.289	3.359	3.360	2.996	2.996	1.274	1.278
21.11.1997	172	284	3.221	3.217	3.297	3.290	3.371	3.361	3.005	2.999	1.285	1.282
29.11.1997	180	320	3.218	3.222	3.291	3.290	3.361	3.361	3.000	3.003	1.289	1.287

A typical subsidence-time characterization example is given for actual measurements of BB' line over panel B14 in Figure 6-4. The typical results obtained from model for station 7 (located at the BB' section of panel B14), namely: time and advance dependent parts of upper and lower face, are presented in Figure 6-5 and also actual field measurements and estimated total subsidence values for this station are displayed.

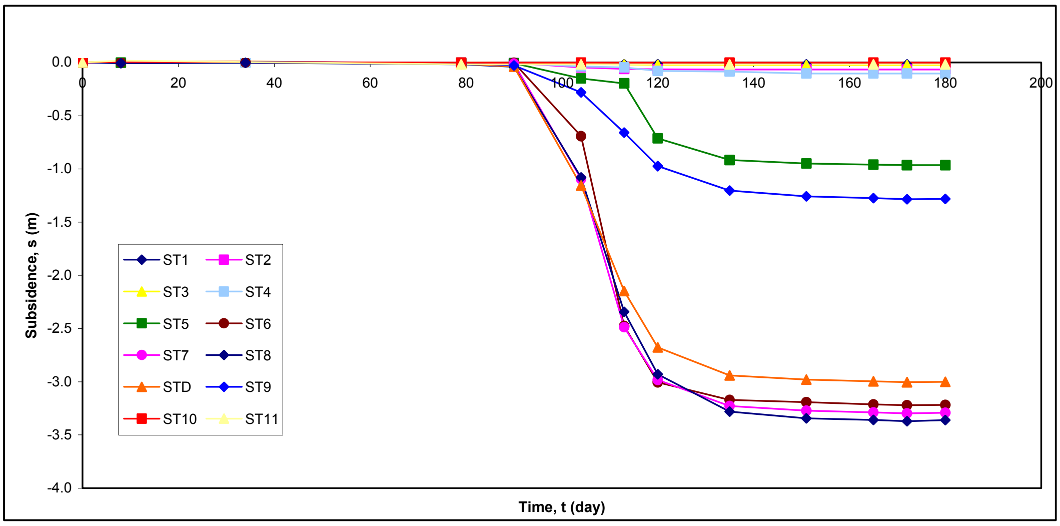

Figure 6-4 Subsidence versus time along BB' section of panel B14.

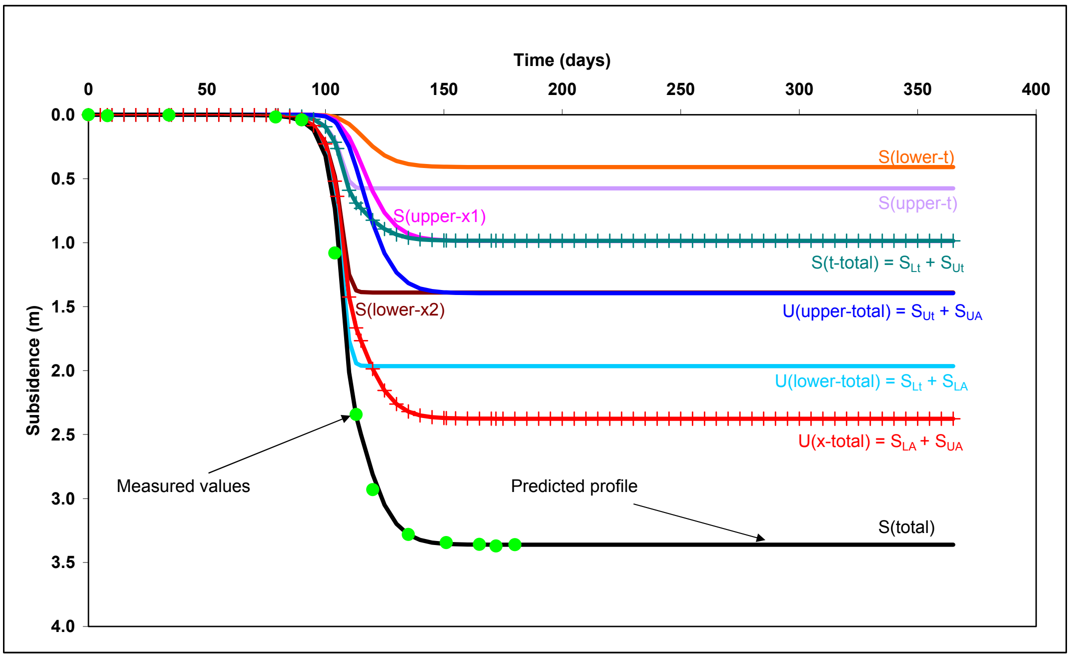

Figure 6-5 Analysis of the subsidence components estimated for St.7.

Subsidence profiles at measurement dates can be seen in the section view along BB' line of panel B14 (Figure 6-6). Precited and actual profiles for the final measurement date along BB' (29.11.1997) are compared and the time-face advance dependents parts of the predicted profile are shown in Figure 6-7.

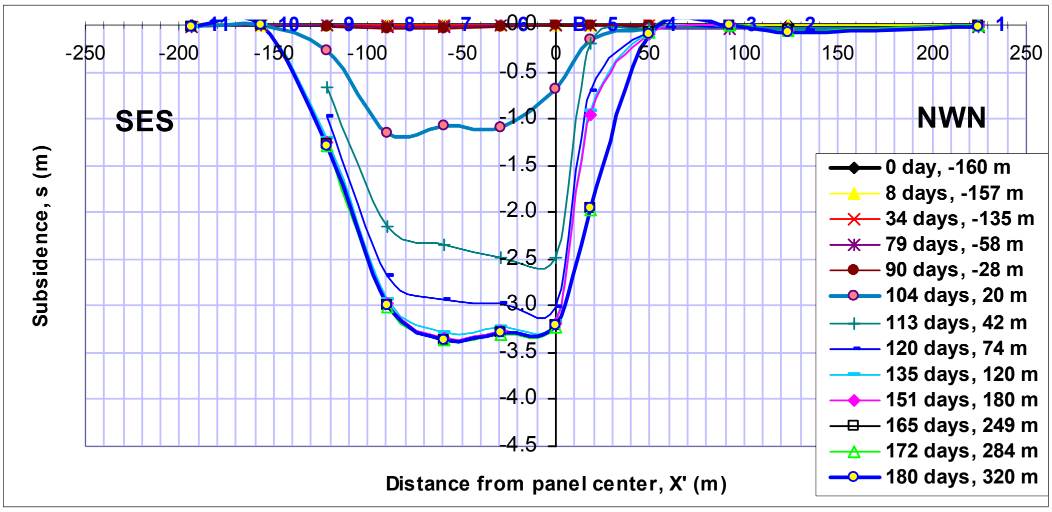

Figure 6-6 Subsidence along BB' section of panel B14 at different dates.

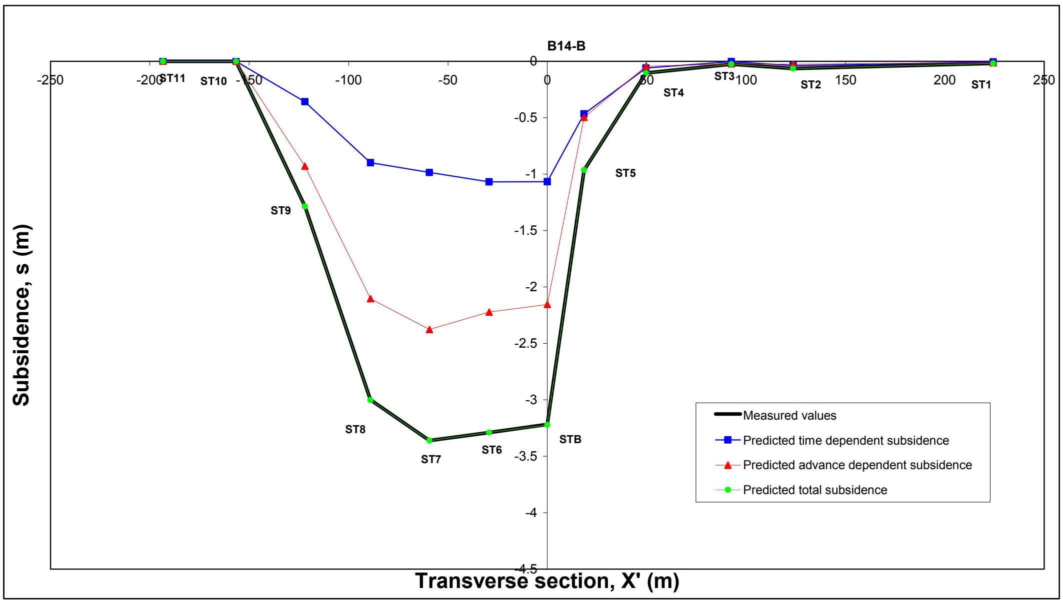

Figure 6-7 Comparison of measured and predicted values for the final measurement date, along BB' section of panel B14.

After the mathematical model is established, the subsidence velocity (mm/day) and subsidence acceleration (mm/day^2) profiles are derived and the typical results are shown in Figure 6-8, using the coefficients estimated for St.7.

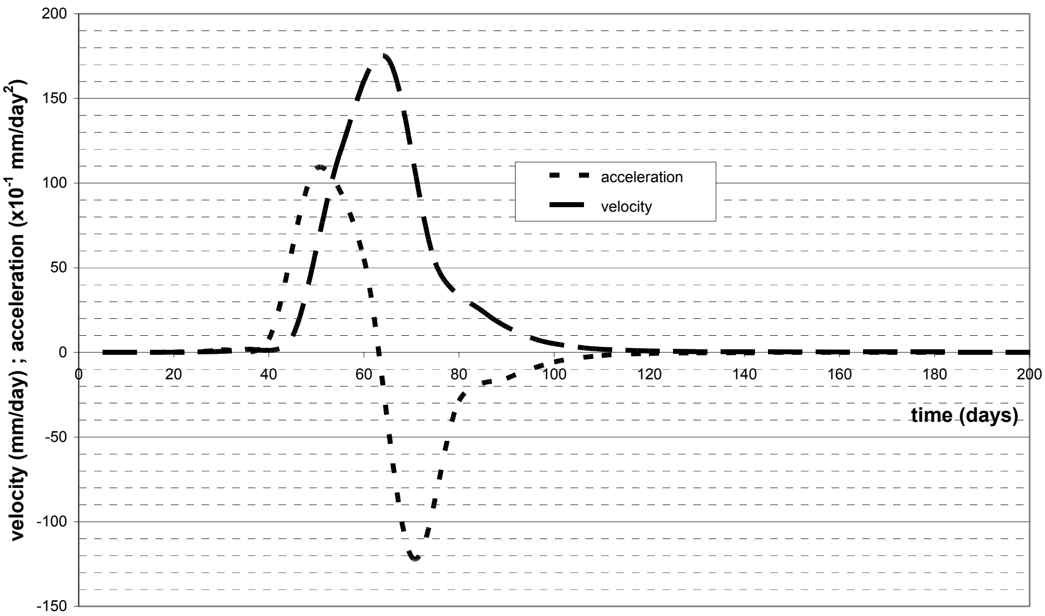

Figure 6-8 Velocity and acceleration profiles of the model for St.7.

6.2. OTHER APPROACHES FOR SUBSIDENCE ESTIMATION

6.2.1. PROFILE FUNCTION METHODS

Indian, Hungarian and Donetz profile functions presented in Chapter 2 are applied to some panels for curve fitting.

Coefficient of determination (R^2) is one of the factors to test the model and can be evaluated as follows:

$$R^2 = 1 - \frac{\sum_{i=1}^{n}(S_i - S_i^p)^2}{\sum_{i=1}^{n}(S_i - \overline{S})^2} \qquad [6\text{-}15]$$

where S_i and S_i^p are i-th measured and predicted subsidence values, respectively. $\overline{S}$ is the average of all the values of S_i.

R^2 is obtained by the principle of least squares. The higher the value of R^2 (R) is, the better is the model. Curve fitting is said to very good for the values greater than 95% (Zhang, 1996). In general however, correlation coefficient (R) of 0.7 is said to be good estimation. As it can be seen from the following figures, R^2 values for profile function estimations are greater than 0.90.

Table 6-3 shows subsidence estimation using Indian profile function for subcritical case for B line of panel B02. By trial and error, best fit ($R^2 = 0.95$) is obtained by taking maximum subsidence as 3.5 m, p (distance of the subsidence trough margin to the subsidence center) as 200 m and n as 5. Following figures (Figure 6-9 to Figure 6-17) show various profile function estimations along some transverse sections. Estimated and measured values can be compared using these figures. Profile function equations, related parameters and R^2 values are presented in the figures.

Table 6-3 Subsidence prediction using Indian profile function for B line over B02.

$s_{meas.}$ (m)	S (m)	n	X (m)	P (m)	$s_{pred.}$ (m)
0.10	3.50	5	149.030	200	-0.01
-0.06	3.50	5	120.623	200	-0.20
-1.13	3.50	5	80.453	200	-1.33
-2.70	3.50	5	58.171	200	-2.20
-3.18	3.50	5	33.606	200	-3.03
-3.29	3.50	5	5.714	200	-3.49
-3.40	3.50	5	-26.154	200	-3.21
-1.60	3.50	5	-70.866	200	-1.71
-0.26	3.50	5	-124.969	200	-0.14
-0.11	3.50	5	-150.044	200	-0.01

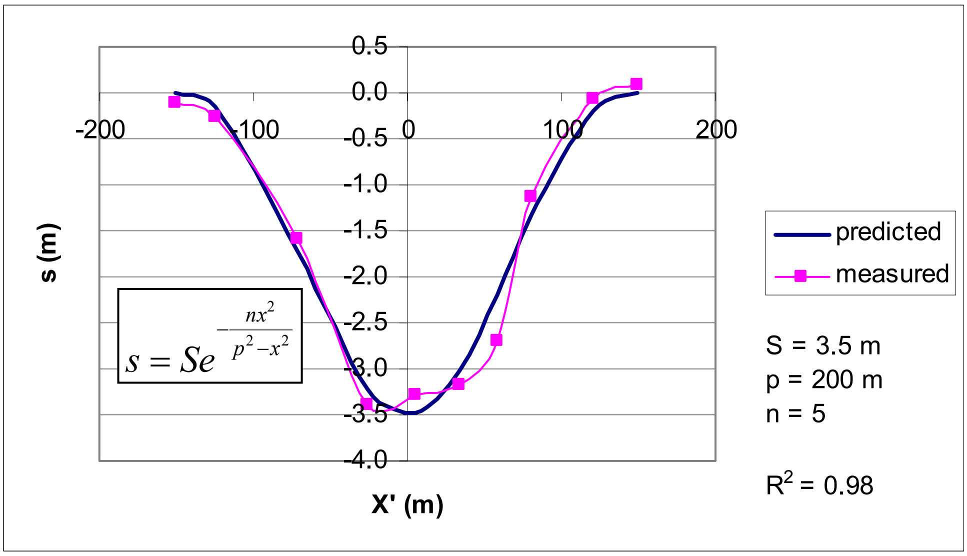

Figure 6-9 Estimation by Indian profile function (subcritical) for B line over B02.

In Figure 6-10 estimated values by Hungarian profile function method and actual measurements (belonging to B section of the B02 panel) are compared, and R^2 is found as 0.96.

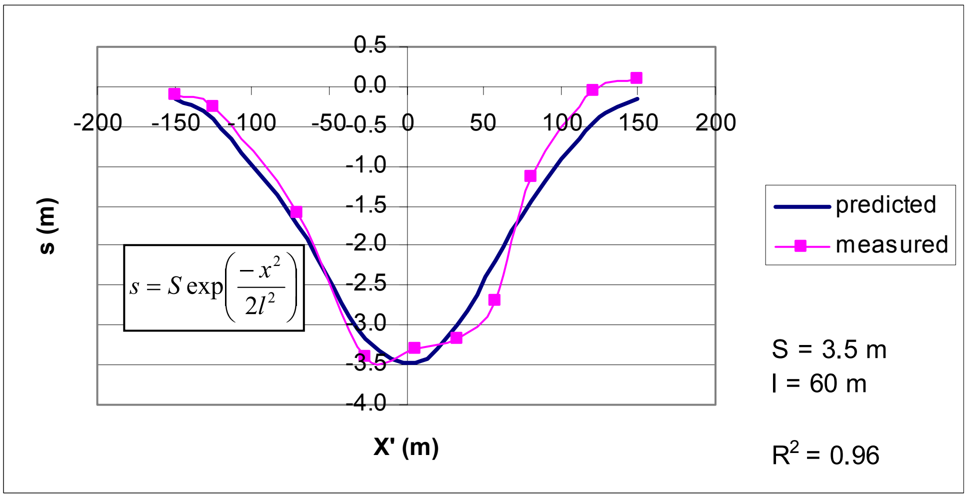

Figure 6-10 Estimation by Hungarian profile function for B line over panel B02.

Left hand side of the B line of B10 panel is similar to the subcritical condition, and right hand side to supercritical condition. Therefore both subcritical and supercritical estimations of Indian profile function are used. Subsidence center is shifted 5m left from the panel center. Therefore necessary corrections are done for x and p values in the model. (Figure 6-11).

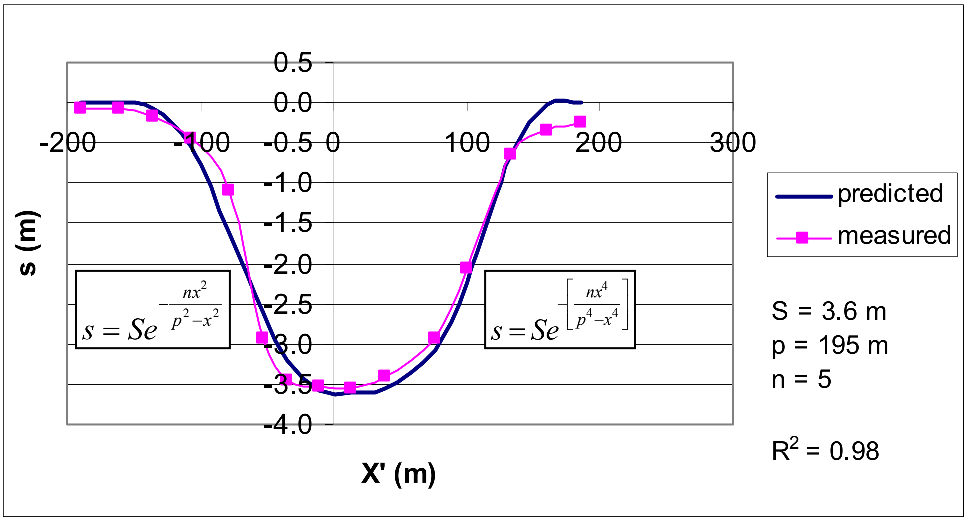

Figure 6-11 Estimation by Indian profile function (subcritical and critical) for B line over panel B10.

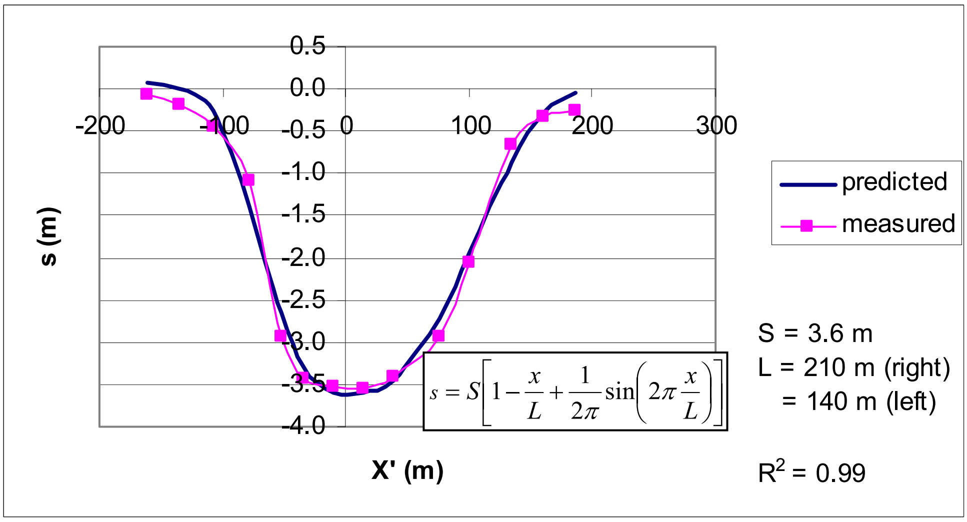

Figure 6-12 Estimation by Donetz profile function for B line of panel B10.

Center of subsidence trough along C section over panel B12 is located 20 m left of panel center.

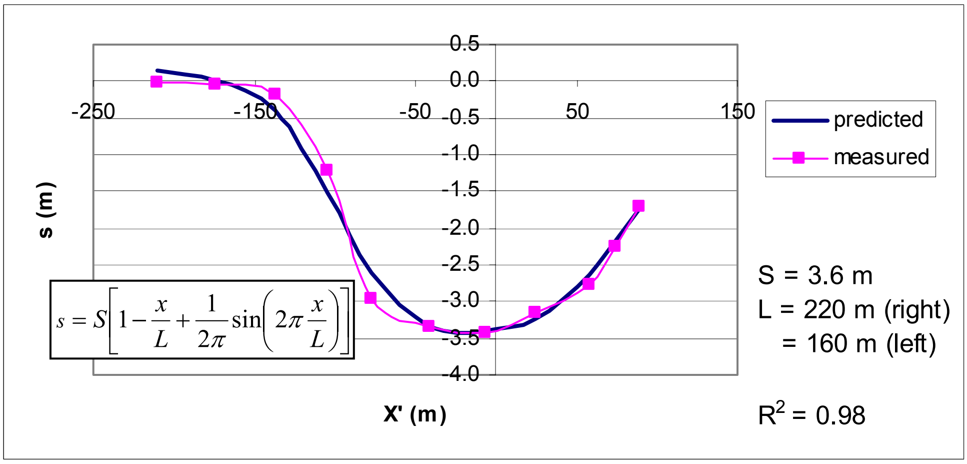

Figure 6-13 Estimation by Donetz profile function for C line over panel B12.

Center of subsidence trough along B section over panel C08 is located 30 m right of panel center.

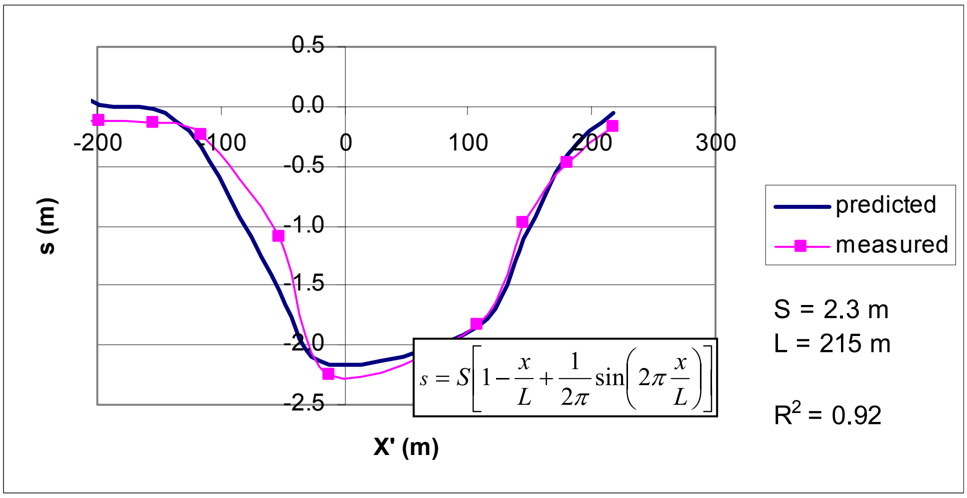

Figure 6-14 Estimation Donetz profile function B line over panel C08.

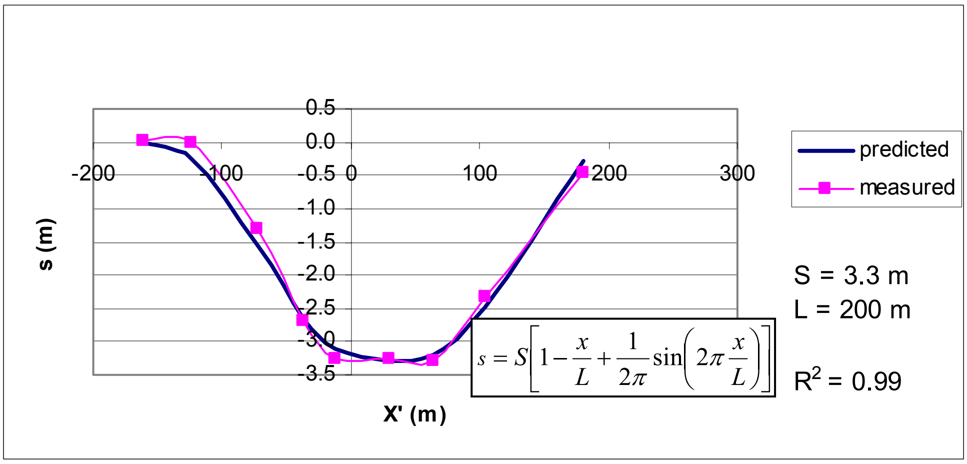

Figure 6-15 Estimation Donetz profile function C line over panel C08.

Center of subsidence trough along B section over panel C10 is located 10 m right of panel center.

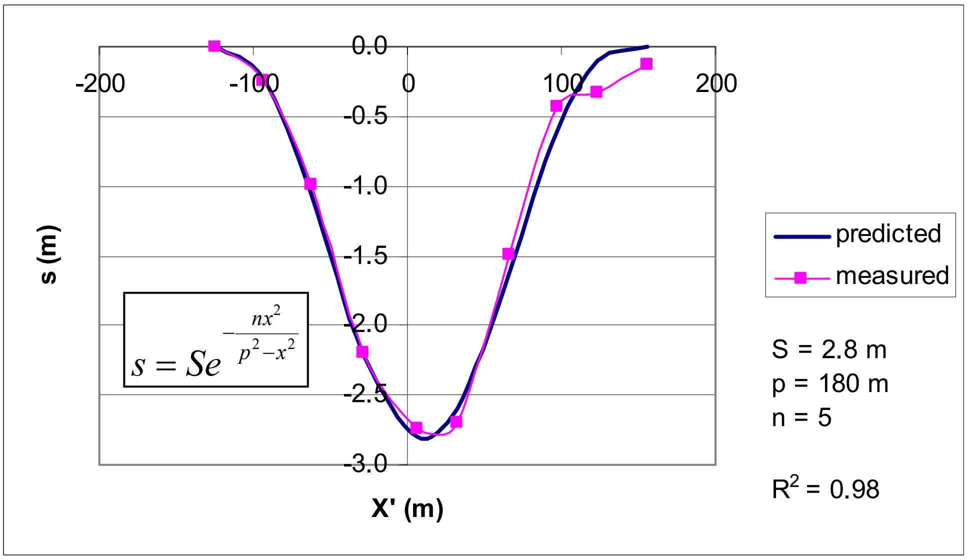

Figure 6-16 Estimation by Indian profile function (subcritical) for B line over C10.

Center of subsidence trough along D section over panel C12 is located 20 m left of panel center.

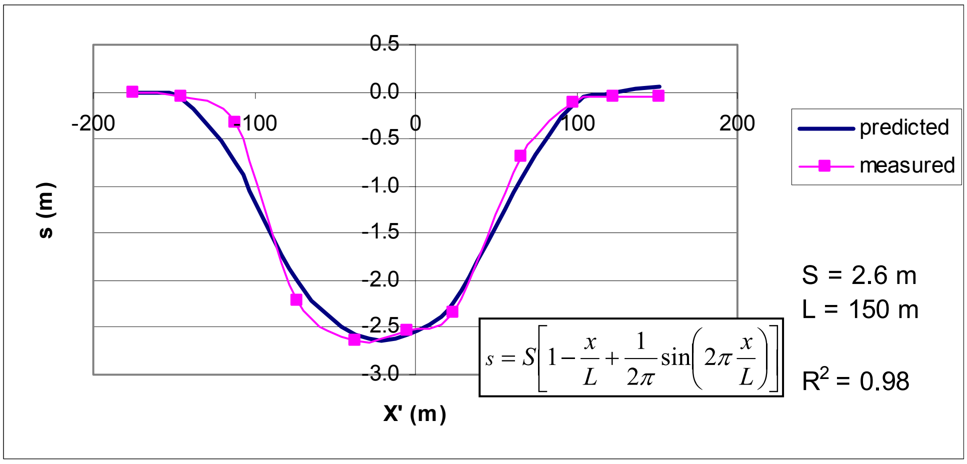

Figure 6-17 Estimation Donetz profile function D line over panel C12.

6.2.2. GRAPHICAL METHOD AND ESTIMATIONS FOR INCLINED SEAMS

Lin et al. (1992 b) stated that the maximum subsidence angle (φ), demonstrated in Figure 6-18, is equal to the dip angle of the seam (α), for gently inclined seams (α up to 20-25º).

In Çayırhan Coal Mine, φ vales determined by section views (demonstaring original surface, subsided surface, coal seam) in Appendix B, are generally smaller than the dip angle.

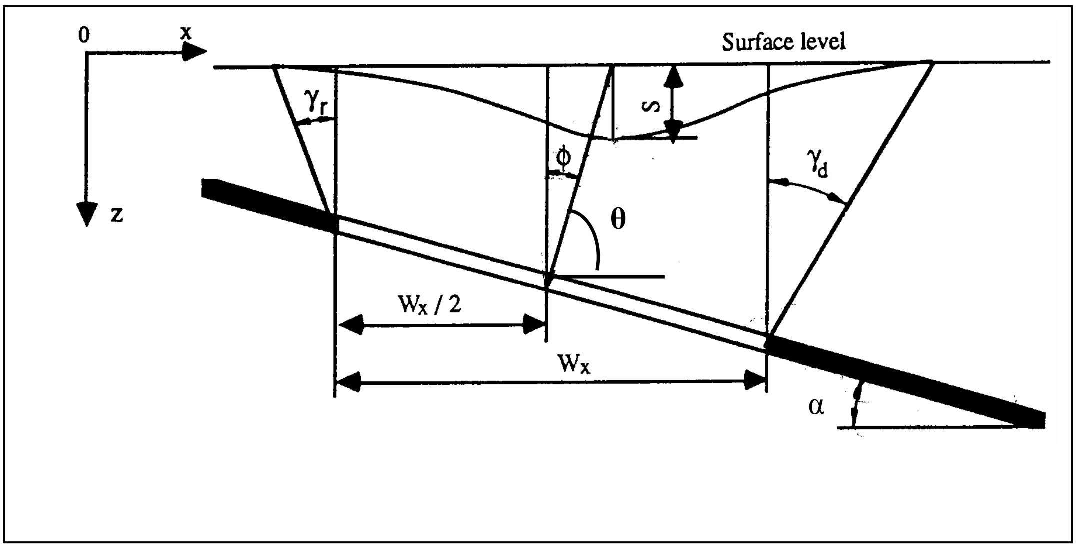

Figure 6-18 An Inclined seam subsidence trough on the transverse cross-section (Lin et al., 1992 b)

Maximum subsidence for inclined seams is given by Liu (1991):

$$S_{max} = S_{\theta\max} \sin\theta = a\, M_\theta \sin\theta \qquad [6\text{-}16]$$

where

θ : angle of extraction influence transmission

$$\theta = 90 - \alpha\, K(Z) \qquad [6\text{-}17]$$

where $K(Z)$ is a coefficient dependent on the properties of the rock mass and changing between 0 and 1.

$S_{\theta\max}$: the maximum ground surface displacement in the direction of θ

M_θ : the effective coal seam thickness in the direction of θ

$$M_\theta = \mathrm{M} / \cos\,[\alpha\,(1\text{-}\mathrm{K})] \qquad [6\text{-}18]$$

For K = 1, the line connecting seam center and maximum subsidence is assumed to be perpendicular to seam:

$\theta = 90 - \alpha$ ($\sin\theta = \cos\alpha$); $M_\theta = M$. So:

$$S_{max} = a\ M \cos\alpha \qquad [6\text{-}19]$$

For K=0, maximum subsidence is assumed to be just above the centroid of the seam:

$\theta = 90$ ($\sin\theta = 1$); $M_\theta = M/\cos\alpha$. So:

$$S_{max} = a\ M/\cos\alpha \qquad [6\text{-}20]$$

(In Equation 6-16, "$M_\theta \sin\theta$" is the vertical component of M_θ. This component is shown in Figure 6-19 as $M_{\theta V}$).

Also in Çayırhan Coal Mine, it is generally observed that the K takes values between 0 and 1.

Assuming a constant panel width of 220 m, for depths smaller than 157 m, the condition becomes supercritical according to the Table E.1 given in Appendix E and the subsidence factor (*a*) is found as 0.9.

Above the panels where subsidence measurements were carried out, minimum subsidence factor (*a*) is found as 0.84 for a width to depth ratio of 1.

For a width to average depth (180 m) ratio of 1.22, average subsidence factor is found as 0.87 by interpolation.

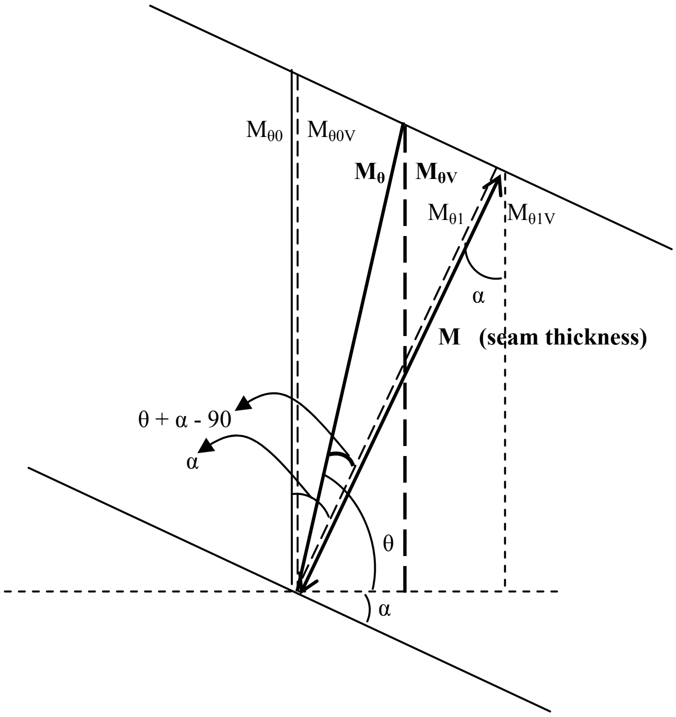

Figure 6-19 Effective extraction thickness (M_θ) and its vertical component ($M_{\theta V}$)

For horizontal seam extraction, maximum subsidence is estimated between 3.1 m and 3.3 m for B panels, and between 3.6 and 3.9 m for C panels.

Maximum strain due to extension and maximum ground tilt values can be also determined using Table E.1.

Sample calculation of maximum subsidence and horizontal starains is given below, for EE' line over panel B4:

- a = 0.9 (W/H > 1.4)

- $Smax = a\ M \cos\alpha$ (K is assumed as 1)

$$= (0.9)(3.7)(\cos 22)$$
$$= 3.09 \text{ m}$$

Actual value of maximum subsidence was measured as 3.14 m for this section.

- $-E = 0.52\ Smax/H = 0.52\ (3.08/110)$
  $= 14.56$ mm/m

- $+E = 0.65\ Smax/H = 0.65\ (3.08/110)$
  $= 18.2$ mm/m

CHAPTER 6

CONCLUSIONS AND RECOMMENDATIONS

7.1. CONCLUSIONS

The analysis of rock mass movements due to excavation operations is one important concept of rock mass mechanics. Based on studies carried out in this thesis, the following conclusions can be drawn.

- Local measurements are essential for a conclusive interpretation of field measurements.

- As shown in this study, the collected data was combined to arrive at a conclusive overall picture of the ground movement, its extent and its duration.

- The study of surface subsidence profiles along the rows of measurement stations led to the following results:

    - Width to depth ratio is about 1.2. So this is a subcritical condition, since this value is smaller than 1.4. However, subsidence profiles show also supercritical property in some parts. This may be because of the change in depth and seam inclination as explained in Graphical Methods in Chapter 6.

    - Subsidence factor *a* is about 0.87.

    - The subsidence profiles were asymmetrical because of inclined seam mining. However, the amout of deviation is not so much.

    - Subsidence center is shifted both to the rise and dip side, but mostly to the dip side which means that K is changing between 0 and 1. The average amount of shifting is about 20 m.

    - Distance from subsidence center to the trough margin changes from 130 m (steeper angle of draw) to 250 m. The influenced area and angle of draw is generally greater in the dip side.

- The exact location of crack initiation mode can be identified better by local deformation measurements.

- The subsidence model in this study was developed as a function of time and the profile functions are used to estimate of subsidence profiles according to distance from panel center. The correlation between the actual and predicted values was high for both estimations.

7.2. RECOMMENDATIONS

It is recommended that, the study conducted throughout this thesis should be extended to include the other panels of Çayırhan coal mine and other mine sites which are liable to subsidence problems. The measurement time before and after the panel production should be extended to be able to measure the residual subsidence and the effect of previous workings.

Physical meaning of the constants used in the model equation should be interpreted in future studies. The mathematical model suggested in this study can be simplified to be more applicable.

REFERENCES

AKSOY C.O., KOSE H., ONARGAN T., KOCA Y. and HEASLY K., 2004. “Estimation of limit angle using laminated displacement discontinuity analysis in Soma coal field, Western Turkey, International Journal of Rock Mechanics and Mining Sciences, vol. 41, pp. 547-556.

ALEJANO L.R., RAMIREZ-OYANGUREN P. and TABOADA J., 1999. “FDM predictive methodology for subsidence due to flat and inclined coal seam mining”, International Journal of Rock Mechanics and Mining Sciences, vol. 36, pp. 475-491.

ASTON T.R.C., TAMMEMAGI H.Y. and POON A.W., 1987. “A Review and Evaluation of Empirical and Analytical Subsidence Prediction Techniques”, Mining Science and Technology, vol. 5, pp. 59-69.

BAHAGUNA P.P., SRIVASTAVA A.M.C. and SAXENA N.C., 1991. “A critical review of mine subsidence prediction methods”, Mining Science and Technology, vol. 13, pp. 369-382.

BELL F.G., STACEY T.R. and GENSKE D.D., 2000. “Mining subsidence and its effect on the environment: some differing examples”, Environmental Geology vol. 40 (1-2), pp 135-152.

CUI X., MIAO X., WANG J., YANG S., LIU H., SONG Y., LIU H. and HU X., 2000. “Improved prediction of differential subsidence caused by underground mining", International Journal of Rock Mechanics and Mining Sciences, vol. 37, pp. 615-627.

DALGIÇ A., 1996. "O.A.L. Çayırhan işletmesinde kömür kesimi aakliyesi ve ramble atımı gibi faaliyetler esnasında oluşan tozun azaltılmasına yönelik çözümler", Maden Mühendisliği Anabilim Dalında Yüksek Lisans Tezi, Ç.Ü., 107 pages.

CUI X. and WANG J., 2001. "Technical note: Prediction of progressive surface subsidence above longwall coal mining using a time function", International Journal of Rock Mechanics and Mining Sciences, vol. 38, pp. 1057-1063.

GARCIA A.B. and MERES J.O., 1997. "Technical Note: Parameter optimization of influence functions in mining subsidence", International Journal of Rock Mechanics and Mining Sciences, vol. 34, 1125-1131.

HEASLEY K.A. and BARTON T.M., 1999. "Coal mine subsidence prediction using a boundary-element program", International Journal of Rock Mechanics and Mining Sciences, vol. 36, pp.475-491.

HOOD M., EWY R.I. and RIDDLE L.R., 1983. "Empirical methods of subsidence prediction—a case study from Illinois", Int. J. of Rock Mech. Min. Sci. Geomech. Abstr., vol. 20 (4), pp. 153–170.

HUAYANG D., INZHUANG W., MEIFENG C., LIXIN W. and ZENGZHANG G., 2002. "Seam dip angle based mining subsidence model and its application", International Journal of Rock Mechanics and Mining Sciences, vol. 39, pp. 115-123.

JEREMIC M.L., 1985. Strata Mechanics in Coal Mining, Rotterdam, Netherlands; Boston: A.A. Balkemia, 400 pages.

KWINTA A., HEJMANOVSKI R. and SROKA A.,1996. “A time function analysis used for the prediction of rock mass subsidence”, Proceedings of the '96 Int. Symp. on Mining Science and Technology; XUZHOU; JIANGSU, China.

KRATZSCH H., 1983. “Mining Subsidence Engineering”, Berlin, New York: Springer-Verlag, 543 pages.

LIAO C.P., 1993. “Fuzzy influence function method for calculating mine subsidence in a horizontal seam”, Geotechnical and Geological Engineering, vol. 11, pp. 235-47.

LIN S, REDDISH D.J. and WHITTAKER B.N., 1992 a. “An integrated analytical model of subsidence induced by level seam extractions”, Geotechnical and Geological Engineering, vol. 10, pp. 203-21.

LIN S., WHITTAKER B.N. and REDDISH D.J., 1992 b. “Application of asymmetrical influence functions for subsidence prediction of gently inclined seam extractions”, International Journal of Rock Mechanics and Mining Sciences, vol. 29, pp. 479-90.

PENG S.S., 1992. “Surface Subsidence Engineering”, Littleton, Colo.: Society for Mining, Metallurgy, 161 pages.

REN G., REDDISH D. J. and WHITTAKER B. N., 1987. “Mining subsidence and displacement prediction using influence function methods”, Mining Science and Technology, vol. 5, pp. 89-104.

SHEOREY P.R., LOUI J.P., and SINGH K.B., SINGH S.K., 2000. “Ground subsidence observations and a modified influence function method for complete subsidence prediction”, International Journal of Rock Mechanics and Mining Sciences, vol. 37, pp. 801-818.

SINGH M.M., 1992. Chapter 10.6, “Mine Subsidence”, SME Mining Engineering Handbook, 2nd Edition, ed., Hartman, vol. 1, pp. 938-971.

SINGH K.B. and SINGH T.N., 1998. “Ground movements over longwall workings in the Kamptee coalfield, India”, Engineering Geology, vol. 50, pp. 125-139.

SUTHERLAND H.J. and MUNSON D.E., 1984. “Prediction of subsidence using complementary influence functions”, International Journal of Rock Mechanics and Mining Sciences, vol.21, no. 4, pp. 195-202.

UNAL E., ÇAKMAKÇI G., ERDEM B. and AYDIN Y., 1998. “Uzun ayak panosu üzerinde oluşan tasmanın yüzeydeki enerji iletim hattı pilonlarına etkisinin incelenmesi”, Türkiye 11. Kömür Kongresi, Bartın-Amasra, pp65-76.

UNAL E., ÖZKAN İ. and ÇAKMAKÇI G., 2001. “Modeling the behavior of longwall coal mine gate roadways subjected to dynamic loading”, International Journal of Rock Mechanics and Mining Sciences, vol.38, pp. 181-197.

UNVER T., 1993. “Subsidence monitoring studies at Çayırhan Lignite Mine, T.K.İ.”, M.Sc. Thesis, Department of Mining Engineering, METU, 74 pages.

WENXIU Li., 1991. “Fuzzy mathematics method for theoretical analysis of ground movements due to underground excavation”, Mining Science and Technology, vol. 13, pp. 45-56.

WHITTAKER B.N. and REDDISH DJ., 1989. “Subsidence: Occurrence, Prediction and Control”, Amsterdam, Elsevier, 528 pages.

WHITTAKER B.N. and REDDISH D.J.(first part); BAOCHEN LIU (second part), 1991. Comprehensive Rock Engineering, Ed. by J. A. Hudson, Pergamon Press, Vol. 4, pp. 751-817.

YONG B.J. and SUNG O.C., 2005. “Ground subsidence estimation and prediction using artificial neural network”, World Tunnel Congress (ITA. AITES, 2005), May 7-12, Istanbul, Turkey. In press.

ZHANG M., 1996. “Critical review of the state-of-art subsidence prediction methods”, Proceedings of the '96 Int. Symp. on Mining Science and Technology; Xuzhou; Jiangsu, China.

APPENDIX – A
Measurements

The raw data consisting of 3D coordinates indicating the location of measurement stations are presented below:

Table A.1 Raw data for Panel B02

Measurements along A line

Station No.	08.08.2001			22.08.2001			27.08.2001		
	X	Y	Z	X	Y	Z	X	Y	Z
A	87734.228	42900.336	778.661	87734.184	42900.348	778.547	87734.260	42900.306	778.664
1	87678.624	42874.244	779.159	87678.577	42874.206	779.166	87678.021	42873.956	778.946
2	87654.510	42862.898	779.395	87654.491	42862.864	779.353	87653.891	42862.721	778.777
3	87621.905	42848.000	779.443	87621.901	42848.048	779.384	87621.716	42848.000	778.395
B	87588.111	42832.340	777.530	87588.149	42832.357	777.540	87588.305	42832.416	777.261
4	87553.493	42816.211	777.109				87553.478	42816.236	777.094
5	87521.938	42801.575	776.578				87521.935	42801.509	776.588
C	87491.701	42787.558	770.343						
6	87458.513	42772.140	773.899						
7	87425.351	42756.805	774.195						
8	87386.332	42738.769	776.050						
9	87344.383	42719.298	775.575						
10	87301.481	42699.379	774.920						

Station No.	01.09.2001			15.09.2001			01.10.2001		
	X	Y	Z	X	Y	Z	X	Y	Z
A	87734.225	42900.313	778.630	87734.114	42900.342	778.692			
1	87677.644	42873.766	778.865	87677.183	42873.592	778.669			
2	87653.436	42862.481	778.431	87652.410	42862.180	778.008			
3	87621.270	42847.736	777.529	87620.021	42847.223	776.440	87619.709	42847.091	776.399
B	87588.522	42832.501	776.779	87588.099	42832.238	774.683	87587.353	42832.005	774.240
4	87553.511	42816.230	777.123	87554.167	42816.451	775.922	87553.758	42816.382	774.476
5	87521.946	42801.596	776.616	87522.210	42801.668	776.436	87522.333	42801.684	774.746
C	87491.664	42787.564	770.370	87491.684	42787.554	770.335	87491.919	42787.740	770.097
6	87458.458	42772.154	773.953	87458.469	42772.141	773.906	87458.480	42772.182	773.981
7				87425.301	42756.796	774.217	87425.261	42756.834	774.277
8							87386.282	42738.786	776.110
9							87344.341	42719.314	775.635

Table A.1 Raw data for Panel B02 (cont.)

Station No.	11.10.2001			13.10.2001			01.11.2001		
	X	Y	Z	X	Y	Z	X	Y	Z
4				87552.698	42815.611	773.929			
5				87521.296	42801.305	773.263	87520.761	42801.047	772.936
C				87491.887	42787.834	767.840	87491.039	42787.626	766.858
6				87459.177	42772.645	772.889			
7				87425.495	42757.047	774.114	87425.639	42757.110	771.939
8				87386.233	42738.801	776.077	87386.775	42739.128	775.499
9				87344.287	42719.313	775.627	87344.311	42719.324	775.519
10				87301.401	42699.371	774.946	87301.377	42699.385	774.911
11	87246.645	42673.865	773.055				87246.614	42673.873	773.022
12	87192.103	42648.582	772.377						
13	87145.529	42626.968	768.889						
14	87107.456	42609.317	765.127						
15	87060.546	42587.575	750.686						
16	86998.331	42558.719	742.875						
17	86941.642	42532.422	736.392						
18	86890.642	42508.805	724.496						
D	86812.566	42472.621	717.567						
19	86753.933	42445.441	729.701						
20	86703.166	42421.926	730.099						

Station No.	16.11.2001			01.12.2001			19.12.2001		
	X	Y	Z	X	Y	Z	X	Y	Z
C	87490.668	42787.549	766.731						
6									
7	87424.603	42756.768	770.697	87424.376	42756.796	770.576			
8	87386.093	42739.040	772.749	87385.458	42738.908	772.357			
9	87344.838	42719.844	774.045	87344.150	42719.614	772.308	87343.500	42719.472	771.900
10	87301.540	42699.575	774.754	87301.997	42699.936	773.191	87301.248	42699.765	771.570
11	87246.617	42673.863	773.046	87246.657	42673.945	772.972	87247.277	42674.609	771.634
12	87192.087	42648.585	772.368	87192.053	42648.579	772.382	87192.052	42648.645	772.357
13				87145.488	42626.950	768.872	87145.470	42627.006	768.862
14							87107.362	42609.360	765.138
15							87060.461	42587.594	750.709

Station No.	02.01.2002			22.01.2002			02.02.2002		
	X	Y	Z	X	Y	Z	X	Y	Z
10	87300.482	42699.544	771.221	87300.230	42699.478	771.079			
11	87246.771	42674.537	769.864	87245.791	42674.394	769.236			
12	87192.438	42648.933	771.746	87191.806	42648.806	769.085			
13	87145.467	42626.951	768.890	87146.050	42627.445	767.173	87143.282	42626.851	764.734
14	87107.354	42609.249	765.127	87107.625	42609.540	764.963	87105.112	42609.424	760.933
15	87060.423	42587.486	750.706	87060.605	42587.696	750.726	87058.945	42587.969	747.568
16	86998.224	42558.655	742.918	86998.407	42558.850	742.892	86998.465	42558.942	742.538
17				86941.712	42532.625	736.404	86941.667	42532.491	736.452
18							86890.635	42508.884	724.540

Table A.1 Raw data for Panel B02 (cont.)

Station No.	07.02.2002			15.02.2002			14.03.2002		
	X	Y	Z	X	Y	Z	X	Y	Z
11	87245.545	42674.473	769.310						
12	87190.824	42648.663	768.832	87190.569	42648.527	768.587			
13	87144.789	42627.177	765.476	87143.942	42626.942	764.925			
14	87107.402	42609.990	763.213	87106.282	42609.696	761.553	87104.709	42609.340	760.799
15	87060.457	42587.694	750.870	87060.110	42588.090	750.090	87058.124	42587.755	746.908
16	86998.359	42558.843	743.042	86998.244	42558.603	742.917	86997.859	42559.036	739.795
17	86941.606	42532.521	736.645	86941.618	42532.391	736.432	86941.372	42532.562	734.806
18							86890.122	42508.901	724.202
D							86812.541	42472.574	717.731
19							86753.912	42445.411	729.855

Station No.	15.04.2002			01.05.2002			17.05.2002		
	X	Y	Z	X	Y	Z	X	Y	Z
16	86997.179	42558.748	739.317						
17	86940.433	42532.159	732.974	86940.152	42532.061	732.969			
18	86888.949	42508.591	721.355	86888.600	42508.300	721.355	86888.525	42508.370	720.949
D	86812.633	42472.523	717.580	86813.095	42472.352	715.309	86813.121	42472.310	714.414
19	86753.950	42445.365	729.743	86754.094	42445.243	729.603	86754.802	42445.504	726.943
20	86703.150	42421.825	730.256	86703.077	42421.090	730.274	86703.665	42421.920	729.612
21	86654.619	42399.426	722.001	86654.440	42397.424	721.964	86654.661	42399.450	721.944
22	86600.648	42374.269	706.635				86600.676	42374.337	706.523
23	86546.191	42349.045	707.319						
24	86502.974	42329.025	701.595						
25	86457.790	42308.075	696.488						
26	86412.395	42287.067	691.549						
E	86368.037	42266.503	683.343						
27	86331.159	42249.405	677.601						
28	86297.981	42234.056	670.499						
29	86230.270	42202.673	657.061						
30	86177.234	42177.965	649.840						
31	86126.066	42154.446	644.575						
32	86078.403	42132.344	641.615						

Station No.	01.06.2002			15.06.2002			01.07.2002		
	X	Y	Z	X	Y	Z	X	Y	Z
D	86812.967	42472.181	714.324						
19	86754.710	42445.060	726.236	86753.901	42444.901	726.090	86753.855	42444.944	726.070
20	86703.505	42421.493	727.162	86702.648	42420.881	726.426	86702.360	42420.746	726.225
21	86654.771	42399.320	721.507	86654.224	42398.488	719.155	86653.667	42398.059	718.460
22	86600.688	42374.336	706.576	86600.806	42374.214	706.282	86600.899	42373.859	704.497
23	86546.200	42349.095	707.312	86546.239	42348.981	707.301	86546.378	42349.092	707.096
24				86503.034	42328.992	701.540	86503.011	42329.097	701.491
25							86457.812	42308.117	696.426
26							86412.386	42287.081	691.559

Station No.	15.07.2002			31.07.2002			16.08.2002		
	X	Y	Z	X	Y	Z	X	Y	Z
21	86653.495	42397.845	718.247	86653.342	42397.739	718.284			
22	86600.544	42373.375	703.676	86600.280	42373.155	703.435	86600.111	42372.894	703.233
23	86546.971	42348.958	706.146	86546.803	42348.473	704.620	86546.191	42347.932	703.843
24	86503.209	42329.047	701.207	86503.413	42328.996	700.630	86503.243	42328.204	698.381
25	86457.845	42308.021	696.318	86457.959	42308.080	696.360	86457.988	42307.761	695.574
26	86412.418	42287.009	691.473	86412.440	42287.054	691.550	86412.529	42286.927	691.307
E	86368.057	42266.520	683.242	86368.008	42266.547	683.328	86368.020	42266.363	683.229
27							86331.159	42249.261	677.505

Table A.1 Raw data for Panel B02 (cont.)

Station No.	02.09.2002			18.09.2002			30.09.2002		
	X	Y	Z	X	Y	Z	X	Y	Z
23	86545.946	42347.736	703.876						
24	86502.636	42327.855	697.962	86502.385	42327.866	697.881			
25	86457.544	42307.385	693.778	86456.933	42307.045	693.095	86456.680	42306.842	692.890
26	86412.787	42286.868	690.902	86412.273	42286.650	689.691	86411.742	42286.182	688.306
E	86368.136	42266.371	683.255	86368.826	42266.821	682.590	86368.847	42266.546	681.060
27	86331.184	42249.151	677.580	86331.304	42249.529	677.480	86331.950	42249.776	677.031
28	86297.979	42234.067	670.388	86297.982	42234.093	670.374	86298.077	42234.084	670.172
29							86230.215	42202.819	656.838

Station No.	16.10.2002			31.10.2002			16.11.2002		
	X	Y	Z	X	Y	Z	X	Y	Z
25	86456.659	42306.813	692.874						
26	86411.398	42285.973	688.067	86411.409	42285.959	688.009			
E	86368.206	42266.023	679.927	86367.919	42265.848	679.773			
27	86331.913	42249.486	675.190	86331.335	42248.940	674.253	86331.161	42249.137	674.123
28	86298.880	42234.222	669.407	86298.434	42233.745	667.483	86298.001	42233.771	667.127
29	86230.323	42202.788	656.812	86230.594	42202.831	656.701	86230.968	42202.938	655.180
30	86177.273	42177.948	649.688	86177.300	42178.089	649.714	86177.308	42178.296	649.690
31				86126.079	42154.546	644.397	86126.079	42154.700	644.415
32							86078.412	42132.556	641.456

Measurements along B line

Station No.	08.08.2001			22.08.2001			27.08.2001		
	X	Y	Z	X	Y	Z	X	Y	Z
B	87588.111	42832.340	777.530	87588.149	42832.357	777.540	87588.305	42832.416	777.261
1	87527.692	42962.416	763.144	87527.627	42962.452	763.212	87527.663	42962.427	763.172
2	87539.571	42936.864	767.466	87539.522	42936.905	767.501	87539.578	42936.885	767.503
3	87556.329	42900.802	771.264	87556.227	42900.828	771.229	87556.365	42900.790	771.254
4	87565.756	42880.440	773.302	87565.668	42880.494	773.321	87565.812	42880.456	773.295
5	87576.302	42857.813	775.076	87576.278	42857.848	775.105	87576.446	42857.848	774.995
6	87602.019	42802.517	783.668	87601.988	42802.565	783.655	87602.207	42802.747	783.391
7	87621.166	42761.295	795.617	87621.059	42761.380	795.626	87621.240	42761.422	795.534
8	87643.533	42713.285	803.816	87643.434	42713.368	803.799	87643.509	42713.328	803.778
9	87654.047	42690.757	801.880	87653.992	42690.795	801.858	87654.054	42690.776	801.888

Station No.	01.09.2001			15.09.2001			01.10.2001		
	X	Y	Z	X	Y	Z	X	Y	Z
B	87588.522	42832.501	776.779	87588.099	42832.238	774.683	87587.353	42832.005	774.240
1	87527.646	42962.443	763.226	87527.767	42962.310	763.137	87527.644	42962.293	763.240
2	87539.562	42936.901	767.552	87539.715	42936.637	767.371	87539.557	42936.505	767.410
3	87556.372	42900.808	771.232	87556.551	42900.373	770.373	87556.254	42899.968	770.132
4	87565.926	42880.440	773.054	87565.747	42879.837	771.083	87565.251	42879.579	770.602
5	87576.621	42857.909	774.607	87576.499	42857.639	772.300	87575.795	42857.391	771.900
6	87602.243	42802.969	782.824	87601.368	42803.019	780.575	87600.551	42802.998	780.267
7	87621.194	42761.730	795.342	87620.373	42762.787	794.376	87619.612	42762.551	794.020
8	87643.484	42713.394	803.780	87643.274	42713.605	803.578	87643.033	42713.776	803.551
9	87654.028	42690.814	801.878	87653.864	42690.897	801.759	87653.668	42691.068	801.769

Table A.1 Raw data for Panel B02 (cont.)

Measurements along C line

Station No.	08.08.2001			01.09.2001			15.09.2001		
	X	Y	Z	X	Y	Z	X	Y	Z
C	87491.701	42787.558	770.343	87491.664	42787.564	770.370	87491.684	42787.554	770.335
1	87427.200	42926.758	762.519	87427.150	42926.739	762.591	87427.199	42926.687	762.483
2	87444.366	42889.532	757.659	87444.265	42889.566	757.757	87444.311	42889.525	757.670
3	87459.267	42857.322	762.536	87459.178	42857.387	762.581	87459.219	42857.337	762.516
4	87469.011	42836.628	766.200	87468.921	42836.632	766.248	87468.929	42836.596	766.167
5	87479.327	42814.322	766.406	87479.254	42814.352	766.455	87479.311	42814.324	766.413
6	87508.352	42751.520	773.210	87508.317	42751.544	773.277	87508.305	42751.554	773.226
7	87523.007	42720.163	776.789	87522.963	42720.195	776.797	87522.949	42720.181	776.739
8	87543.315	42676.347	781.506	87543.254	42676.379	781.524	87543.245	42676.362	781.495
9	87560.583	42638.897	781.847	87560.546	42638.936	781.855	87560.543	42638.901	781.854

Station No.	01.10.2001			13.10.2001		
	X	Y	Z	X	Y	Z
C	87491.919	42787.740	770.097	87491.887	42787.834	767.840
1	87427.167	42926.723	762.642	87427.088	42926.709	762.632
2	87444.289	42889.553	757.841	87444.322	42889.390	757.636
3	87459.247	42857.388	762.559	87459.569	42857.062	761.512
4	87469.152	42836.719	766.057	87469.706	42836.663	765.129
5	87479.464	42814.514	766.090			
6	87508.642	42751.826	772.889	87508.466	42752.255	771.046
7	87522.981	42720.467	776.654	87522.737	42721.154	775.768
8				87543.009	42676.817	781.279
9	87560.454	42639.020	781.872	87560.325	42639.161	781.769

Measurements along D line

Station No.	11.10.2001			15.04.2002			01.05.2002		
	X	Y	Z	X	Y	Z	X	Y	Z
D	86812.566	42472.621	717.567	86812.633	42472.523	717.580	86813.095	42472.352	715.309
1	86725.068	42663.285	735.551	86725.077	42663.230	735.667	86724.112	42661.311	735.624
2	86747.893	42612.667	731.447	86747.914	42612.589	731.531	86747.899	42612.483	731.573
3	86767.103	42570.741	730.997	86767.169	42570.629	731.065	86767.187	42570.327	730.932
4	86790.412	42520.460	721.722	86790.351	42520.225	721.761	86790.246	42519.327	719.871
5	86830.740	42433.452	714.119	86830.765	42433.439	714.157	86831.253	42433.911	712.619
6	86860.440	42369.406	726.365	86860.416	42369.308	726.473	86860.228	42368.007	726.361
7	86870.356	42347.946	731.310	86870.264	42347.843	731.394	86870.244	42346.501	731.413
8	86881.680	42323.486	736.648	86881.658	42323.391	736.729	86881.654	42322.089	736.692

Station No.	17.05.2002			01.06.2002		
	X	Y	Z	X	Y	Z
D	86813.121	42472.310	714.414	86812.967	42472.181	714.324
1	86725.075	42663.145	735.663	86725.065	42663.113	735.620
2	86747.936	42612.443	731.559	86747.938	42612.408	731.477
3	86767.219	42570.294	730.736	86767.153	42570.184	730.731
4	86790.206	42519.235	719.090	86790.100	42519.116	719.045
5	86831.021	42433.914	711.627	86830.797	42433.815	711.529
6	86860.044	42369.835	726.161	86859.858	42369.818	726.030
7	86870.117	42348.052	731.277	86869.959	42347.974	731.221
8	86881.473	42323.465	736.668	86881.349	42323.411	736.669

Table A.1 Raw data for Panel B02 (cont.)

Measurements along E line

Station No.	15.04.2002			16.08.2002			02.09.2002		
	X	Y	Z	X	Y	Z	X	Y	Z
E	86368.037	42266.503	683.343	86368.020	42266.363	683.229	86368.136	42266.371	683.255
1	86296.650	42420.523	692.371	86296.715	42420.501	692.263	86296.648	42420.309	692.279
2	86312.136	42387.102	686.277	86312.194	42387.042	686.144	86312.158	42386.962	686.162
3	86329.866	42349.014	680.706	86329.784	42348.792	680.573	86329.885	42348.823	680.631
4	86348.543	42308.642	681.222	86348.564	42308.470	681.058	86348.656	42308.348	681.112
5	86400.295	42197.412	633.873	86400.339	42197.267	633.738	86400.301	42197.065	633.830
6	86411.864	42173.028	636.113	86411.814	42172.899	635.915	86411.824	42172.675	635.942
7	86427.087	42139.983	636.578	86427.074	42139.725	636.514			

Station No.	18.09.2002			30.09.2002			16.10.2002		
	X	Y	Z	X	Y	Z	X	Y	Z
E	86368.826	42266.821	682.590	86368.847	42266.546	681.060	86368.206	42266.023	679.927
1	86296.715	42420.567	692.388	86296.722	42420.467	692.366	86296.692	42420.354	692.350
2	86312.192	42387.107	686.202	86312.238	42386.975	686.187	86312.210	42386.717	686.121
3	86329.927	42348.854	680.395	86329.977	42348.329	679.527	86329.839	42347.583	678.897
4	86349.075	42308.703	680.650	86348.836	42308.291	679.206	86348.353	42307.512	678.203
5									
6	86411.740	42172.735	636.075	86411.689	42172.726	636.012			

Station No.	31.10.2002		
	X	Y	Z
E	86367.919	42265.848	679.773
1	86296.683	42420.454	692.347
2	86312.236	42386.683	686.126
3	86329.811	42347.520	678.710
4	86348.227	42307.415	677.936

Table A.2 Raw data for Panel B10

Location of face at underground measurement dates

Date	Front Face Intersection Point		Back Face Intersection Point	
	X_{front}	Y_{front}	X_{back}	Y_{back}
01.02.2000	87249.082	43622.740	87271.762	43633.274
01.03.2000	87131.166	43567.974	87152.047	43577.672
01.04.2000	87024.161	43518.275	87040.471	43525.851
01.05.2000	86916.278	43468.169	86938.999	43478.722
01.06.2000	86844.611	43434.883	86865.484	43444.577
01.07.2000	86804.700	43416.346	86825.574	43426.041
01.08.2000	86705.846	43370.433	86726.692	43380.115
01.09.2000	86614.178	43327.858	86635.097	43337.574
02.10.2000	86554.392	43300.090	86575.232	43309.769
01.11.2000	86475.082	43263.255	86496.386	43273.149
01.12.2000	86390.770	43224.095	86411.612	43233.776
02.01.2001	86294.561	43179.411	86314.587	43188.712
01.02.2001	86185.726	43128.862	86205.754	43138.164
01.03.2001	86074.265	43077.094	86097.808	43088.029
02.04.2001	85962.654	43025.256	85986.272	43036.225
01.05.2001	85897.559	42995.022	85916.124	43003.645

Table A.2 Raw data for Panel B10 (cont.)

Measurements along B line

Station No.	26.02.2000			01.05.2000			16.05.2000		
	X	Y	Z	X	Y	Z	X	Y	Z
B	86859.378	43456.349	711.193	86859.371	43456.371	711.177	86859.629	43456.453	711.107
1	86772.119	43643.820	749.302	86772.050	43643.782	749.279	86772.076	43643.748	749.271
2	86786.168	43613.712	738.589	86786.102	43613.656	738.608	86786.050	43613.600	738.597
3	86796.766	43590.840	730.979	86796.670	43590.787	730.961	86796.641	43590.729	730.963
4	86807.943	43566.879	723.934	86807.866	43566.837	723.923	86807.901	43566.776	723.915
5	86821.712	43537.225	717.108	86821.685	43537.197	717.088	86821.757	43537.147	717.018
6	86832.348	43514.418	711.341	86832.340	43514.399	711.319	86832.460	43514.400	711.252
7	86848.613	43479.471	707.900	86848.620	43479.477	707.882	86848.845	43479.506	707.819
8	86869.574	43434.376	714.609	86869.570	43434.398	714.582	86869.777	43434.476	714.536
9	86879.929	43412.146	719.307	86879.955	43412.176	719.263	86880.064	43412.253	719.219
10	86887.819	43395.176	723.125	86887.823	43395.205	723.109	86887.894	43395.297	723.061
11	86898.359	43372.586	728.151	86898.352	43372.606	728.120	86898.407	43372.705	728.070
12	86910.653	43346.135	731.833	86910.643	43346.150	731.803	86910.675	43346.192	731.788
13	86922.142	43321.431	734.819	86922.109	43321.457	734.756	86922.119	43321.507	734.741
14	86932.895	43298.298	736.838	86932.882	43298.317	736.811	86932.876	43298.331	736.820
15	86945.012	43272.107	739.061	86944.983	43272.139	739.023	86944.994	43272.130	739.032

Station No.	01.06.2000			17.06.2000			18.07.2000		
	X	Y	Z	X	Y	Z	X	Y	Z
B	86860.137	43456.865	710.031	86860.107	43456.941	709.014	86859.078	43456.714	707.656
1	86772.076	43643.633	749.265	86772.062	43643.566	749.208	86772.085	43643.289	749.092
2	86786.072	43613.466	738.563	86786.072	43613.369	738.512	86786.049	43613.053	738.386
3	86796.702	43590.551	730.896	86796.702	43590.414	730.831	86796.669	43590.057	730.662
4	86808.022	43566.529	723.764	86808.040	43566.332	723.634	86808.020	43565.667	723.330
5	86822.117	43536.882	716.426	86822.161	43536.592	715.902	86821.853	43535.807	715.135
6	86832.899	43514.303	710.406	86832.884	43514.051	709.581	86832.336	43513.290	708.470
7	86849.398	43479.795	706.847	86849.433	43479.891	705.906	86848.553	43479.452	704.494
8	86870.230	43434.977	713.599	86870.218	43435.037	712.574	86869.209	43435.014	711.124
9	86880.343	43412.713	718.560	86880.269	43412.860	717.493	86879.396	43413.040	715.922
10	86888.046	43395.745	722.629	86887.957	43396.038	721.790	86887.062	43396.339	720.259
11	86898.445	43372.977	727.919	86898.370	43373.217	727.664	86897.678	43373.746	727.105
12	86910.632	43346.341	731.741	86910.621	43346.489	731.627	86910.370	43346.787	731.430
13	86922.094	43321.543	734.760	86922.077	43321.611	734.689	86921.964	43321.771	734.620
14	86932.862	43298.361	736.834	86932.846	43298.382	736.786	86932.800	43298.465	736.725
15	86944.966	43272.130	739.092	86944.948	43272.154	739.019	86944.952	43272.183	739.011

Station No.	02.08.2000		
	X	Y	Z
B	86858.960	43456.601	707.650
1	86772.074	43643.150	749.088
2	86786.036	43612.929	738.341
3	86796.636	43589.894	730.642
4	86807.999	43565.516	723.280
5	86821.797	43535.664	715.057
6	86832.259	43513.147	708.414
7	86848.501	43479.326	704.491
8	86869.092	43434.971	711.083
9	86879.283	43412.994	715.865
10	86886.971	43396.311	720.194
11	86897.613	43373.735	727.057
12	86910.298	43346.814	731.383
13	86921.897	43321.788	734.643
14	86932.799	43298.515	736.758
5	86944.978	43272.239	738.979

Table A.3 Raw data for Panel B12

Location of face at underground measurement dates

Date	Front Face Intersection Point		Back Face Intersection Point	
	X_{front}	Y_{front}	X_{back}	Y_{back}
01.12.1998	87044.559	43772.956	87068.118	43783.904
01.01.1999	86900.378	43705.956	86920.325	43715.225
01.02.1999	86800.623	43659.6	86824.185	43670.549
01.03.1999	86677.13	43602.212	86692.699	43609.447
01.04.1999	86546.688	43541.596	86567.554	43551.292
01.05.1999	86463.435	43502.908	86483.534	43512.248
01.06.1999	86360.777	43455.203	86380.741	43464.481
01.07.1999	86274.62	43415.166	86293.67	43424.018
01.08.1999	86122.282	43344.374	86143.134	43354.064
01.09.1999	86016.164	43295.061	86037.027	43304.756
01.10.1999	85932.745	43256.297	85955.422	43266.835
01.11.1999	85832.992	43209.941	85855.668	43220.479
24.11.1999	85804.877	43196.876		
20.11.1999	85792.172	43190.972		

Table A.4 Raw data for Panel B12

Measurements along B line

Station No.	24.10.1998			31.10.1998			19.12.1998		
	X	Y	Z	X	Y	Z	X	Y	Z
B							86945.873	43641.457	754.554
1	86820.938	43910.293	758.152	86820.948	43910.303	758.155	86820.945	43910.317	758.146
2	86834.445	43881.196	758.108	86834.486	43881.243	758.1	86834.459	43881.252	758.103
3	86855.323	43836.263	763.522	86855.336	43836.289	763.514	86855.297	43836.307	763.499
4	86873.729	43796.638	768.346	86873.756	43796.677	768.339	86873.734	43796.686	768.333
5	86885.737	43770.869	769.789	86885.753	43770.894	769.788	86885.741	43770.918	769.784
6	86898.989	43742.347	771.562	86898.995	43742.374	771.568	86898.997	43742.384	771.553
7	86913.745	43710.578	771.768	86913.76	43710.59	771.79	86913.8	43710.592	771.8
8	86924.562	43687.326	768.381	86924.532	43687.327	768.358	86924.602	43687.295	768.39
9	86935.007	43664.736	761.873	86935.014	43664.75	761.846	86935.043	43664.738	761.879
10	86957.252	43616.875	746.74	86957.274	43616.875	746.709	86957.294	43616.85	746.747
11	86967.347	43595.089	739.723	86967.351	43595.101	739.698	86967.375	43595.078	739.739
12	86977.433	43573.383	733.43	86977.432	43573.416	733.414	86977.472	43573.395	733.448
13	86985.669	43555.605	726.394	86985.686	43555.607	726.368	86985.713	43555.572	726.4
14	87000.278	43524.291	727.449	87000.289	43524.304	727.436			
15	87016.469	43489.362	727.8	87016.474	43489.371	727.773			
16	87031.182	43457.652	729.747	87031.187	43457.658	729.722			
17	87046.244	43425.286	732.944	87046.248	43425.309	732.733			

Table A.3 Raw data for Panel B12 (cont.)

Station No.	31.12.1998			15.01.1999			31.01.1999		
	X	Y	Z	X	Y	Z	X	Y	Z
B				86945.633	43641.855	751.297	86945.208	43641.69	751.041
1	86820.945	43910.311	758.142	86820.976	43910.293	758.139	86820.981	43910.255	758.127
2	86834.389	43881.248	758.108	86834.317	43881.213	758.095	86834.267	43881.159	758.099
3	86855.236	43836.27	763.514	86855.2	43836.26	763.465	86855.14	43836.167	763.449
4	86873.693	43796.628	768.36	86873.615	43796.57	768.21	86873.551	43796.448	768.161
5	86885.823	43770.827	769.651	86885.593	43770.277	768.638	86885.305	43769.969	768.317
6	86899.229	43742.362	771.201	86898.89	43741.836	769.118	86898.461	43741.509	768.723
7	86914.275	43710.715	771.462	86913.495	43710.499	768.83	86913.047	43710.25	768.43
8	86924.924	43687.441	767.894	86924.085	43687.355	765.024	86923.567	43687.145	764.735
9	86935.369	43664.992	761.384	86934.742	43664.789	758.821	86934.217	43664.589	758.501
10	86957.518	43617.03	746.442	86956.927	43617.122	744.578	86956.614	43617.035	744.432
11	86967.439	43595.122	739.646	86967.152	43594.935	739.351	86967.098	43594.875	739.299
12	86977.468	43573.433	733.412	86977.396	43573.468	733.345	86977.345	43573.457	733.349
13	86985.699	43555.606	726.385	86985.683	43555.645	726.352	86985.639	43555.61	726.346
14	87000.302	43524.301	727.477	87000.298	43524.317	727.429	87000.311	43524.305	727.455
15	87016.493	43489.349	727.813	87016.486	43489.369	727.795	87016.488	43489.351	727.81
16	87031.219	43457.652	729.771	87031.197	43457.656	729.748	87031.242	43457.654	729.757
17	87046.291	43425.277	732.973	87046.29	43425.302	732.968	87046.302	43425.289	732.986

Measurements along C line

Station No.	20.12.1998			21.12.1998			26.02.1999		
	X	Y	Z	X	Y	Z	X	Y	Z
C	86542.901	43454.257	697.765				86542.911	43454.293	697.767
1				86402.435	43757.564	738.176	86402.43	43757.562	738.164
2				86411.496	43737.846	733.857	86411.52	43737.863	733.858
3				86420.391	43718.641	728.587	86420.398	43718.657	728.593
4				86431.427	43694.715	727.473	86431.447	43694.746	727.473
5				86443.953	43667.601	731.459	86443.948	43667.597	731.469
6				86453.432	43646.627	738.638	86453.439	43646.618	738.638
7				86462.569	43627.247	747.662	86462.579	43627.262	747.657
8	86471.843	43607.197	753.671				86471.854	43607.226	753.697
9	86478.012	43593.825	752.027				86478.039	43593.838	752.034
10	86485.407	43577.914	746.843				86485.414	43577.934	746.866
11	86499.491	43547.727	733.292				86499.505	43547.712	733.31
12	86513.182	43518.275	720.468				86513.192	43518.293	720.476
13	86527.87	43486.668	708.527				86527.867	43486.687	708.531
14	86554.505	43429.336	690.625				86554.497	43429.32	690.636
15	86567.814	43400.698	685.737				86567.802	43400.645	685.752
16	86583.696	43366.508	693.184				86583.658	43366.499	693.197
17	86598.882	43333.805	705.749				86598.865	43333.801	705.756
18	86614.561	43300.012	714.847				86614.571	43300.036	714.842
19	86628.771	43269.485	721.148				86628.778	43269.491	721.146
20	86643.187	43238.488	725.559				86643.171	43238.516	725.557

Table A.3 Raw data for Panel B12 (cont.)

Station No.	19.03.1999			01.04.1999			15.04.1999		
	X	Y	Z	X	Y	Z	X	Y	Z
C	86542.901	43454.257	697.765	86542.912	43454.289	697.734	86543.213	43454.537	697.447
1	86402.429	43757.574	738.165	86402.417	43757.577	738.168	86402.411	43757.602	738.162
2	86411.523	43737.873	733.86	86411.521	43737.882	733.862	86411.501	43737.892	733.854
3	86420.405	43718.669	728.593	86420.397	43718.673	728.591	86420.385	43718.694	728.581
4	86431.435	43694.751	727.473	86431.429	43694.766	727.477	86431.42	43694.791	727.467
5	86443.952	43667.62	731.471	86443.934	43667.612	731.466	86443.937	43667.633	731.443
6	86453.423	43646.626	738.633	86453.424	43646.641	738.622	86453.451	43646.619	738.58
7	86462.569	43627.274	747.652	86462.58	43627.264	747.625	86462.669	43627.239	747.544
8	86471.829	43607.177	753.681	86471.88	43607.224	753.616	86472.231	43607.183	753.366
9	86478.009	43593.833	752.013	86478.034	43593.858	751.994	86478.506	43593.862	751.626
10	86485.392	43577.929	746.828	86485.409	43577.955	746.808	86485.88	43578.111	746.452
11	86499.469	43547.731	733.284	86499.501	43547.729	733.261	86500.03	43547.893	732.923
12	86513.166	43518.309	720.45	86513.193	43518.29	720.429	86513.754	43518.552	720.037
13	86527.846	43486.666	708.514	86527.875	43486.691	708.491	86528.403	43487.016	708.094
14	86554.493	43429.332	690.627	86554.504	43429.344	690.602	86554.637	43429.523	690.431
15	86567.812	43400.677	685.746	86567.832	43400.664	685.743	86567.818	43400.733	685.698
16	86583.679	43366.518	693.187	86583.688	43366.517	693.184	86583.675	43366.526	693.169
17	86598.872	43333.821	705.758	86598.874	43333.816	705.75	86598.871	43333.832	705.746
18	86614.552	43300.045	714.837	86614.564	43300.031	714.838	86614.56	43300.05	714.843
19	86628.784	43269.499	721.143	86628.778	43269.501	721.142	86628.771	43269.497	721.142
20	86643.202	43238.479	725.553	86643.185	43238.493	725.559	86643.199	43238.519	725.56

Station No.	05.05.1999			18.05.1999			01.06.1999		
	X	Y	Z	X	Y	Z	X	Y	Z
C	86542.81	43454.874	695.234	86542.358	43454.599	694.867	86542.261	43454.479	694.791
1	86402.405	43757.618	738.171	86402.421	43757.627	738.174	86402.438	43757.603	738.168
2	86411.504	43737.922	733.863	86411.508	43737.913	733.858	86411.533	43737.908	733.829
3	86420.37	43718.704	728.585	86420.367	43718.699	728.567	86420.389	43718.681	728.546
4	86431.421	43694.786	727.462	86431.437	43694.747	727.443	86431.415	43694.66	727.399
5	86443.949	43667.549	731.399	86443.957	43667.444	731.318	86443.91	43667.334	731.24
6	86453.546	43646.344	738.433	86453.569	43646.137	738.317	86453.492	43645.932	738.236
7	86462.844	43626.621	747.123	86462.789	43626.213	746.885	86462.663	43625.95	746.754
8	86472.303	43606.137	752.514	86472.082	43605.573	752.112	86471.967	43605.264	751.966
9	86478.456	43592.839	750.381	86478.163	43592.316	749.928	86478.029	43592.029	749.77
10	86485.54	43577.402	744.789	86485.153	43576.901	744.245	86484.989	43576.647	744.07
11	86499.491	43547.511	730.842	86498.958	43547.131	730.311	86498.79	43546.943	730.126
12	86513.182	43518.348	717.684	86512.624	43517.976	717.193	86512.438	43517.845	717.052
13	86527.954	43487.08	705.703	86527.407	43486.774	705.254	86527.306	43486.63	705.169
14	86554.279	43429.954	689.602	86554.118	43429.992	689.445	86554.063	43429.972	689.415
15	86567.77	43400.836	685.602	86567.677	43400.852	685.578	86567.708	43400.839	685.552
16	86583.672	43366.55	693.146	86583.611	43366.575	693.141	86583.637	43366.564	693.128
17	86598.867	43333.836	705.741	86598.829	43333.846	705.753	86598.848	43333.831	705.734
18	86614.54	43300.025	714.834	86614.538	43300.049	714.838	86614.545	43300.001	714.832
19	86628.775	43269.491	721.139	86628.767	43269.504	721.139	86628.785	43269.483	721.138
20	86643.196	43238.511	725.557	86643.172	43238.498	725.559	86643.174	43238.476	725.556

Table A.3 Raw data for Panel B12 (cont.)

Measurements along D line

Station No.	21.12.1998			20.04.1999			02.08.1999		
	X	Y	Z	X	Y	Z	X	Y	Z
D				86129.796	43262.345	670.369	86129.839	43262.395	670.313
1	85970.441	43605.534	707.095	85970.435	43605.509	707.076	85970.449	43605.485	707.071
2	85976.140	43593.196	703.333	85976.149	43593.205	703.324	85976.161	43593.186	703.325
3	85986.416	43571.143	697.573	85986.408	43571.133	697.605	85986.411	43571.106	697.585
4	85999.011	43543.998	698.649	85999.010	43543.978	698.658	85999.021	43543.976	698.649
5	86010.163	43520.003	699.443	86010.163	43520.003	699.452	86010.167	43519.972	699.442
6	86023.008	43492.343	693.656	86023.001	43492.345	693.660	86022.998	43492.305	693.637
7	86033.584	43469.557	684.373	86033.567	43469.561	684.377	86033.569	43469.522	684.366
8	86050.153	43434.052	679.756	86050.117	43434.052	679.764	86050.158	43434.025	679.712
9	86059.531	43413.716	685.131	86059.541	43413.718	685.138	86059.617	43413.749	685.042
10	86072.081	43386.652	689.375	86072.079	43386.655	689.371	86072.164	43386.760	689.288
11	86086.976	43354.478	681.035	86086.971	43354.476	681.052	86087.045	43354.530	680.997
12	86112.546	43299.385	662.869	86112.533	43299.391	662.875	86112.629	43299.450	662.817
13	86121.193	43280.943	667.398	86121.182	43280.960	667.391	86121.237	43281.020	667.353
14	86138.109	43244.449	672.558	86138.132	43244.440	672.580	86138.138	43244.476	672.552
15	86149.619	43219.815	677.685	86149.615	43219.811	677.684	86149.600	43219.840	677.658
16	86157.151	43203.494	679.981	86157.146	43203.476	680.017	86157.127	43203.488	679.997
17	86165.799	43184.877	680.978	86165.779	43184.871	680.983	86165.763	43184.880	680.970
18	86178.386	43157.693	682.576	86178.387	43157.693	682.595	86178.378	43157.698	682.610
19	86192.729	43126.796	684.272	86192.738	43126.769	684.286	86192.704	43126.768	684.285
20	86208.970	43091.871	686.762	86208.978	43091.852	686.757	86208.946	43091.859	686.760

Station No.	16.08.1999			01.09.1999			15.09.1999		
	X	Y	Z	X	Y	Z	X	Y	Z
D	86129.892	43263.084	669.421	86129.182	43263.411	668.278	86128.905	43263.374	668.130
1	85970.467	43605.470	707.049	85970.467	43605.408	707.004	85970.458	43605.407	706.969
2	85976.156	43593.154	703.290	85976.158	43593.127	703.248	85976.135	43593.121	703.220
3	85986.408	43571.074	697.566	85986.415	43571.021	697.549	85986.398	43570.990	697.533
4	85999.049	43543.925	698.632	85999.051	43543.836	698.584	85999.004	43543.721	698.535
5	86010.189	43519.887	699.410	86010.202	43519.714	699.360	86010.157	43519.535	699.296
6	86022.990	43492.203	693.605	86022.998	43492.017	693.528	86022.973	43491.816	693.462
7	86033.582	43469.420	684.308	86033.581	43469.207	684.208	86033.523	43469.014	684.118
8	86050.325	43433.822	679.462	86050.314	43433.371	679.195	86050.209	43433.098	679.074
9	86059.861	43413.554	684.353	86059.720	43413.010	683.777	86059.560	43412.714	683.584
10	86072.470	43386.835	688.269	86072.117	43386.205	687.286	86071.829	43385.885	687.032
11	86087.346	43354.596	679.665	86086.934	43354.138	678.191	86086.581	43353.846	677.717
12	86112.781	43299.853	661.347	86112.206	43300.118	660.004	86111.821	43299.979	659.780
13	86121.348	43281.775	666.100	86120.608	43281.913	664.750	86120.279	43281.824	664.565
14	86138.168	43244.785	672.121	86137.652	43245.262	671.453	86137.368	43245.306	671.318
15	86149.603	43220.073	677.508	86149.471	43220.256	677.308	86149.331	43220.311	677.264
16	86157.121	43203.642	679.910	86157.056	43203.742	679.836	86156.965	43203.777	679.816
17	86165.759	43184.998	680.936	86165.712	43185.044	680.928	86165.627	43185.082	680.909
18	86178.364	43157.769	682.597	86178.344	43157.786	682.600	86178.289	43157.783	682.585
19	86192.721	43126.800	684.303	86192.674	43126.833	684.296	86192.597	43126.848	684.289
20	86208.955	43091.901	686.763	86208.943	43091.914	686.771	86208.876	43091.896	686.772

Table A.5 Raw data for Panel C08

Location of face at underground measurement dates

Date	Face Intersection Point	
	X	Y
01.07.2002	90100.669	44530.105
01.08.2002	90027.957	44505.110
31.08.2002	89915.077	44466.308
01.10.2002	89785.270	44421.687
01.11.2002	89654.190	44376.628
01.12.2002	89506.895	44325.995
31.12.2002	89388.206	44285.196
01.02.2003	89253.088	44238.749
01.03.2003	89172.930	44211.195
01.04.2003	89026.351	44160.808
01.05.2003	88872.313	44107.858
02.06.2003	88720.501	44055.672
16.06.2003	88675.829	44040.316

Measurements along B line

Station No.	07.06.2002			04.07.2002			11.07.2002		
	X	Y	Z	X	Y	Z	X	Y	Z
B	90095.927	44516.023	936.495	90095.892	44516.024	936.460	90095.963	44516.002	936.564
1	90021.394	44732.433	945.170	90021.443	44732.422	945.157	90021.452	44732.419	945.227
2	90033.152	44698.493	942.576	90033.173	44698.515	942.541	90033.208	44698.484	942.593
3	90044.823	44664.471	939.661	90044.812	44664.453	939.693	90044.866	44664.450	939.700
4	90057.040	44628.871	938.189	90057.053	44628.842	938.098	90057.114	44628.860	938.234
5	90109.591	44476.232	934.048	90109.603	44476.250	934.040	90109.662	44476.211	934.131
6	90129.929	44417.082	932.609	90129.965	44417.075	932.598	90129.953	44417.075	932.668
7	90142.438	44380.669	934.889	90142.438	44380.668	934.891	90142.465	44380.655	934.971
8	90156.520	44339.791	935.777	90156.514	44339.782	935.762	90156.533	44339.778	935.840
9	90169.472	44302.175	939.870	90169.454	44302.175	939.895	90169.478	44302.158	939.943
10	90193.668	44231.790	956.461						

Station No.	16.07.2002			17.07.2002			20.07.2002		
	X	Y	Z	X	Y	Z	X	Y	Z
B	90095.916	44516.036	936.431	90095.911	44515.991	936.417	90095.884	44516.019	936.310
1	90021.442	44732.404	945.128						
2	90033.113	44698.478	942.525						
3	90044.829	44664.443	939.581						
4	90057.054	44628.855	938.054				90057.130	44628.849	937.895
5	90109.631	44476.236	934.012	90109.593	44476.240	933.995	90109.633	44476.241	933.930
6	90129.927	44417.085	932.588				90129.947	44417.116	932.530
7	90142.434	44380.672	934.849						
8	90156.521	44339.792	935.763						
9	90169.452	44302.192	939.839						

Table A.4 Raw data for Panel C08 (cont.)

Station No.	22.07.2002		24.07.2002			31.07.2002		
	Y	Z	X	Y	Z	X	Y	Z
B	44516.021	936.262	90095.863	44516.020	936.150	90095.592	44515.919	935.064
1	44732.370	945.100				90021.456	44732.293	945.090
2	44698.391	942.460				90033.230	44698.264	942.209
3	44664.394	939.453				90044.921	44664.191	939.024
4	44628.867	937.895	90057.050	44628.825	937.800	90057.082	44628.611	937.134
5	44476.268	933.988	90109.556	44476.286	933.900	90109.383	44476.379	933.585
6	44417.076	932.581	90129.896	44417.123	932.530	90129.866	44417.203	932.496
7	44380.636	934.877				90142.377	44380.724	934.833
8	44339.783	935.750				90156.445	44339.820	935.730
9	44302.151	939.830				90169.424	44302.219	939.833

Station No.	16.08.2002			02.09.2002		
	X	Y	Z	X	Y	Z
B	90094.876	44515.631	934.352	90094.833	44515.492	934.242
1	90021.499	44732.167	944.976	90021.506	44732.105	944.998
2	90033.184	44698.037	942.164	90033.188	44697.955	942.104
3	90044.779	44663.851	938.823	90044.788	44663.706	938.683
4	90056.822	44628.171	936.469	90056.767	44628.011	936.359
5	90108.667	44476.327	933.004	90108.603	44476.272	932.960
6	90129.575	44417.222	930.744	90129.567	44417.435	932.378
7	90142.277	44380.880	934.762	90142.204	44380.913	934.751
8	90156.391	44340.026	935.682	90156.304	44339.989	935.651
9	90169.311	44302.375	939.836	90169.289	44302.401	939.765

Measurements along C line

Station No.	31.07.2002			02.09.2002			18.09.2002		
	X	Y	Z	X	Y	Z	X	Y	Z
C	89856.509	44433.726	926.105	89856.497	44433.684	926.132	89856.971	44433.964	925.329
1	89793.332	44617.005	930.900	89793.466	44616.931	930.880	89793.597	44616.683	930.782
2	89818.395	44544.400	929.105	89818.478	44544.392	929.101	89819.082	44544.172	928.446
3	89831.570	44506.022	928.158	89831.609	44506.024	928.163	89832.399	44506.011	927.254
4	89842.582	44474.059	927.765	89842.576	44474.028	927.777	89843.292	44474.125	926.979
5	89864.724	44409.749	924.575	89864.725	44409.730	924.600	89865.104	44410.087	923.952
6	89876.858	44374.634	924.566	89876.808	44374.614	924.581	89877.021	44374.948	924.452
7	89892.979	44327.943	926.650	89893.057	44327.694	926.664	89893.012	44327.711	926.680
8	89905.463	44291.763	928.601	89905.438	44291.765	928.616	89905.423	44291.774	928.631

Station No.	30.09.2002			16.10.2002		
	X	Y	Z	X	Y	Z
C	89856.680	44433.869	923.614	89855.907	44433.656	922.851
1	89793.664	44616.430	930.580	89793.718	44616.186	930.427
2	89819.117	44543.553	927.363	89818.758	44543.008	926.771
3	89832.314	44505.488	925.692	89831.643	44505.097	924.875
4	89843.039	44473.796	925.237	89842.185	44473.482	924.499
5	89865.006	44410.149	922.606	89864.267	44410.056	921.876
6	89876.745	44375.343	923.680	89876.084	44375.566	923.255
7	89892.941	44327.782	926.643	89892.836	44327.851	926.631
8	89905.358	44291.776	928.605	89905.320	44291.788	928.629

Table A.6 Raw data for Panel C10

Location of face at underground measurement dates

Date	Face Intersection Point	
	X	Y
02.04.2001	90093.361	44765.569
01.05.2001	90041.489	44747.751
01.06.2001	89906.609	44701.420
02.07.2001	89736.249	44642.901
01.08.2001	89558.159	44581.728
01.09.2001	89404.220	44528.850
01.10.2001	89274.997	44484.462
01.11.2001	89137.519	44437.238
01.12.2001	88997.900	44389.279
31.12.2001	88865.902	44343.937
01.02.2002	88709.276	44290.136
01.03.2002	88606.830	44254.946
23.03.2002	88566.835	44241.208

Measurements along B line

Station No.	20.03.2001			28.03.2001			11.04.2001		
	X	Y	Z	X	Y	Z	X	Y	Z
B	90101.148	44738.093	946.934	90101.175	44738.075	946.925	90101.113	44738.076	946.904
1	90041.048	44912.531	964.584				90041.023	44912.528	964.651
2	90051.666	44881.793	960.985				90051.665	44881.782	961.185
3	90060.075	44857.380	958.172				90060.072	44857.351	958.186
4	90069.938	44828.547	955.561				90069.915	44828.545	955.585
5	90079.822	44800.105	952.644				90079.823	44800.112	952.600
6	90089.723	44771.386	950.394	90089.701	44771.383	950.375	90089.755	44771.382	950.352
7	90112.325	44705.716	944.203	90112.322	44705.750	944.221	90112.283	44705.752	944.183
8	90122.739	44676.109	941.199				90122.512	44676.113	941.219
9	90132.661	44647.278	939.598				90132.400	44647.298	939.655
10	90146.990	44605.793	938.246						
11	90161.433	44563.687	938.454				90161.182	44563.693	938.528
12	90172.657	44531.206	943.254				90172.401	44531.193	943.297

Station No.	19.04.2001			21.04.2001			24.04.2001		
	X	Y	Z	X	Y	Z	X	Y	Z
B	90101.156	44738.083	946.781	90101.118	44738.104	946.771	90101.206	44738.128	946.693
1							90041.134	44912.462	964.569
2							90051.708	44881.704	960.896
3							90060.116	44857.309	958.014
4				90069.909	44828.497	955.448	90069.974	44828.447	955.328
5	90079.820	44800.088	952.442	90079.867	44800.109	952.300	90079.933	44800.100	952.028
6	90089.725	44771.400	950.125	90089.736	44771.473	950.019	90089.765	44771.517	949.810
7	90112.274	44705.757	944.135	90112.267	44705.772	944.124	90112.299	44705.785	944.060
8	90122.435	44676.108	941.110	90122.422	44676.136	941.144	90122.438	44676.122	941.140
9				90132.363	44647.296	939.567	90132.396	44647.280	939.616

Table A.5 Raw data for Panel C10 (cont.)

Station No.	27.04.2001			30.04.2001			02.05.2001		
	X	Y	Z	X	Y	Z	X	Y	Z
B	90101.220	44738.152	946.580	90101.196	44738.189	946.288	90101.248	44738.192	946.216
1	90041.068	44912.440	964.548	90041.040	44912.400	964.548	90041.091	44912.402	964.591
2	90051.719	44881.682	960.852	90051.629	44881.648	960.852	90051.704	44881.651	960.907
3	90060.080	44857.307	957.984	90060.035	44857.214	957.972	90060.035	44857.216	958.014
4	90070.004	44828.406	955.185	90069.936	44828.317	954.931	90069.983	44828.326	954.972
5	90079.979	44800.107	951.636	90079.958	44800.121	951.210	90079.991	44800.115	951.196
6	90089.839	44771.584	949.378	90089.788	44771.601	948.904	90089.861	44771.583	948.870
7	90112.311	44705.794	944.050	90112.270	44705.789	943.918	90112.327	44705.823	943.937
8	90122.483	44676.152	941.131	90122.414	44676.142	941.107	90122.454	44676.151	941.155
9	90132.402	44647.303	939.573	90132.365	44647.304	939.593	90132.385	44647.276	939.606

Station No.	04.05.2001			07.05.2001			12.05.2001		
	X	Y	Z	X	Y	Z	X	Y	Z
B	90101.213	44738.229	945.970	90101.172	44738.231	945.613	90101.038	44738.177	945.018
1	90041.065	44912.383	964.496	90041.011	44912.355	964.584	90040.941	44912.258	964.448
2	90051.604	44881.638	960.841	90051.600	44881.588	960.801	90051.516	44881.477	960.695
3	90060.053	44857.185	957.914	90059.992	44857.138	957.899	90059.897	44857.017	957.762
4	90069.934	44828.304	954.843	90069.939	44828.243	954.677	90069.813	44828.048	954.270
5	90079.891	44800.117	951.005	90079.872	44800.061	950.777	90079.710	44799.933	950.252
6	90089.788	44771.600	948.708	90089.688	44771.585	948.369	90089.516	44771.447	947.897
7	90112.275	44705.810	943.870	90112.194	44705.851	943.771	90112.040	44705.826	943.466
8	90122.361	44676.162	941.101	90122.374	44676.175	941.060	90122.342	44676.205	941.008
9	90132.331	44647.313	939.590	90132.305	44647.320	939.576	90132.280	44647.330	939.572

Station No.	18.05.2001		
	X	Y	Z
B	90100.881	44738.106	944.741
1	90040.950	44912.199	964.459
2	90051.532	44881.366	960.656
3	90059.921	44856.898	957.736
4	90069.762	44827.909	954.072
5	90079.597	44799.843	949.939
6	90089.418	44771.368	947.649
7	90111.923	44705.841	943.208
8	90122.281	44676.230	940.955
9	90132.368	44647.313	939.594

Measurements along 8 line

Station No.	02.05.2001			18.05.2001			01.06.2001		
	X	Y	Z	X	Y	Z	X	Y	Z
8	90005.815	44705.191	945.158	90005.912	44705.240	944.964	90005.523	44704.988	942.972
1	89956.857	44847.893	963.973	89956.976	44847.707	963.708	89957.051	44847.032	962.949
2	89966.930	44818.242	961.435	89967.078	44818.211	961.026	89966.982	44817.619	959.725
3	89976.650	44789.763	956.648	89976.829	44789.755	956.205	89976.720	44789.169	954.474
4	89985.859	44762.952	952.605	89986.015	44763.006	952.209	89985.714	44762.532	949.984
5	89995.207	44735.860	948.189	89995.373	44735.944	947.866	89995.019	44735.578	945.674
6	90016.593	44673.710	942.830	90016.608	44673.733	942.767	90016.394	44673.816	941.418
7	90027.065	44643.315	939.544	90027.040	44643.329	939.517	90026.935	44643.417	939.012
8	90035.254	44619.576	937.986	90035.214	44619.599	937.938	90035.183	44619.625	937.787

Table A.5 Raw data for Panel C10 (cont.)

Station No.	15.06.2001		
	X	Y	Z
8	90005.441	44704.756	942.656
1	89956.913	44846.672	962.574
2	89966.789	44817.281	959.322
3	89976.519	44788.882	954.012
4	89985.538	44762.277	949.604
5	89994.926	44735.362	945.310
6	90016.296	44673.661	941.117
7	90026.886	44643.337	938.861
8	90035.149	44619.610	937.755

Measurements along C line

Station No.	21.06.2001			01.08.2001			15.08.2001		
	X	Y	Z	X	Y	Z	X	Y	Z
C	89627.631	44574.885	938.948	89627.675	44575.231	936.942	89626.788	44575.189	936.200
1	89550.852	44797.724	922.861	89550.983	44797.689	922.722	89550.811	44797.522	922.643
2	89565.191	44756.124	918.952	89565.276	44755.634	918.680	89565.153	44755.367	918.490
3	89582.212	44706.811	919.369	89582.520	44706.070	918.252	89582.044	44705.594	917.667
4	89616.862	44606.113	934.390	89616.684	44606.356	932.215	89615.757	44606.345	931.433
5	89638.919	44542.093	939.534	89639.015	44542.659	938.291	89638.263	44542.678	937.639
6	89652.462	44502.854	938.538	89652.445	44503.398	938.208	89652.068	44503.535	937.947
7	89665.474	44465.177	936.478	89665.488	44465.300	936.467	89665.384	44465.349	936.419
8	89675.065	44437.322	933.987	89675.102	44437.399	933.943	89675.044	44437.412	933.938
9	89685.519	44406.880	931.445	89685.534	44406.938	931.491	89685.515	44406.950	931.407

Measurements along D line

Station No.	07.09.2001			16.11.2001			05.12.2001		
	X	Y	Z	X	Y	Z	X	Y	Z
D	89069.628	44382.784	903.085	89069.772	44382.855	902.967	89068.866	44383.042	900.430
1	89021.116	44523.421	906.526	89021.358	44523.270	906.285	89021.486	44522.052	905.218
2	89032.619	44490.555	907.542	89033.139	44490.455	907.150	89032.782	44489.388	905.163
3	89039.544	44470.309	903.857	89040.064	44470.349	903.549	89039.154	44469.565	901.117
4	89049.190	44442.118	901.785	89049.617	44442.340	901.394	89049.094	44441.966	898.837
5	89059.622	44411.879	901.824	89059.793	44411.887	901.727	89059.373	44411.722	899.110
6	89079.345	44354.529	901.041	89079.466	44354.641	900.919	89078.592	44355.168	898.801
7	89095.826	44306.581	897.439	89095.826	44306.628	897.364	89095.521	44307.396	896.587
8	89108.088	44271.020	897.445	89108.040	44270.992	897.420	89108.083	44271.185	897.372
9	89119.213	44238.479	897.350	89119.169	44238.425	897.325	89119.178	44238.453	897.352
10	89128.714	44211.107	895.761	89128.687	44211.064	895.746	89128.721	44211.136	895.764

Station No.	19.12.2001			02.01.2002		
	X	Y	Z	X	Y	Z
D	89068.333	44382.991	900.017	89068.352	44383.036	899.897
1	89021.147	44521.783	905.014	89021.187	44521.738	904.974
2	89032.311	44489.030	904.851	89032.276	44488.967	904.808
3	89038.691	44469.250	900.827	89038.656	44469.248	900.750
4	89048.536	44441.718	898.443	89048.535	44441.709	898.380
5	89058.878	44411.614	898.849	89058.891	44411.618	898.828
6	89078.190	44355.192	898.462	89078.130	44355.225	898.407
7	89095.216	44307.500	897.076	89095.267	44307.558	896.169
8	89107.947	44271.212	897.308	89107.946	44271.210	897.300
9	89119.108	44238.476	897.326	89119.155	44238.487	897.332
10	89128.649	44211.161	895.746	89128.677	44211.096	895.747

Table A.7 Raw data for Panel C12

Location of face at underground measurement dates

Date	Face Intersection Point	
	X	Y
01.12.1999	89993.532	44959.775
01.01.2000	89959.395	44948.034
01.02.2000	89845.035	44908.700
01.03.2000	89690.832	44855.662
01.04.2000	89536.709	44802.651
01.05.2000	89465.800	44778.262
01.06.2000	89425.151	44764.281
01.07.2000	89398.615	44755.154
01.08.2000	89285.115	44716.115
01.09.2000	89145.166	44667.980
02.10.2000	89029.803	44628.301
01.11.2000	88892.685	44581.139
01.12.2000	88740.450	44528.778
02.01.2001	88581.585	44474.136
31.01.2001	88471.384	44436.233

Measurements along C line

Station No.	08.03.2000			30.09.2000			18.10.2000		
	X	Y	Z	X	Y	Z	X	Y	Z
C	89056.362	44598.151	922.070	89056.984	44598.340	921.523	89055.737	44597.988	919.193
1	88975.778	44832.470	914.779				88975.862	44832.409	914.787
2	88992.255	44784.437	914.334						
3	88998.652	44765.950	907.995	88998.695	44765.926	908.045	88998.721	44765.835	907.931
4	89003.525	44745.605	900.643	89003.545	44745.557	900.698	89003.521	44745.481	900.472
5	89015.496	44711.541	913.406	89015.642	44711.467	913.403	89015.473	44710.982	913.072
6	89022.579	44693.529	922.024	89022.849	44693.386	921.947	89022.385	44692.465	921.140
7	89029.441	44676.346	929.424	89030.004	44676.044	929.212	89029.164	44674.920	927.761
8	89045.647	44629.310	923.697	89046.260	44629.371	923.118	89045.028	44628.957	920.622
9	89066.540	44568.365	917.107	89066.825	44568.664	916.745	89065.682	44568.851	914.712
10	89076.100	44540.853	911.178	89076.206	44541.023	911.059	89075.648	44541.576	910.180
11	89087.828	44506.620	907.872	89087.825	44506.619	907.898	89087.721	44506.723	907.799
12	89097.858	44477.551	907.438	89097.845	44477.543	907.416	89097.845	44477.577	907.014
13	89107.648	44449.184	907.016	89107.676	44449.177	907.010	89107.645	44449.188	907.014

Station No.	03.11.2000			16.11.2000		
	X	Y	Z	X	Y	Z
C	89055.288	44597.882	918.926	89055.261	44597.845	918.914
1	88975.897	44832.341	914.717	88975.923	44832.315	914.709
2						
3	88998.772	44765.710	907.834	88998.770	44765.668	907.831
4				89003.604	44745.218	900.405
5	89015.249	44710.648	912.882	89015.246	44710.642	912.850
6	89022.081	44692.164	920.896	89022.033	44692.115	920.878
7	89028.810	44674.617	927.457	89028.786	44674.574	927.410
8	89044.648	44628.752	920.350	89044.606	44628.737	920.317
9	89065.330	44568.692	914.515	89065.342	44568.681	914.479
10	89075.408	44541.546	910.007	89075.405	44541.547	909.989
11	89087.696	44506.763	907.756	89087.697	44506.754	907.746
12	89097.797	44477.576	908.872	89097.207	44478.149	907.371
13	89107.621	44449.208	906.980	89107.670	44449.200	906.992

Table A.6 Raw data for Panel C12 (cont.)

Measurements along D line

Station No.	21.10.2000			15.12.2000			05.01.2001		
	X	Y	Z	X	Y	Z	X	Y	Z
D	88649.682	44458.218	863.036	88649.666	44458.206	863.063	88649.378	44458.546	860.512
1	88581.566	44656.849	878.275	88581.634	44656.874	878.251	88581.627	44656.819	878.278
2	88588.509	44636.294	880.422	88588.564	44636.309	880.381	88588.627	44636.242	880.385
3	88597.683	44609.380	878.937	88597.744	44609.375	878.963	88597.787	44609.291	878.913
4	88605.546	44586.711	872.982	88605.598	44586.742	872.954	88605.655	44586.647	872.947
5	88615.898	44556.406	863.464	88615.950	44556.435	863.444	88615.968	44556.198	862.858
6	88629.872	44515.723	863.548	88629.850	44515.717	863.541	88629.339	44515.854	861.287
7	88639.309	44488.420	864.390	88639.322	44488.423	864.344	88638.867	44488.584	861.937
8	88661.625	44423.546	863.182	88661.623	44423.526	863.193	88661.194	44424.341	861.063
9	88673.990	44387.530	865.445	88674.008	44387.498	865.444	88673.793	44388.031	865.168
10	88684.690	44356.399	868.703	88684.691	44356.374	868.692	88684.676	44356.451	868.650
11	88694.664	44327.589	871.660	88694.662	44327.593	871.645	88694.658	44327.624	871.649

Station No.	17.01.2001		
	X	Y	Z
D	88649.214	44458.457	860.392
1	88581.656	44656.776	878.237
2	88588.638	44636.205	880.363
3	88597.796	44609.224	878.881
4	88605.621	44586.562	872.863
5	88615.917	44556.123	862.777
6	88629.278	44515.785	861.195
7	88638.772	44488.515	861.851
8	88661.007	44424.297	860.960
9	88673.714	44388.057	865.112
10	88684.661	44356.451	868.653
11	88694.655	44327.597	871.646

APPENDIX – B

Subsidence and horizontal displacement profiles.

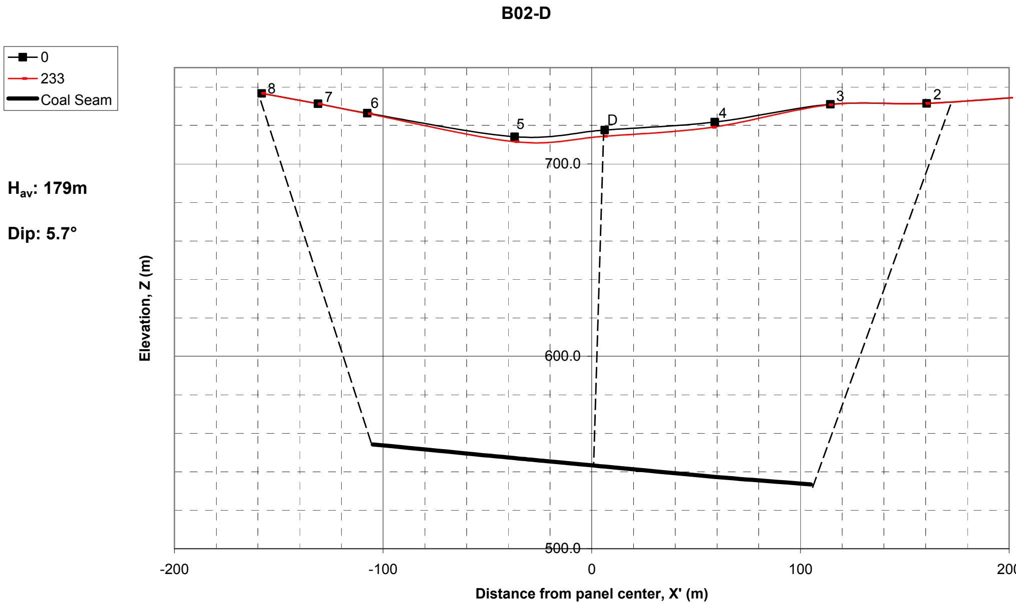

Figure B.1 Section view of D line of panel B02.

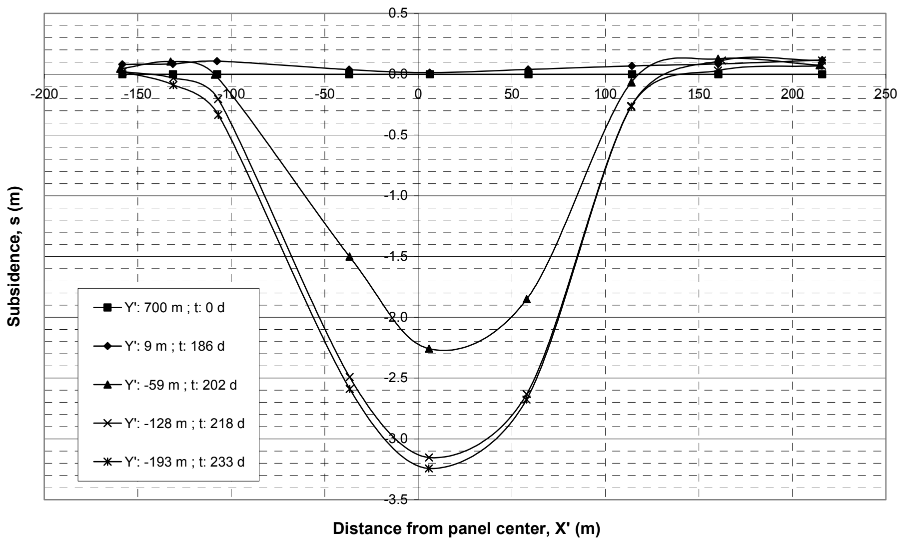

Figure B.2 Subsidence versus distance to the panel center plot along D line of B02.

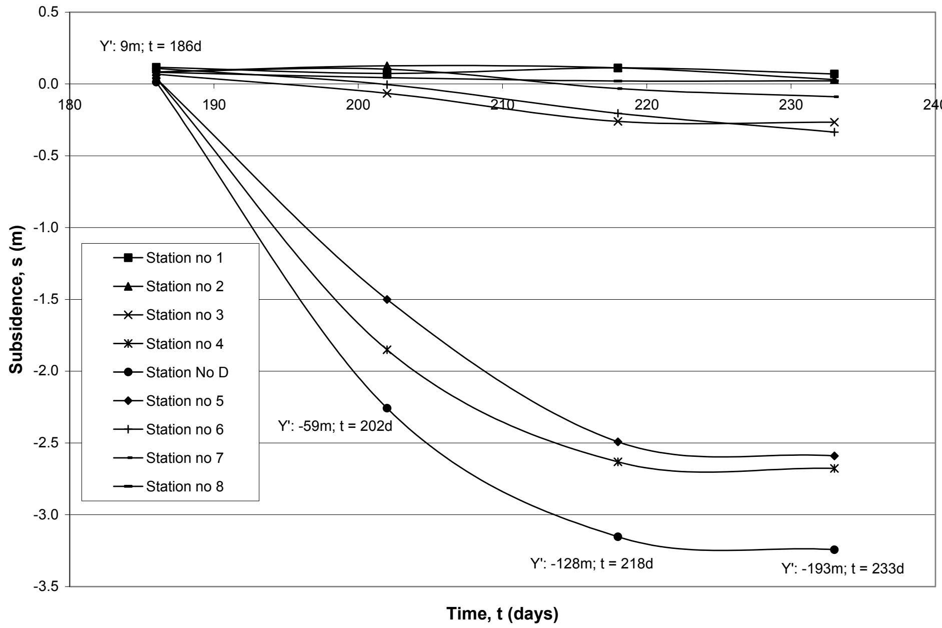

Figure B.3 Subsidence versus time plot for the stations along D line of B02 panel.

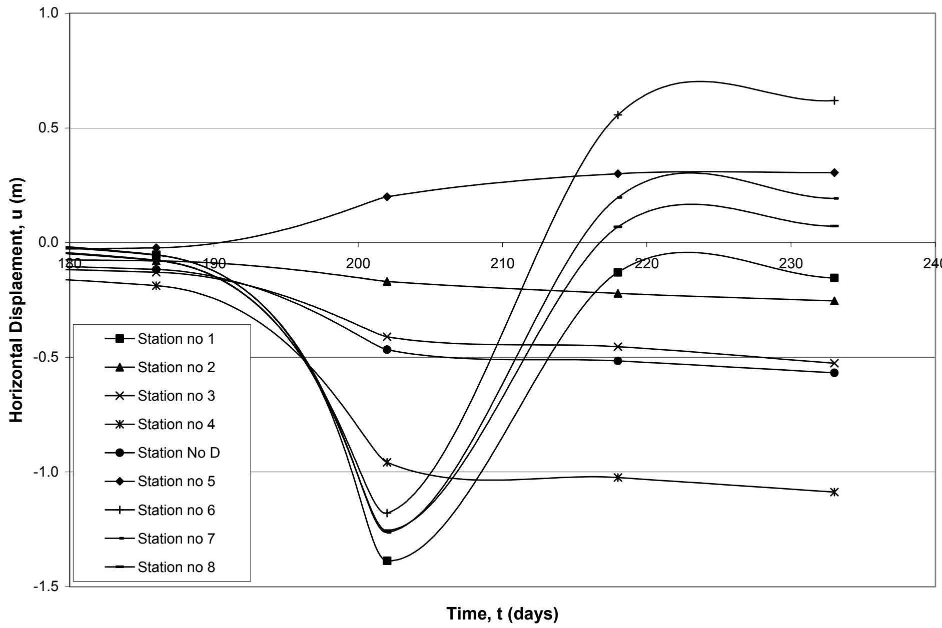

Figure B.4 Horizontal displacement versus time plot for the stations along D line of B02 panel.

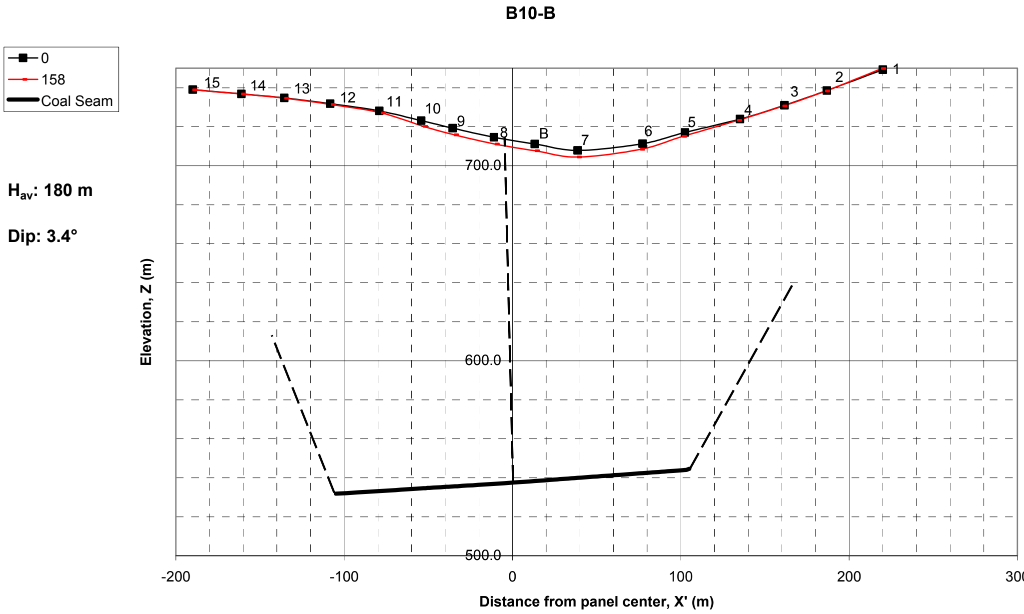

Figure B.5 Section view of B line of panel B10.

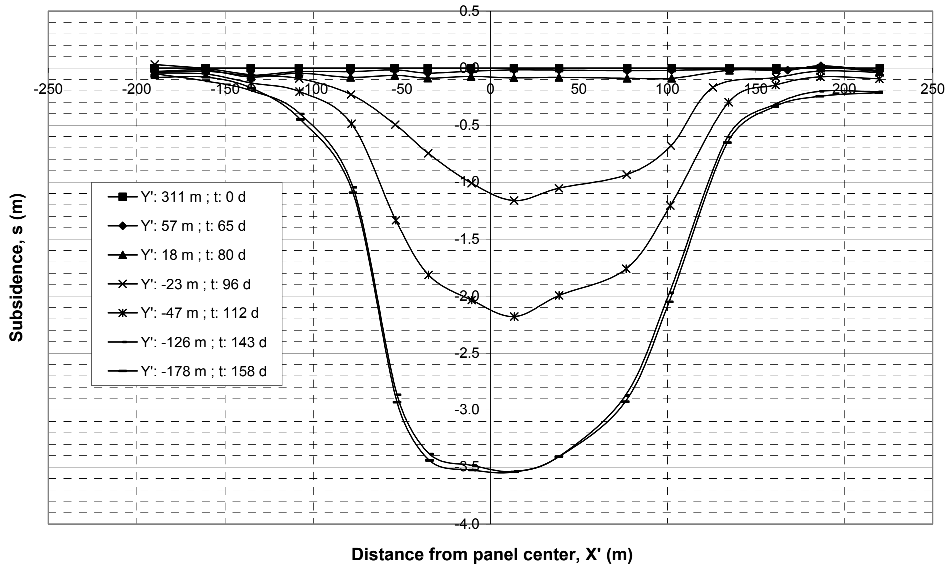

Figure B.6 Subsidence versus distance to the panel center plot along B line of B10.

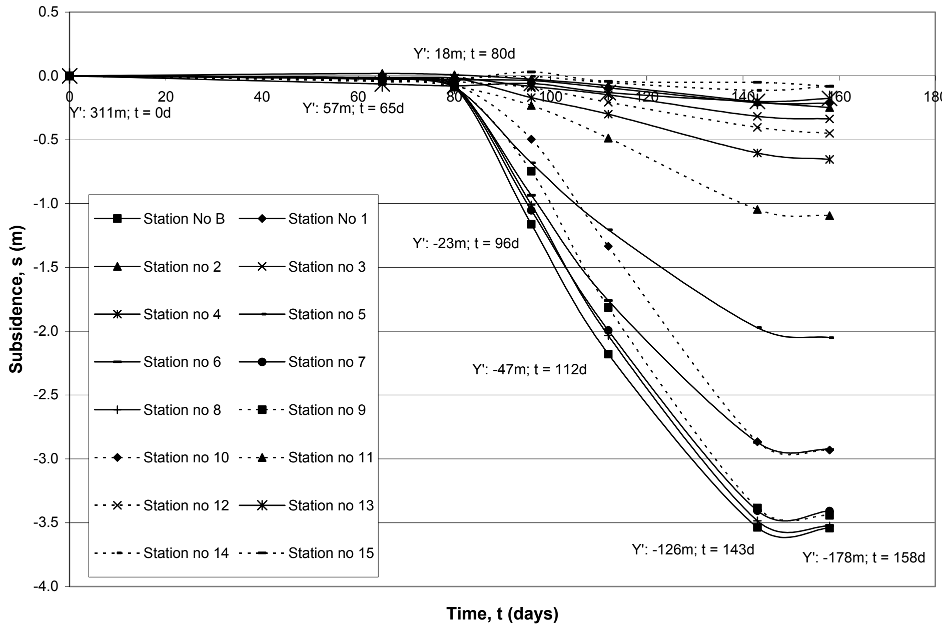

Figure B.7 Subsidence versus time plot for the stations along B line of panel B10.

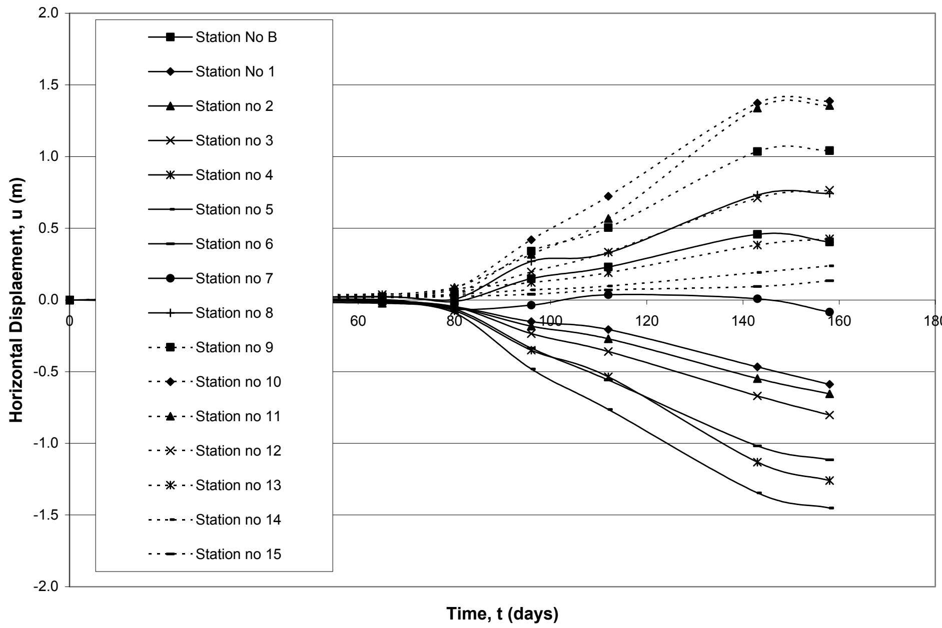

Figure B.8 Horizontal displacement versus time plot for the stations along B line of panel B10 .

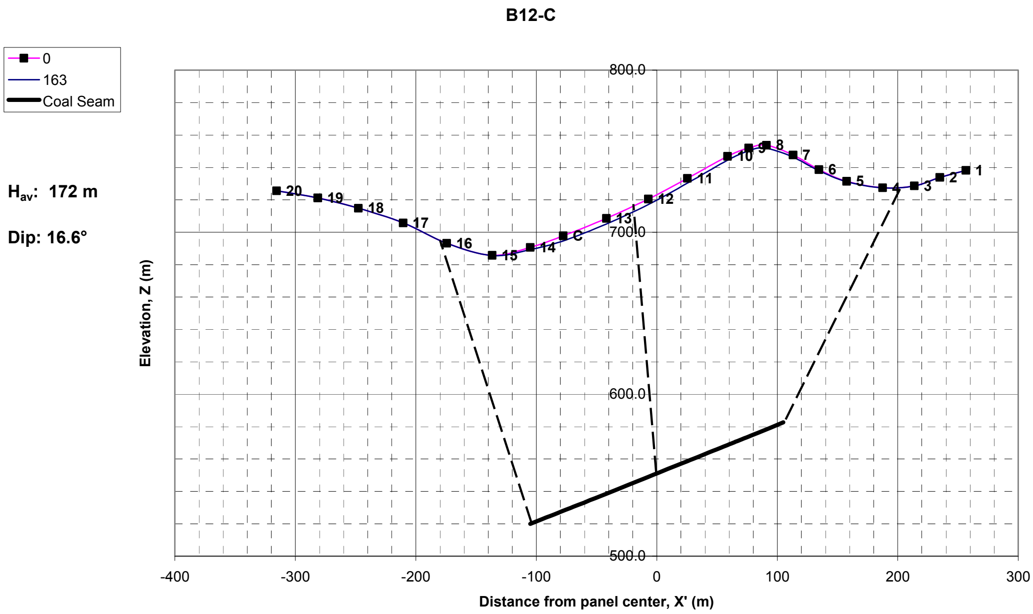

Figure B.9 Section view of C line of panel B12.

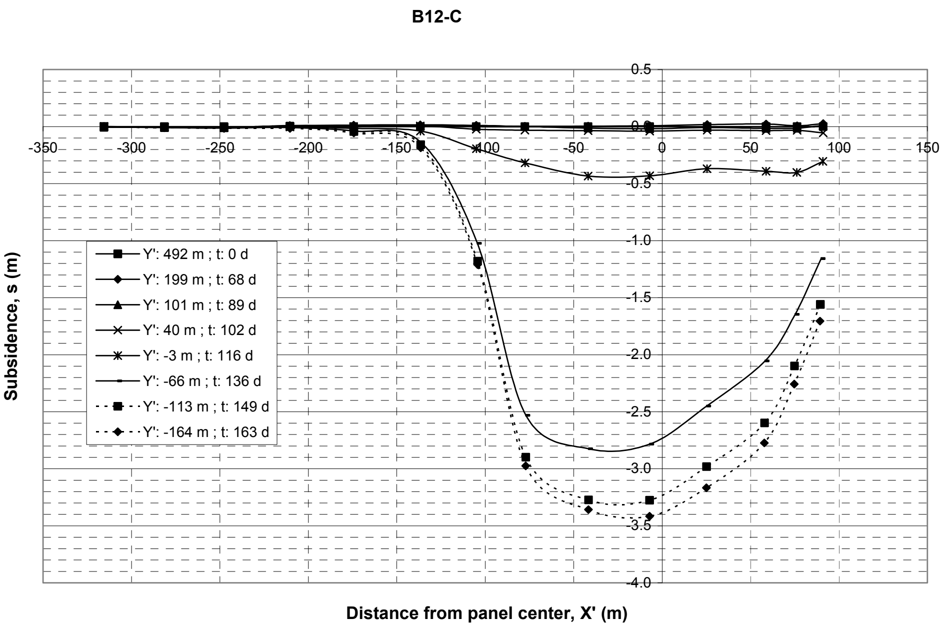

Figure B.10 Subsidence versus distance to the panel center plot along C line of panel B12.

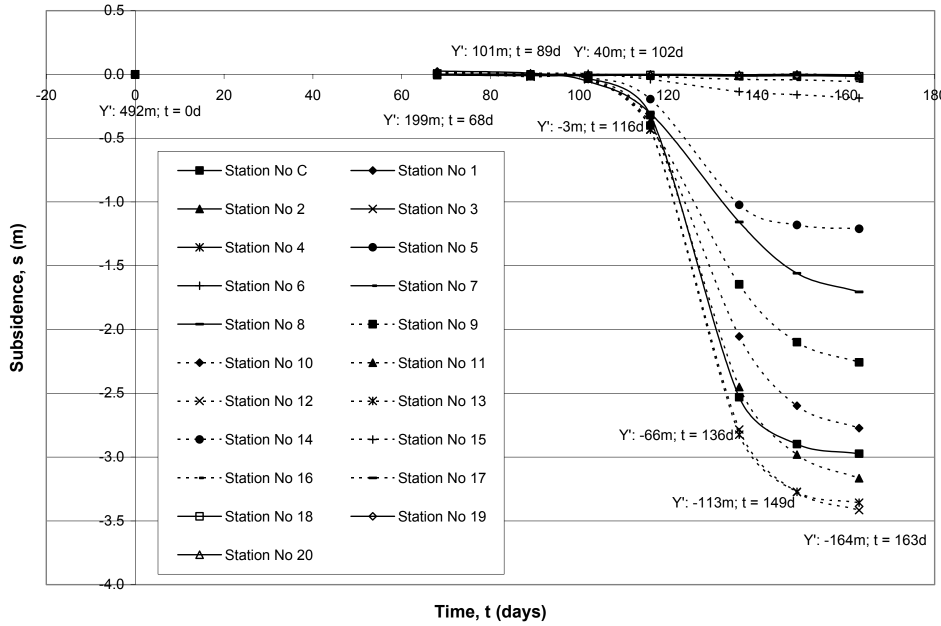

Figure B.11 Subsidence versus time plot for the stations along C line of pabel B12.

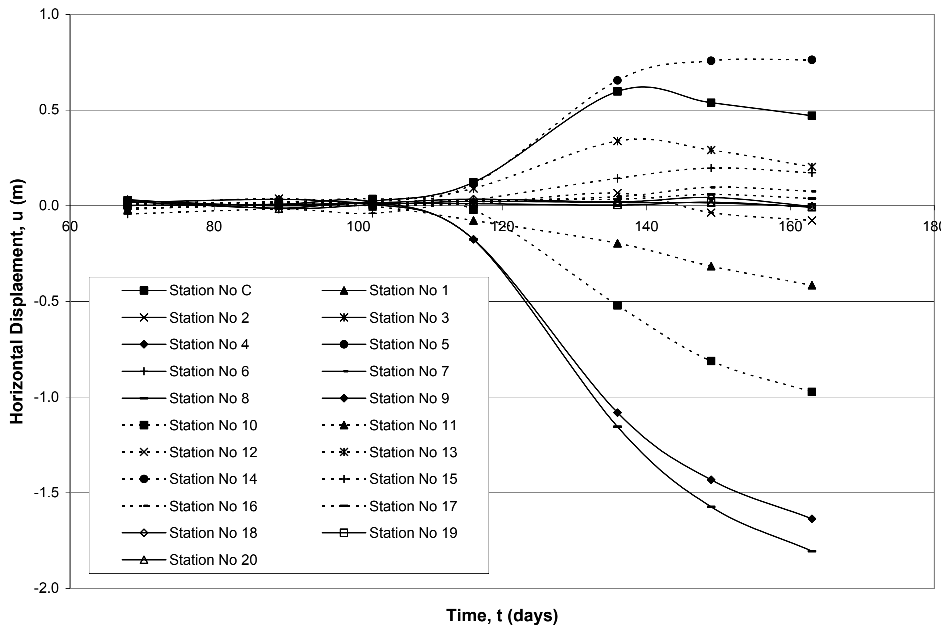

Figure B.12 Horizontal displacement versus time plot for the stations along C line of panel B12.

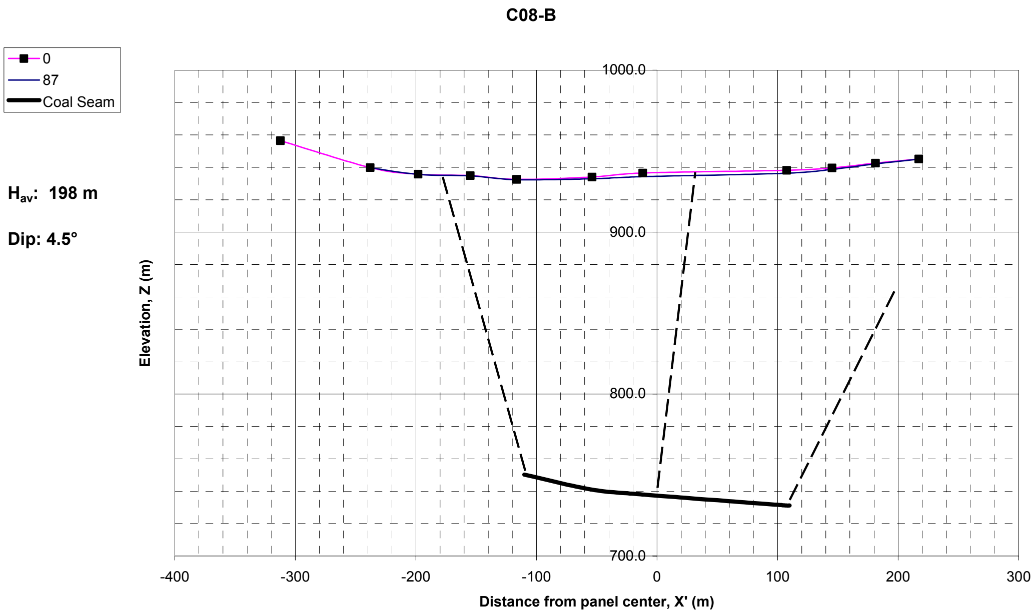

Figure B.13 Section view of B line of panel C08.

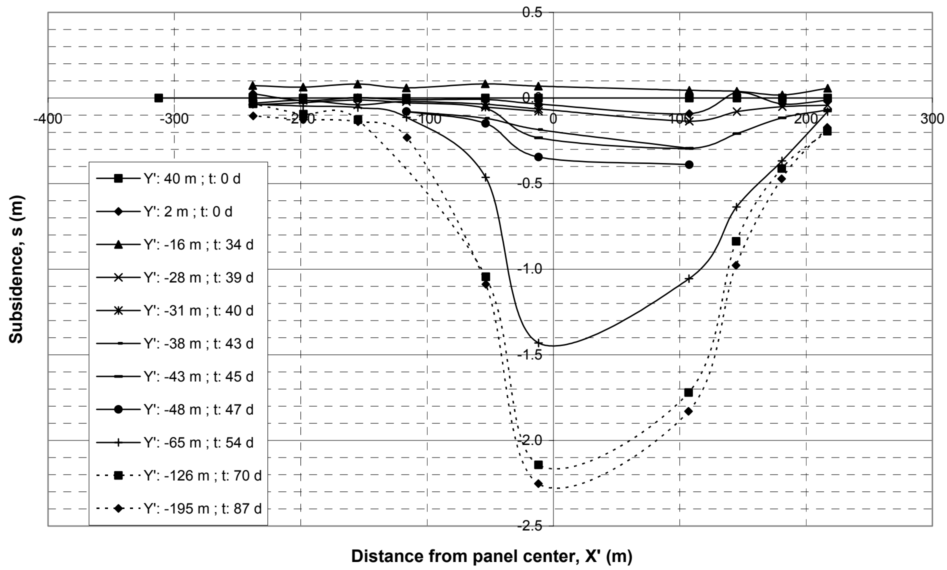

Figure B.14 Subsidence versus distance to the panel center plot along B line of panel C08.

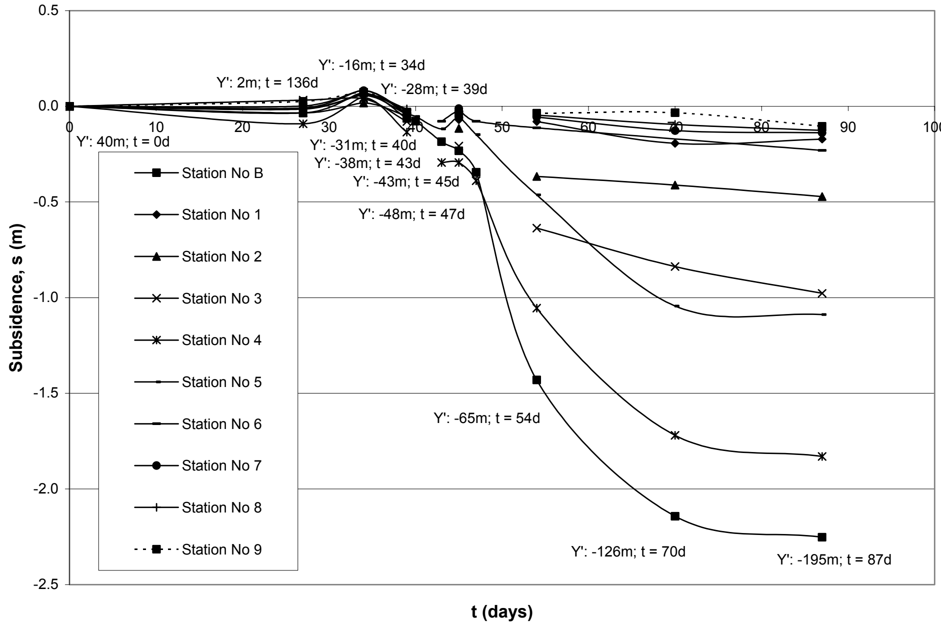

Figure B.15 Subsidence versus time plot for the stations along B line of panel C08.

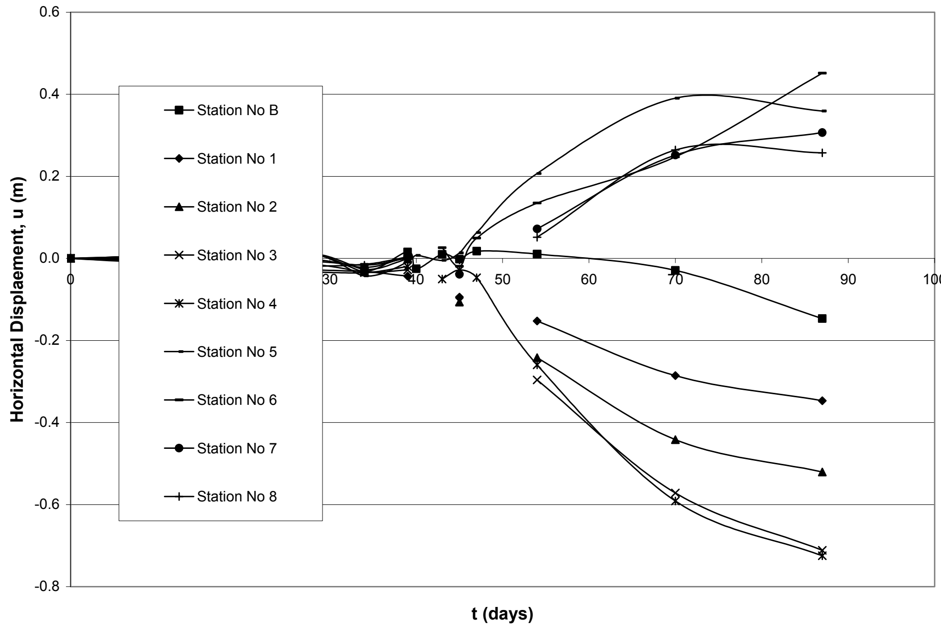

Figure B.16 Horizontal displacement versus time plot for the stations along B line of panel C08.

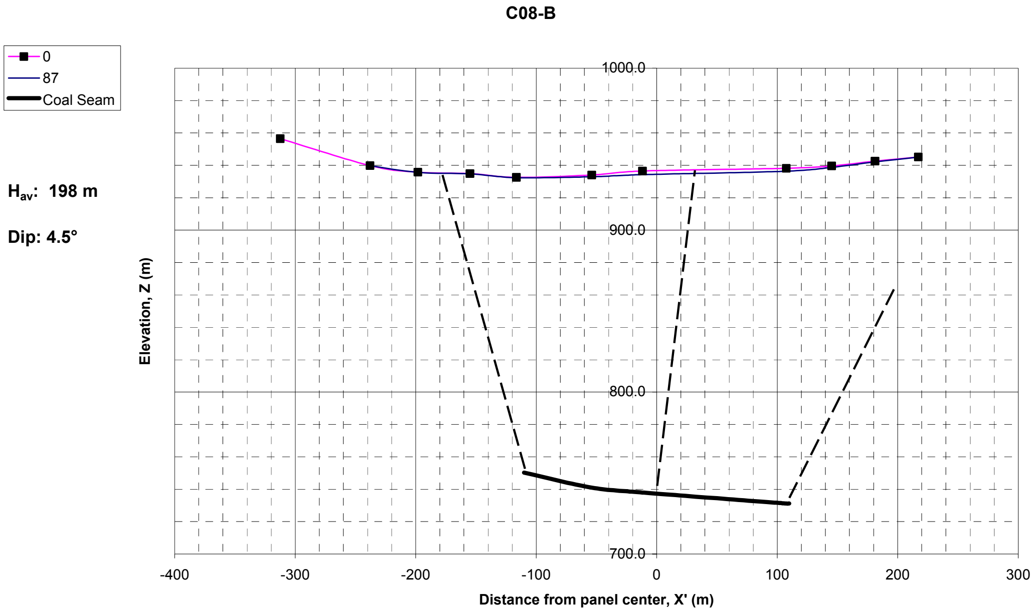

Figure B.17 Section view of B line of panel C08.

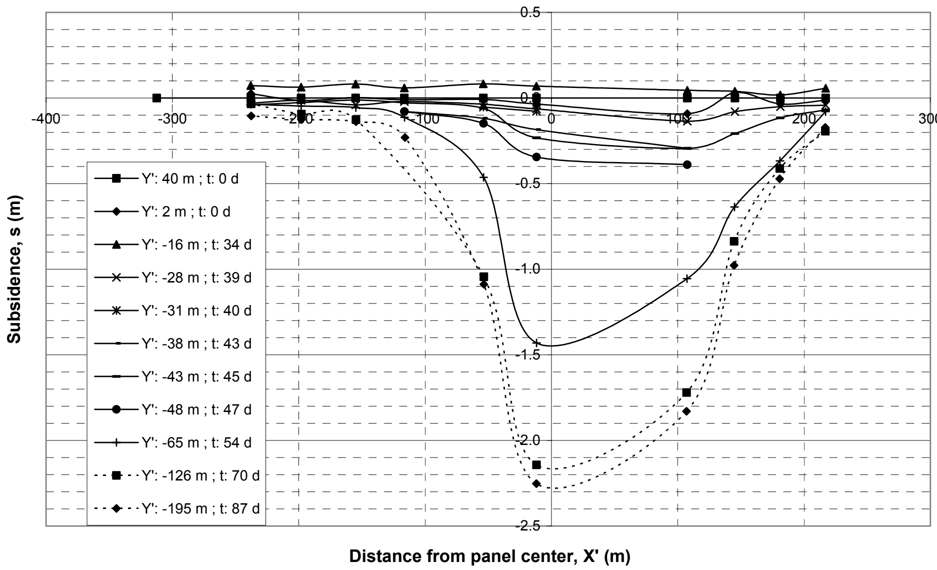

Figure B.18 Subsidence versus distance to the panel center plot along B line of panel C08.

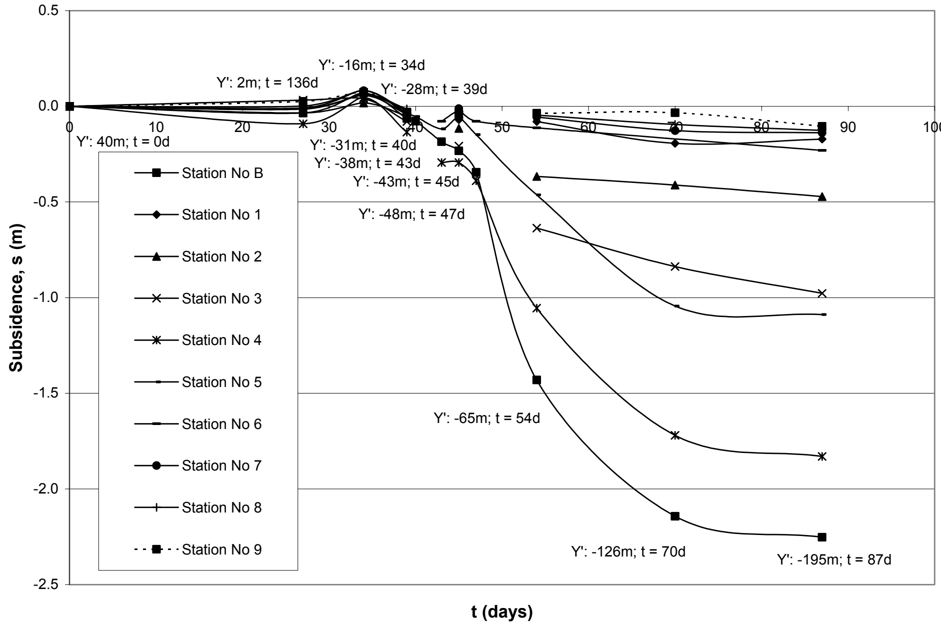

Figure B.19 Subsidence versus time plot for the stations along B line of panel C08.

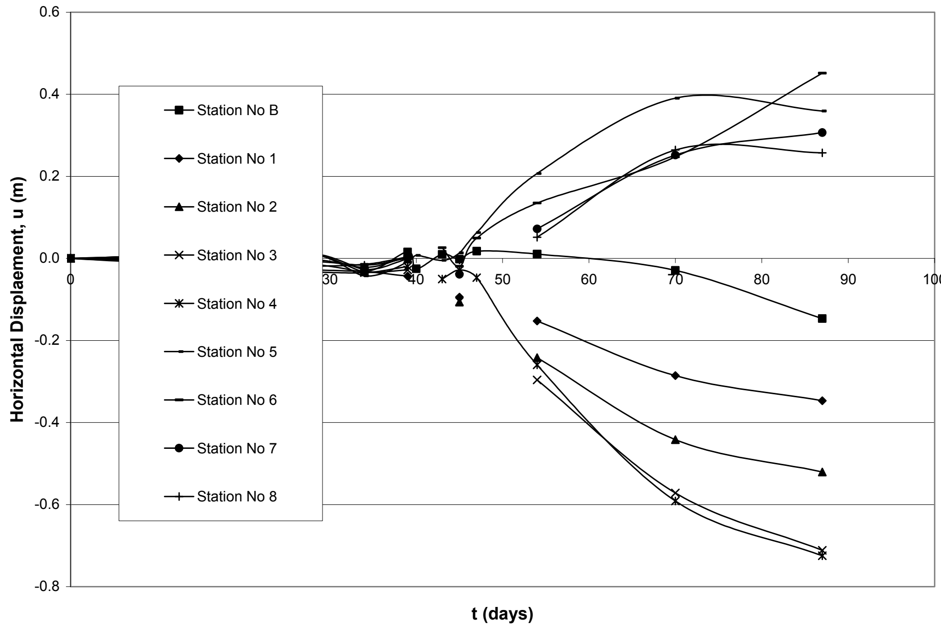

Figure B.20 Horizontal displacement versus time plot for the stations along B line of panel C08.

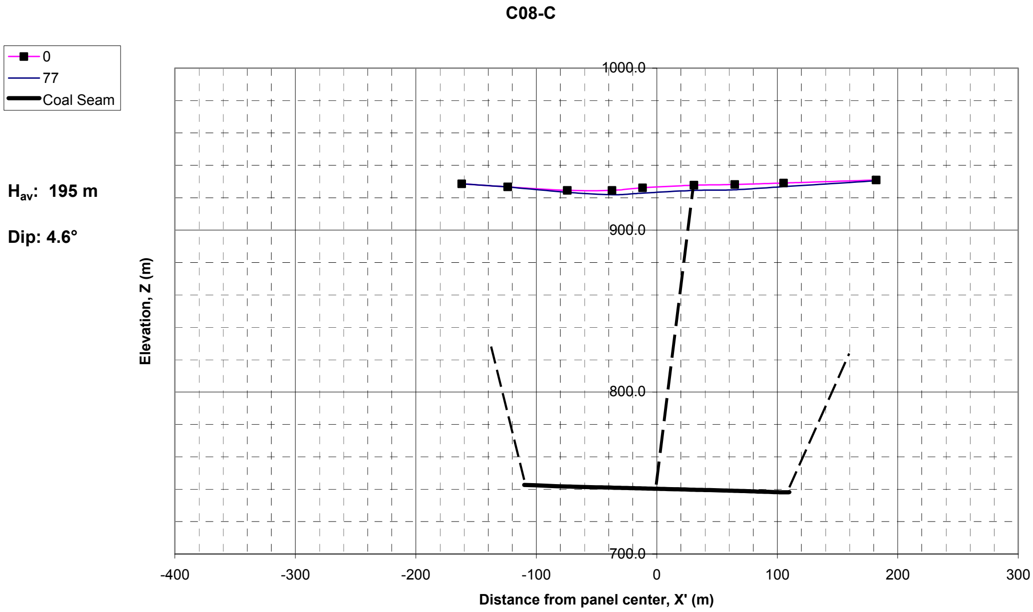

Figure B.21 Section view of C line of panel C08.

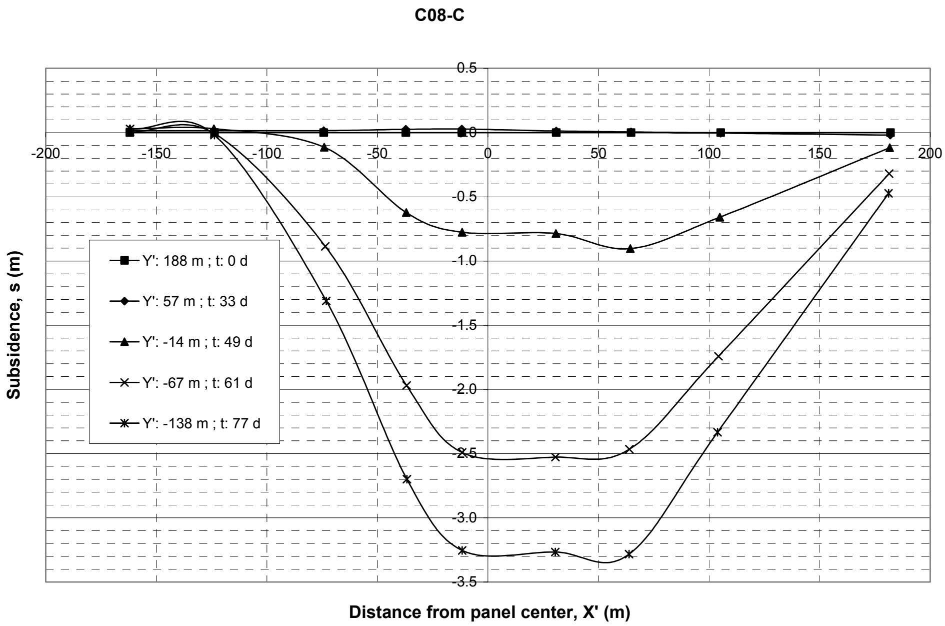

Figure B.22 Subsidence versus distance to the panel center plot along C line of panel C08.

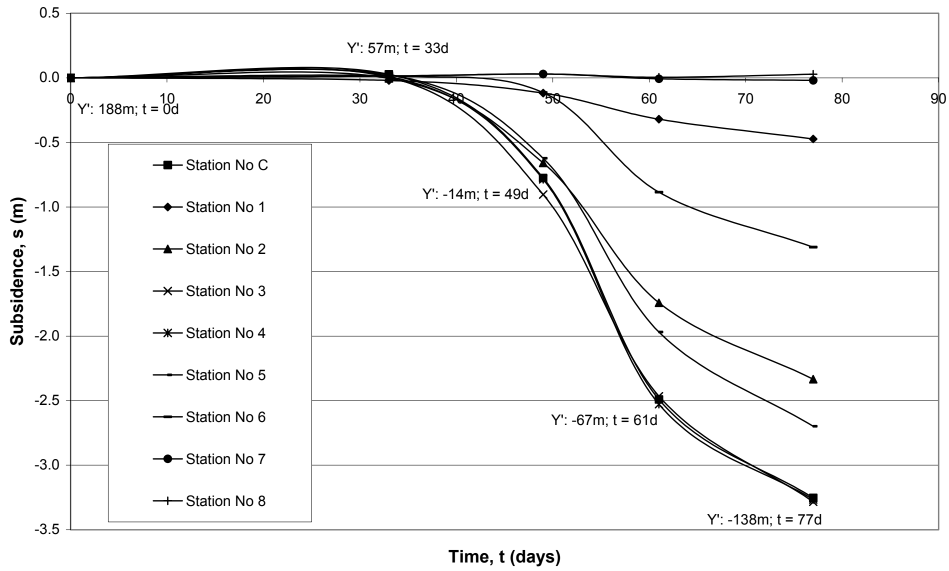

Figure B.23 Subsidence versus time plot for the stations along C line of panel C08.

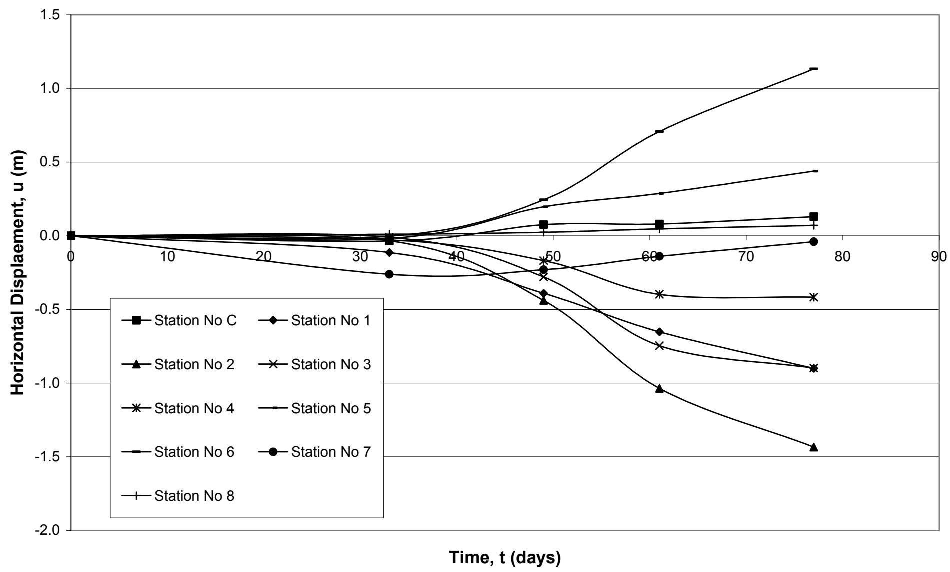

Figure B.24 Horizontal displacement versus time plot for the stations along C line of panel C08 .

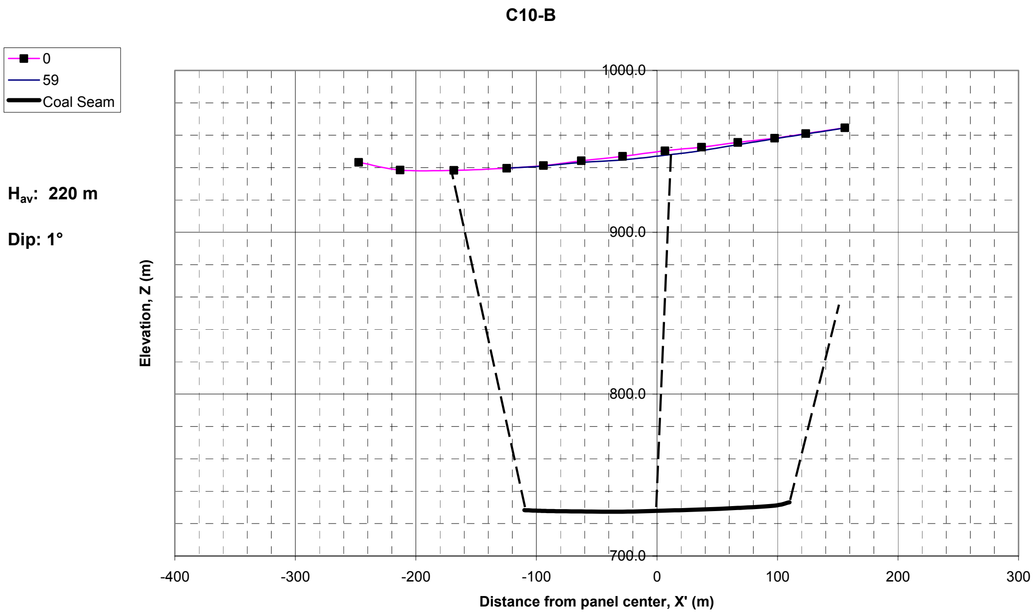

Figure B.25 Section view of B line of panel C10.

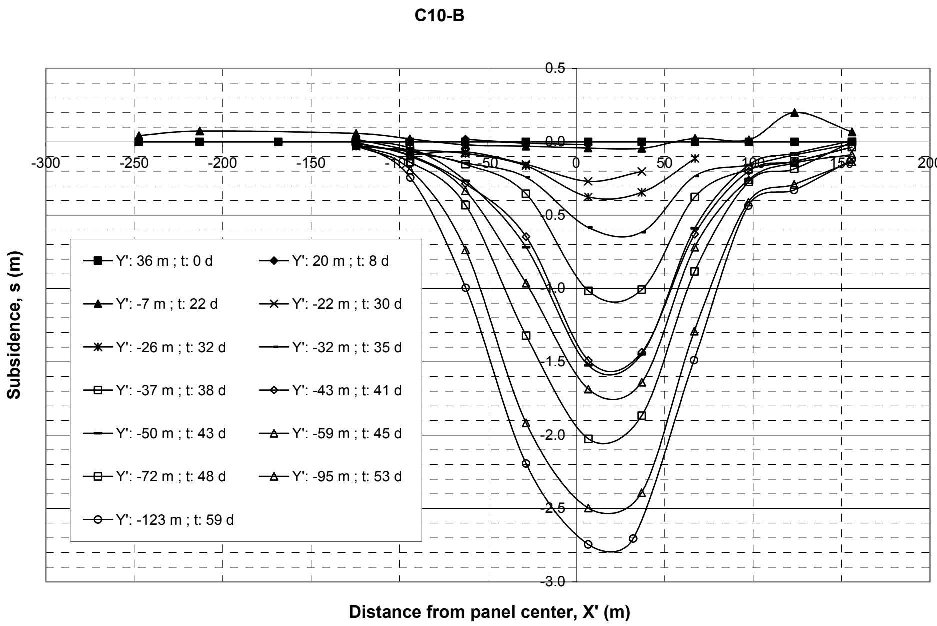

Figure B.26 Subsidence versus distance to the panel center plot along B line of panel C10.

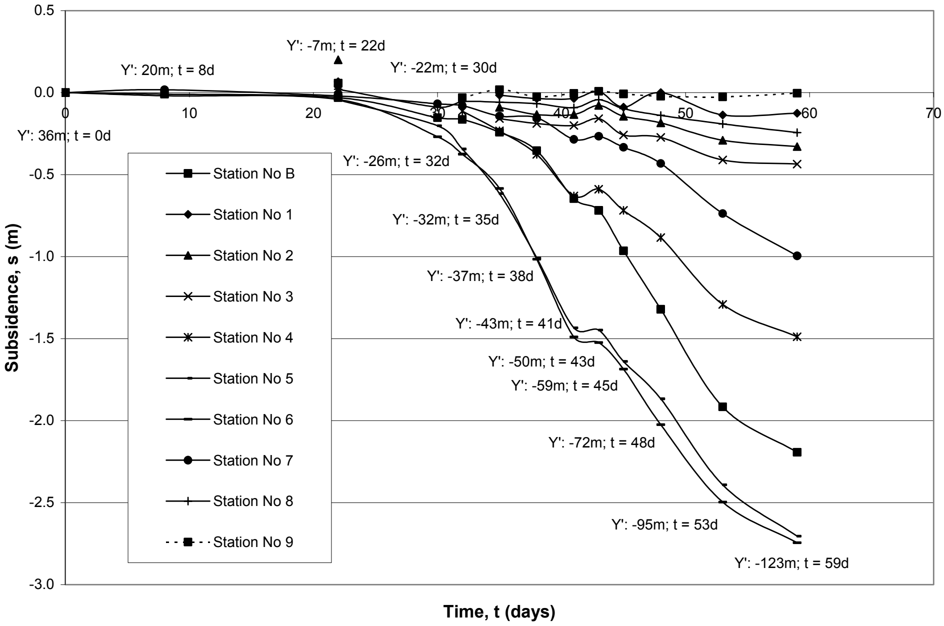

Figure B.27 Subsidence versus time plot for the stations along B line of panel C10.

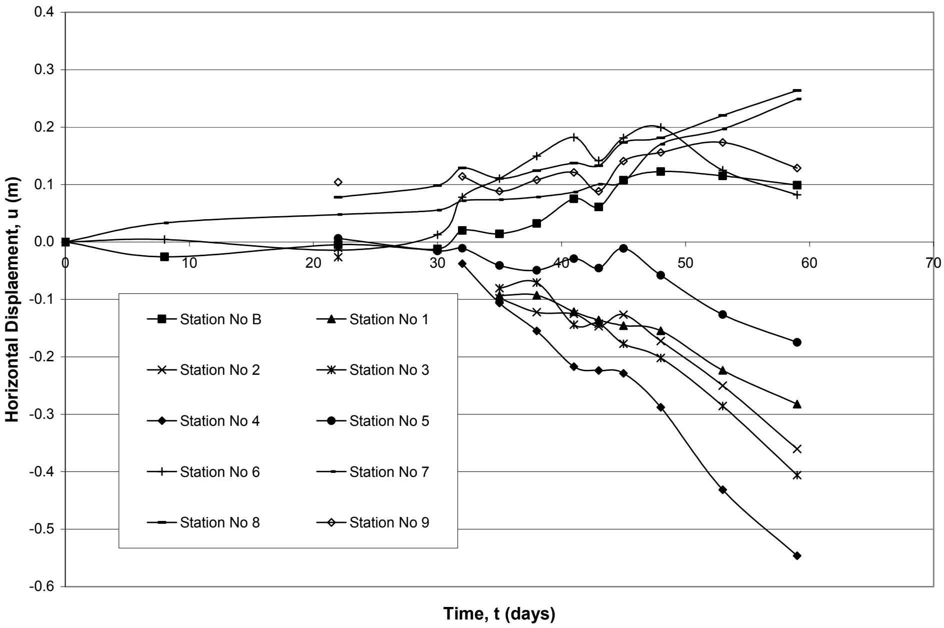

Figure B.28 Horizontal displacement versus time plot for the stations along B line panel C10.

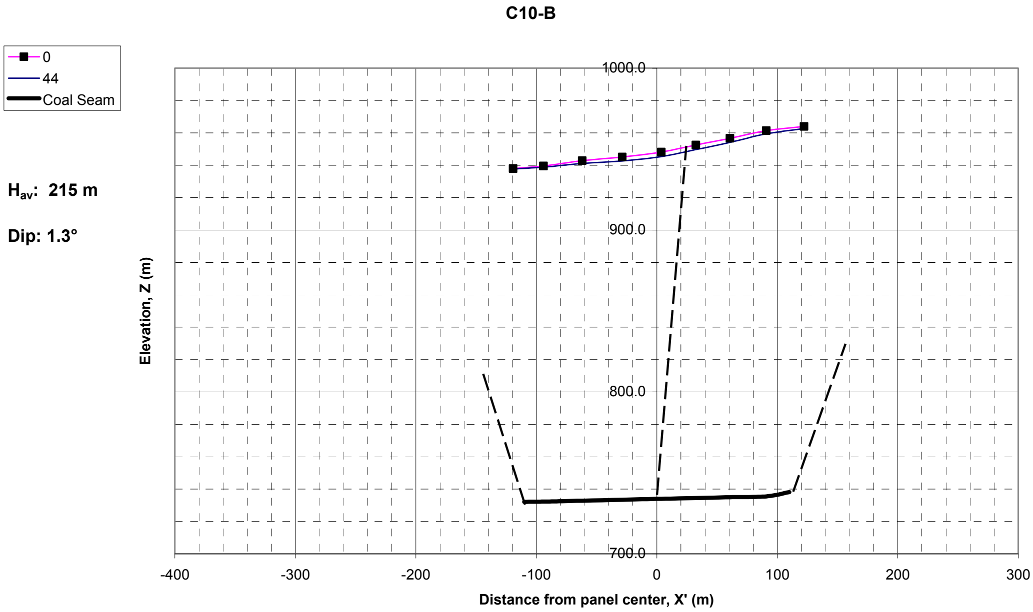

Figure B.29 Section view of "8" line of panel C10.

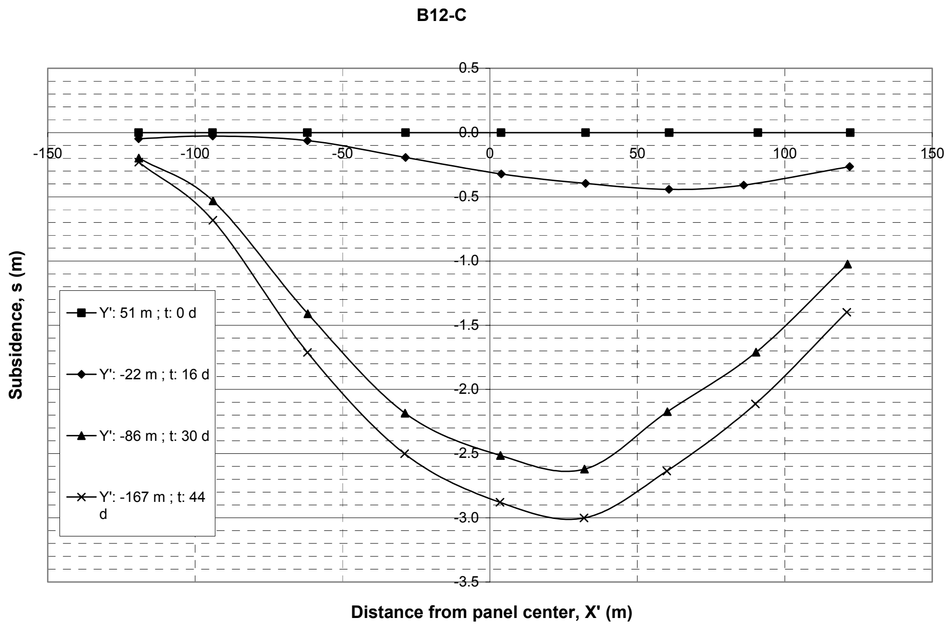

Figure B.30 Subsidence versus distance to the panel center plot along "8" line of panel C10.

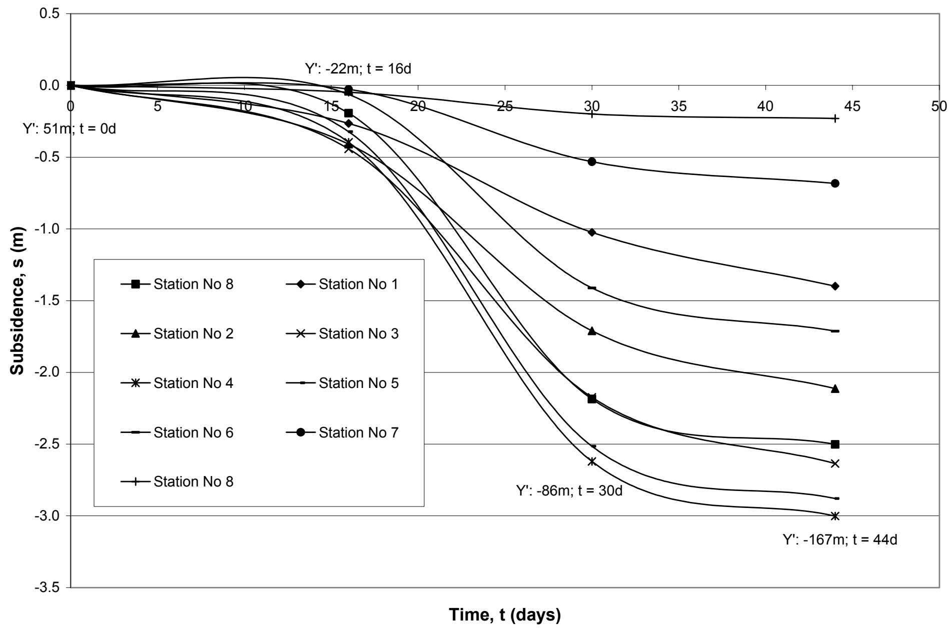

Figure B.31 Subsidence versus time plot for the stations along “8” line of panel C10.

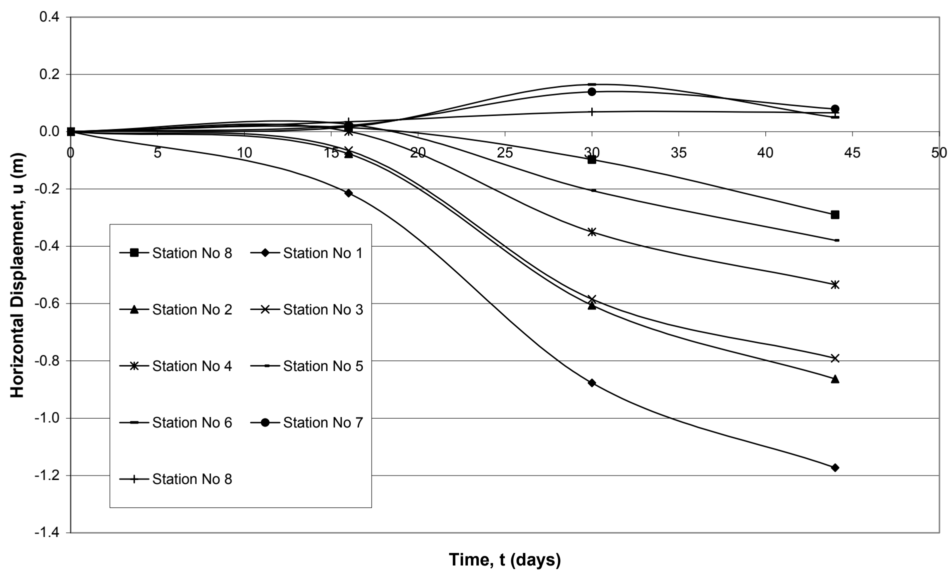

Figure B.32 Horizontal displacement versus time plot for the stations along “8” line of panel C10.

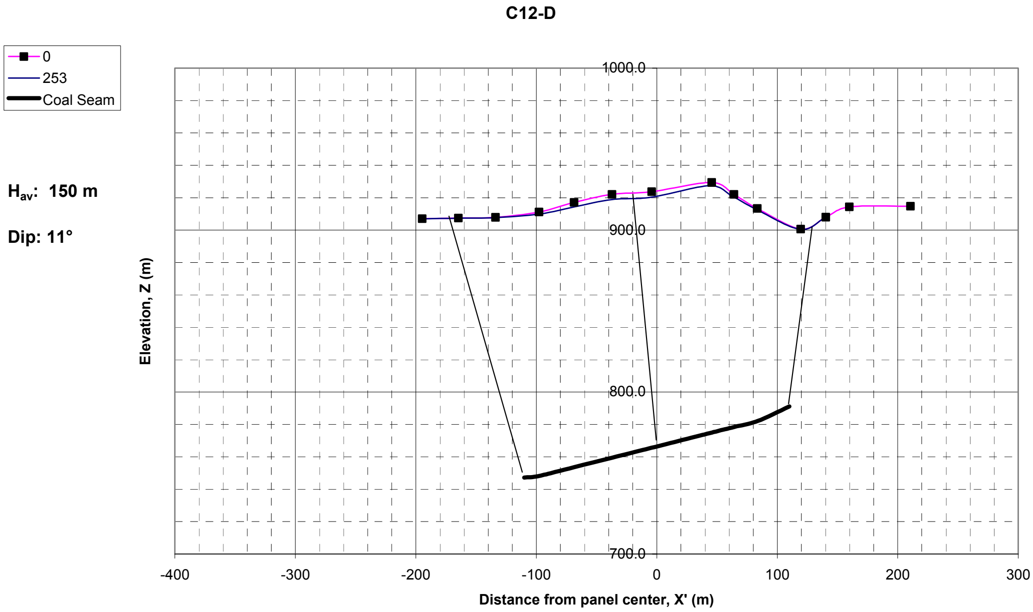

Figure B.33 Section view of D line of panel C12.

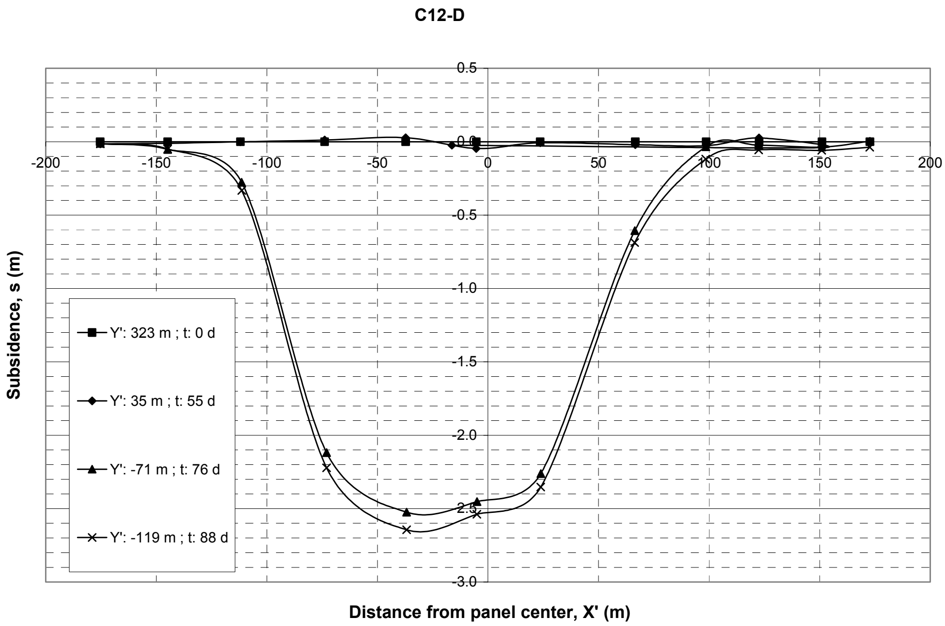

Figure B.34 Subsidence versus distance to the panel center plot along D line of panel C12.

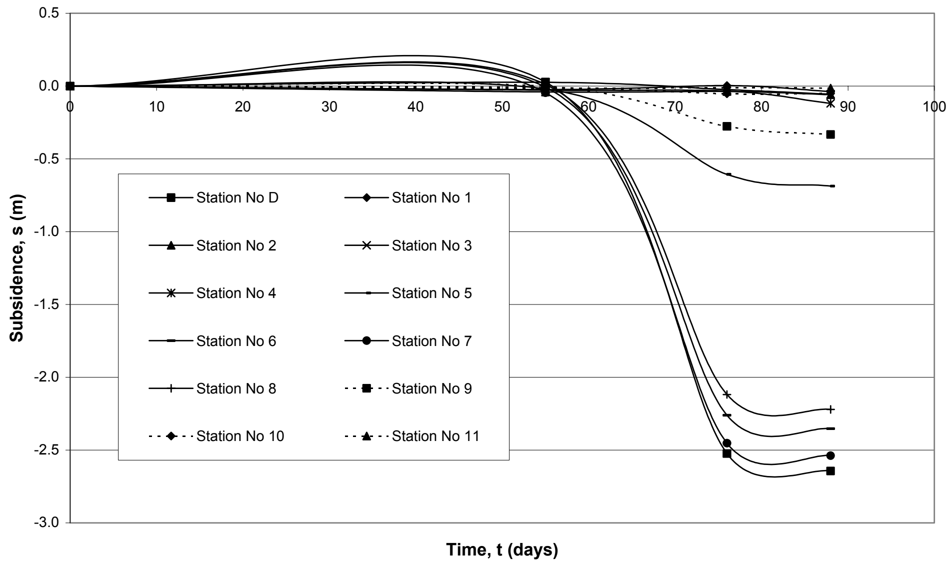

Figure B.35 Subsidence versus time plot for the stations along D line of panel C12.

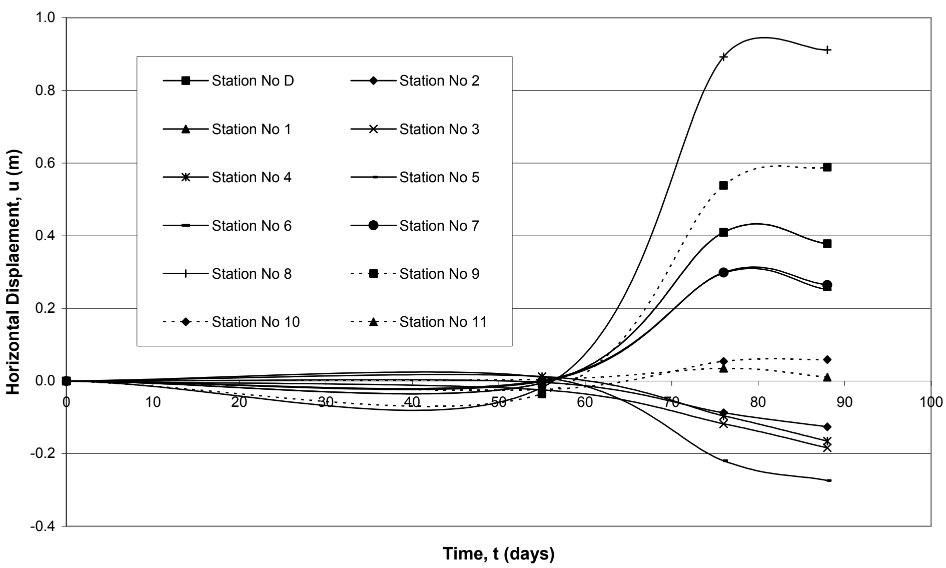

Figure B.36 Horizontal displacement versus time plot for the stations along D line of panel C12.

APPENDIX – C

Macros written for the database calculations

Code C.1

```
Sub TRANSFORMATION()
Sheets("B02").Select
'Sheets("B10").Select
'Sheets("B12").Select
'Sheets("B14").Select
'Sheets("C08").Select
'Sheets("C10").Select
'Sheets("C12").Select

'k = 8 for double face extraction; k = 6 for single face extraction
k = Cells(2, 10)
'Cells(3, 10) = total number of measurement lines perpendicular to panel axis
For m = 1 To Cells(3, 10)
n = 3 * (m - 1) + 11
'cells(3, n) = row number of first measurement of each line
'cells(3, n + 1) = total number of measurements
For i = Cells(3, n) To (Cells(3, n) + Cells(3, n + 1) - 1)
'time(days)
Cells(i, 3) = Cells(i, 2) - Cells(Cells(3, n), 2)
'Dist. btw. Front and Back Face
If k = 8 Then
Cells(i, 6) = (Cells(i, 5) - Cells(i, 4)) / Cos(Cells(3, 9))
End If
```

```
'Gob length (of the front face)
Cells(i, k - 1) = (Cells(3, 1) - Cells(i, 4)) / Cos(Cells(3, 9))
'cells(3, n + 1) = total number of stations for each line
For j = 1 To Cells(3, n + 2)
'x',yf
If Cells(i, (k + 1) + 8 * (j - 1)) = "" Then
Cells(i, (k + 4) + 8 * (j - 1)) = ""
Cells(i, (k + 6) + 8 * (j - 1)) = ""
Else
Cells(i, (k + 4) + 8 * (j - 1)) = (Cells(i, (k + 1) + 8 * (j - 1)) - Cells(i, 4)) * -Sin(Cells(3, 9)) + (Cells(i, (k + 2) + 8 * (j - 1)) - Cells(3, 5) * Cells(i, 4) - Cells(3, 7)) * Cos(Cells(3, 9))
Cells(i, (k + 6) + 8 * (j - 1)) = (Cells(i, (k + 1) + 8 * (j - 1)) - Cells(i, 4)) * -Cos(Cells(3, 9)) + (Cells(i, (k + 2) + 8 * (j - 1)) - Cells(3, 5) * Cells(i, 4) - Cells(3, 7)) * -Sin(Cells(3, 9))
End If
Next j
Next i
For i = Cells(3, n) To (Cells(3, n) + Cells(3, n + 1) - 1)
'Front Face advance
Cells(i, k) = Cells(i, k - 1) - Cells(Cells(3, n), k - 1)
For j = 1 To Cells(3, n + 2)
'change in x'
If Cells(Cells(3, n), (k + 4) + 8 * (j - 1)) = "" Or Cells(i, (k + 4) + 8 * (j - 1)) = "" Then
Cells(i, (k + 5) + 8 * (j - 1)) = ""
Else
Cells(i, (k + 5) + 8 * (j - 1)) = Cells(i, (k + 4) + 8 * (j - 1)) - Cells(Cells(3, n), (k + 4) + 8 * (j - 1))
End If
```

```
'yd
If Cells(Cells(3, n), (k + 6) + 8 * (j - 1)) = "" Or Cells(i, (k + 6) + 8 * (j - 1)) = ""
Then
Cells(i, (k + 7) + 8 * (j - 1)) = ""
Else
Cells(i, (k + 7) + 8 * (j - 1)) = Cells(i, (k + 6) + 8 * (j - 1)) - Cells(Cells(3, n), (k +
6) + 8 * (j - 1)) + Cells(i, k)
End If
'change in z
If Cells(Cells(3, n), (k + 3) + 8 * (j - 1)) = "" Or Cells(i, (k + 3) + 8 * (j - 1)) = ""
Then
Cells(i, (k + 8) + 8 * (j - 1)) = ""
Else
Cells(i, (k + 8) + 8 * (j - 1)) = Cells(i, (k + 3) + 8 * (j - 1)) - Cells(Cells(3, n), (k +
3) + 8 * (j - 1))
End If
Next j
Next i
Next
End Sub
```

Code C.2

```
Sub CLASSIFICATION ACCORDING TO TIME()

Sheets("B02").Select
'Sheets("B10").Select
'Sheets("B12").Select
'Sheets("C08").Select
'Sheets("C10").Select
'Sheets("C12").Select

k = Cells(2, 10)
For m = 1 To Cells(3, 10)
n = 3 * (m - 1) + 11
h = Cells(3, 10) * 3 + 12 + m - 1
Cells(3, h + 1) = Cells(3, h) + Cells(3, n + 2) + 3

For j = 1 To Cells(3, (n + 1))
For i = Cells(3, h) To (Cells(3, h) + Cells(3, n + 2) - 1)
Cells(i, 1) = Cells(Cells(3, n) - 2, (k + 1) + 8 * (i - Cells(3, h)))
Cells(i, 2 + 6 * (j - 1)) = Cells(Cells(3, n) + j - 1, (k + 1) + 8 * (i - Cells(3, h)))
Cells(i, 3 + 6 * (j - 1)) = Cells(Cells(3, n) + j - 1, (k + 2) + 8 * (i - Cells(3, h)))
Cells(i, 4 + 6 * (j - 1)) = Cells(Cells(3, n) + j - 1, (k + 3) + 8 * (i - Cells(3, h)))
Cells(i, 5 + 6 * (j - 1)) = Cells(Cells(3, n) + j - 1, (k + 4) + 8 * (i - Cells(3, h)))
Cells(i, 6 + 6 * (j - 1)) = Cells(Cells(3, n) + j - 1, (k + 7) + 8 * (i - Cells(3, h)))
Cells(i, 7 + 6 * (j - 1)) = Cells(Cells(3, n) + j - 1, (k + 8) + 8 * (i - Cells(3, h)))
Next i
Next j
Next
End Sub
```

APPENDIX – D

Pylons in the area of influence above panel B14

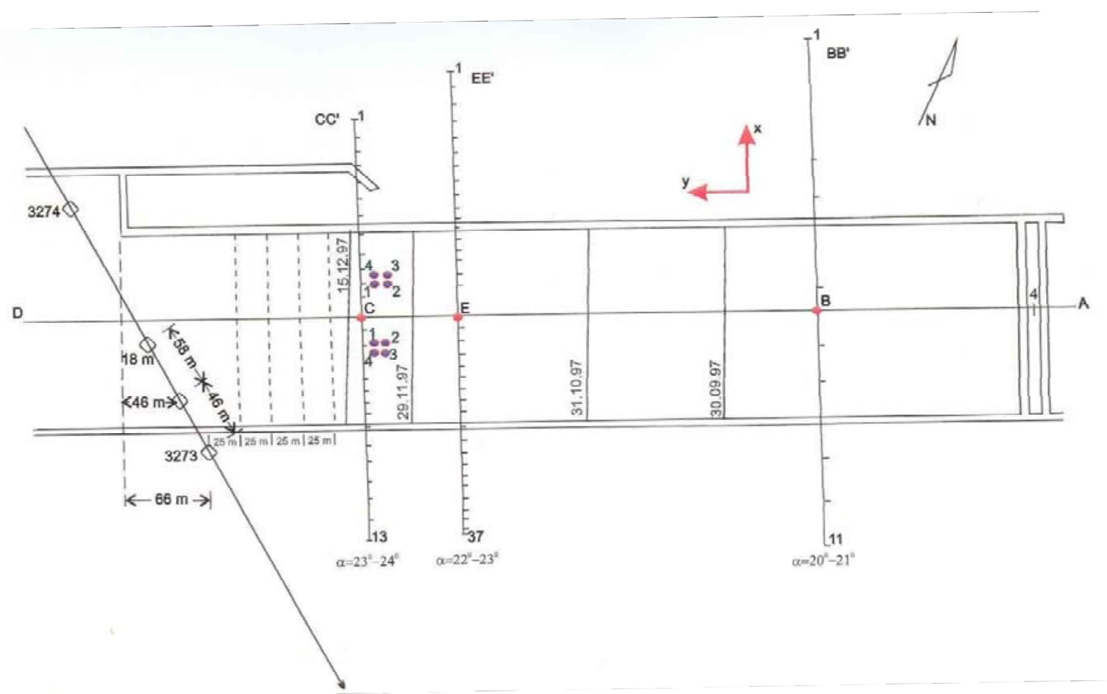

Figure D.1 Alternative 2 (Unal et al.,1998).

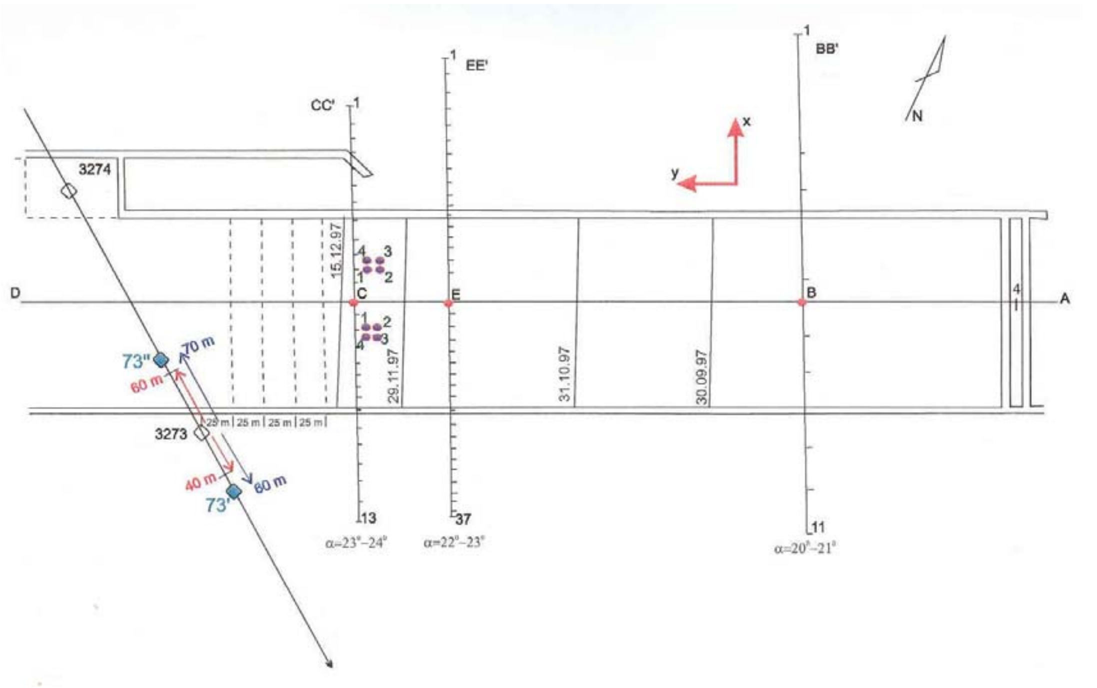

Figure D.2 Alternative 3 (Unal et al., 1998).

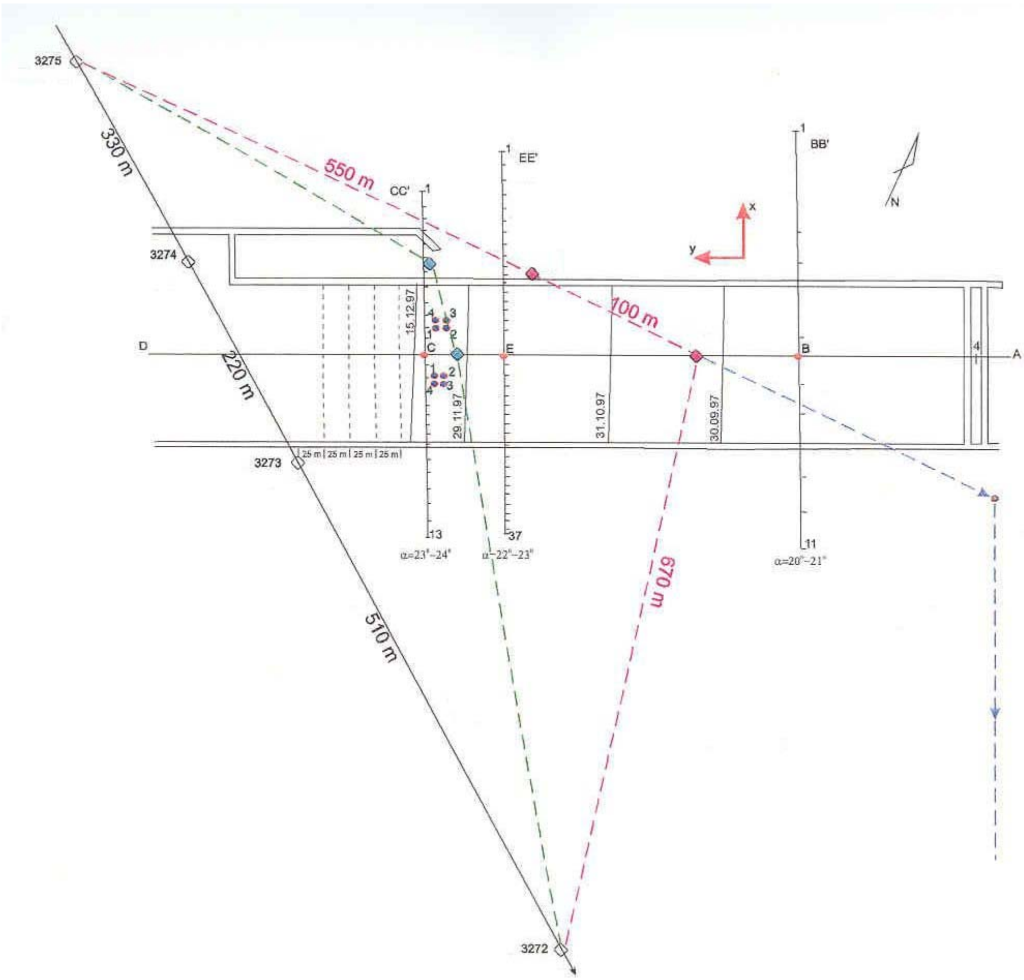

Figure D.3 Alternative 4 (Unal et al., 1998).

APPENDIX – E

Figures, Graphs and Functions from Literature

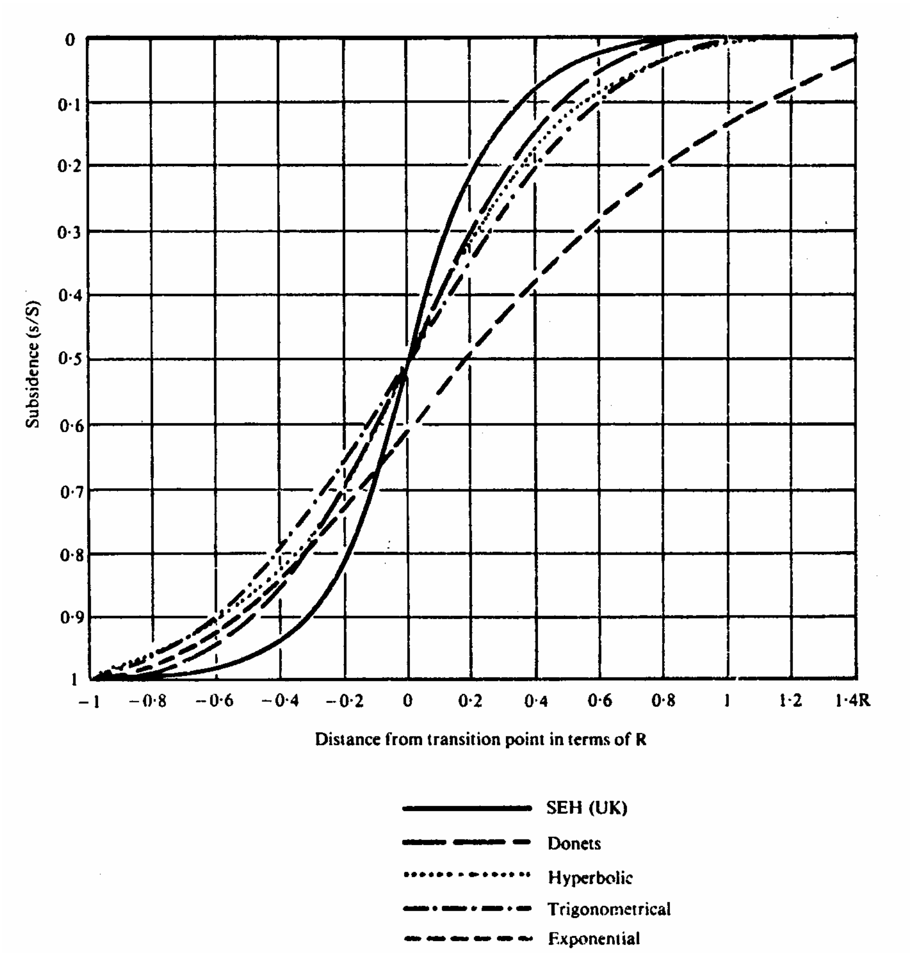

Figure E.1 Comparison of profile functions (Whittaker and Reddish, 1989).

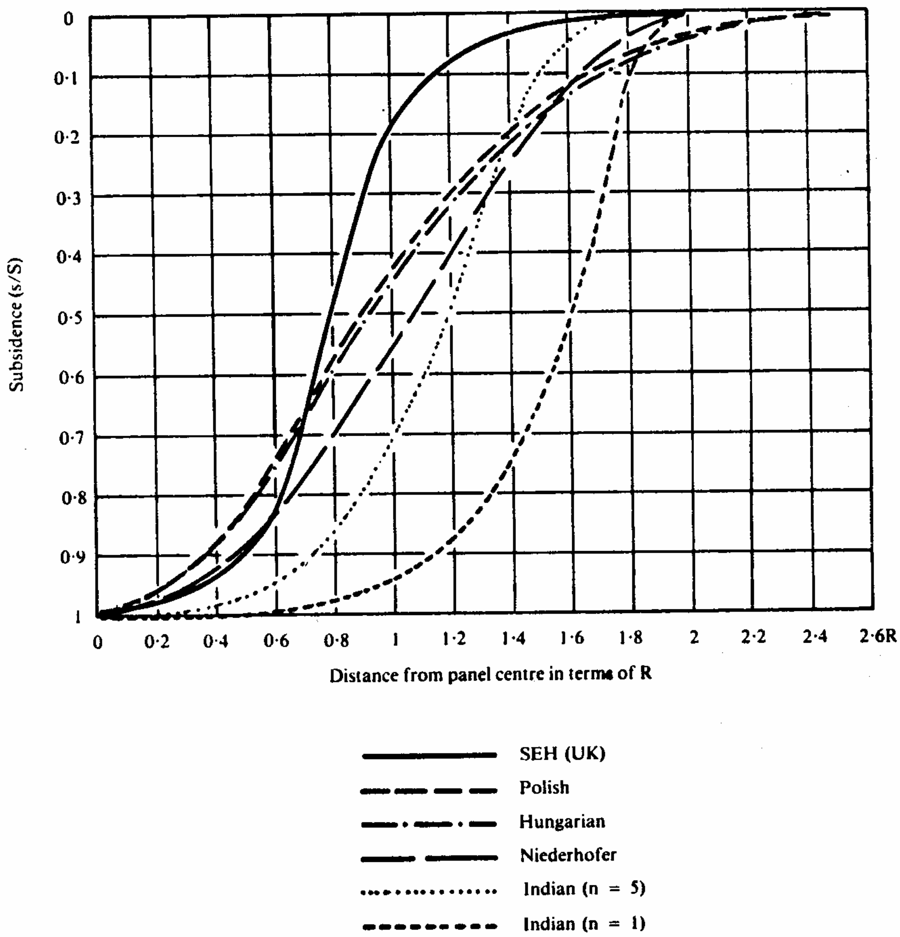

Figure E.2 Comparison of profile functions II (Whittaker and Reddish, 1989).

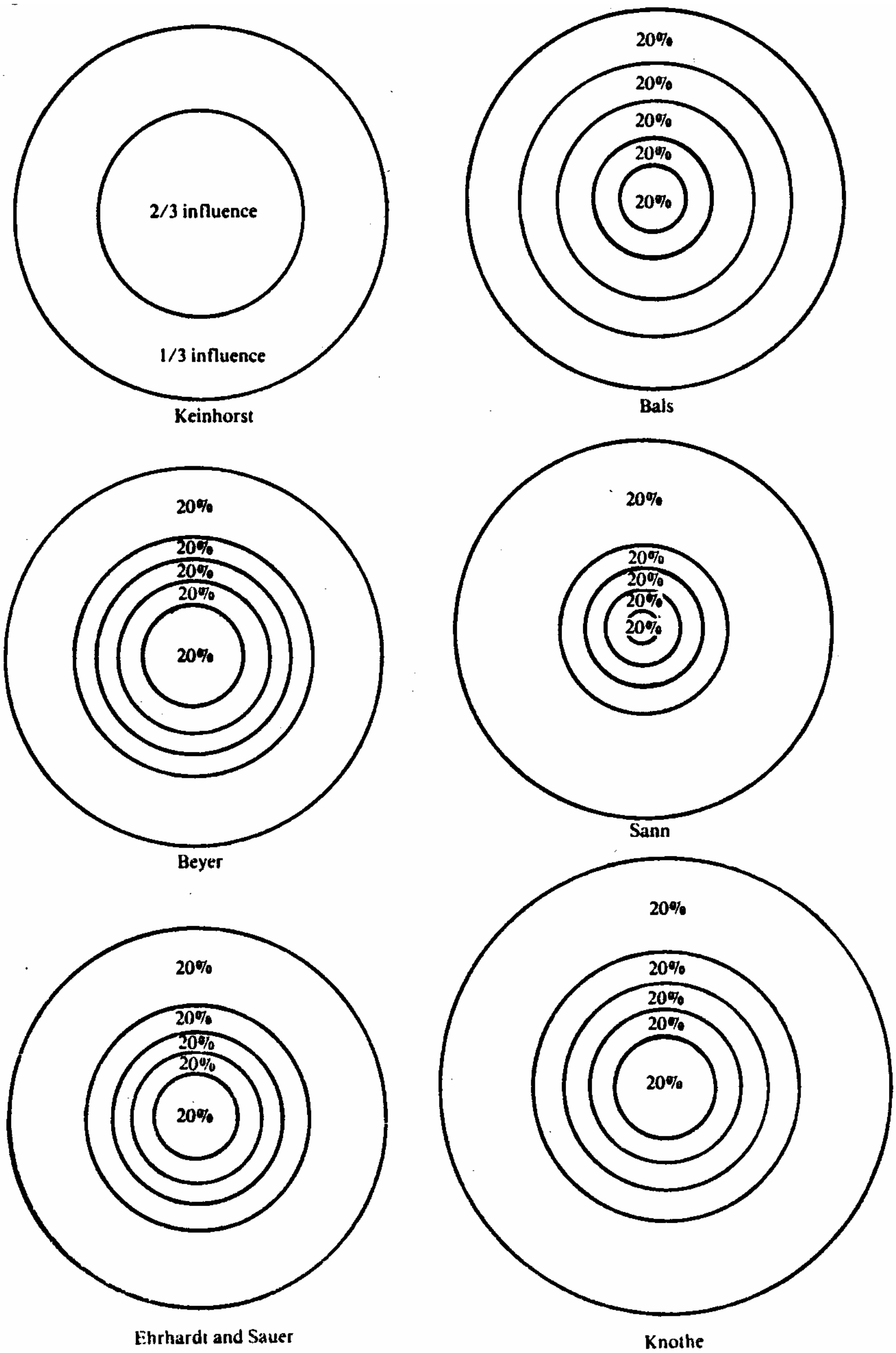

Figure E.3 Comparison of influence functions (Whittaker and Reddish, 1989).

Table E.1 Values of maximum subsidence, surface ground strains and tilt due to longwall mining (Whittaker and Reddish, 1989).

Longwall width/depth (w/h)	0·2	0·25	0·33	0·5	0·75	1·0	1·4
Max. subsidence/extracted seam height S/M; caved wastes	8%	12%	22%	45%	70%	84%	90% (max.)
Coefficients for deducing magnitude and position of maximum ground strains and tilt							
Max. strain due to compression (−E)	2·2S/h	2·15S/h	1·9S/h	1·35S/h	0·75S/h	0·55S/h	0·5S/h
Position of −E from centre line (−Ex)	0	0	0	0·02h	0·10h	0·20h	0·39h
Max. strain due to extension (+E)	0·5S/h	0·65S/h	0·75S/h	0·8S/h	0·65S/h	0·65S/h	0·65S/h
Position of +E from centre line (+Ex)	0·49h	0·42h	0·34h	0·32h	0·40h	0·51h	0·70h
Max. ground tilt (G) (at transition pt.)	2·2S/h	2·6S/h	3·15S/h	3·35S/h	2·85S/h	2·75S/h	2·75S/h
Position of G from centre line (Gx)	0·32h	0·27h	0·22h	0·21h	0·26h	0·37h	0·56h

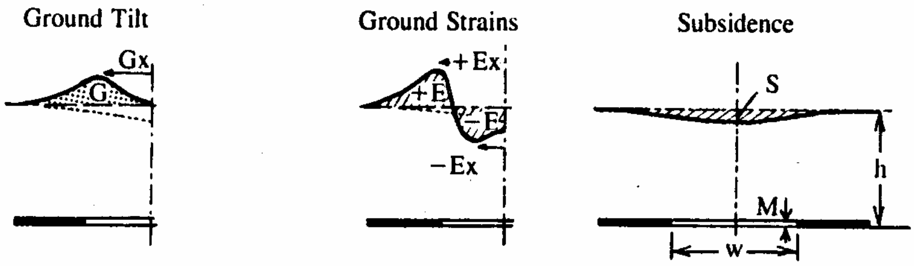

Time functions below are reviewed by *Jarosz, 1989*:

The function representing the influence of time is expressed as

$z(t) = 1 - \exp(\text{-ct})$

So, $\dot{S}(t) = c(t)\left[S^f(t) - S(t)\right]$ and its solution is $\dot{S}(t) = c(t)\left[S^f(t) - S(t)\right]$

where

$\dot{S}(t)$ = subsidence development rate

Sf(t) = final (asymptotic) subsidence at time t

$S(t)$ = actual subsidence at time t

$[S^f(t) - S(t)]$ = subsidence potential at time t

Keinhorst, H. (1928)

$S(t) = aMf(t)z(t)$

$f(t)$ = influence function

Kolmogoroff, A. (1931)

$\dot{S}(t) = V.S'(x)$

$$\dot{S}(t) = \frac{\partial S(t)}{\partial t}$$

$$S'(x) = \frac{\partial S(x)}{\partial x}$$

V = change in the origin

Aviershin, S.G. (1940)

$\dot{S}(t) = A\exp(kt^n)$

A, k, n = empirical parameters

Perz, F. (1948)

$S(t) = \int_0^{x_t = vt} z(t)S'(x)dx$

$$S'(x) = \frac{\partial S(x)}{\partial x}$$

Salustowicz, A. (1951)

$$\dot{S}(t) = c\left[S^f - S(t)\right]$$

Knothe, S. (1953)

$$\dot{S}(t) = c\left[S^f(t) - S(t)\right]$$

Martos, F. (1967)

$$z(t) = 1 - \exp(-ct^2)$$

Trojanowski, K. (1972)

$$\dot{S}(t) = c(t)\left[S^f(t) - S(t)\right]$$

Sroka, A., F. Shober (1983)

$$\Delta M(t) = a\Delta V\left[1 + \frac{\xi}{c-\xi}\mathbf{exp}(-ct) - \frac{c}{c-\xi}\mathbf{exp}(-\xi\, t)\right]$$

$\Delta M(t)$ = volume of elemantary subisdence trough at time t

a = subsidence parameter

ΔV = elementary extracted void

ξ = time compaction coefficient

Three time stages of subsidence:

$$\begin{aligned}
&S(x_t, x_o, x_1, x_2, z, \Delta t) = \\
&S^f(x_t, x_o, y_1, y_2, z) \\
&-\mathbf{exp}\left(\frac{u_z^2}{4\pi}\right)\mathbf{exp}\left(\frac{u_z x_t}{r_z}\right)S^f\left(x_t + \frac{r_z u_z}{2\pi}, x_o + \frac{r_z u_z}{2\pi}, y_1, y_2, z\right) \\
&+\Delta S^f(x_t, x_o, y_1, y_2, z)\left[1 - \mathbf{exp}(-c\Delta t)\right]
\end{aligned}$$

final (asymptotic) subsidence

subsidence development while the face advances with constant speed

subsidence development after the face has stopped and until local maximum subsidence is reached